X-650-65-24

NASA TMX-55219

DIGITAL COMPUTER SIMULATION OF THE INFRARED INTERFEROMETER SPECTROMETER (IRIS) AND INTERFEROGRAM ANALYSIS

BY
L. H. BYRNE

JANUARY 1965

NASA — GODDARD SPACE FLIGHT CENTER
GREENBELT, MARYLAND

DIGITAL COMPUTER SIMULATION

OF THE

INFRARED INTERFEROMETER SPECTROMETER (IRIS)

AND

INTERFEROGRAM ANALYSIS

by

L. H. Byrne

GODDARD SPACE FLIGHT CENTER

GREENBELT, MD.

JANUARY 1965

ACKNOWLEDGEMENT

The author is indebted to the IRIS experimenter, Dr. R. Hanel, without whom this work would not have been possible. Also, gratitude is due Mr. F. Bartko, Dr. C. Hammer, and Dr. R. Roper for the many stimulating discussions on the subject topic. Mr. G. Nichols has provided the necessary information on the electronics of the system, and Mr. A. Simmons is credited with the computer coding and his tireless assistance in setting up computer and plotter runs.

A-B-S-T-R-A-C-T

A digital computer program for the simulation of the output of the Infrared Interferometer Spectrometer (IRIS) and a program for the analysis of the resultant interferogram are being effectively utilized for two purposes: (i) determination and verification of instrument design parameters, and (ii) provision of the basis for operational computer programs which will be needed to process and analyze the data from the actual instrument. Both programs are required to satisfy (i), and, with proper program design, (ii) is fulfilled automatically. The two programs, then, form a "closed-loop" synthesis/analysis model for testing the effects of instrumentation and design parameters on both the interferogram and the transformed spectral profile.

Results indicate that a sampling rate for IRIS of approximately four times the highest frequency present is desirable. The effect on the transformed spectral profile due to digitizing is, as anticipated, about the same as the effect due to the mean expected signal-to-noise ratio at the detector. The effect due to finiteness of the optical solid angle is less than that caused by digitization or noise at the detector. Additional distortions of the data from the actual interferometer may be anticipated due to secondary effects not included in the simulation.

TABLE OF CONTENTS

1.0 INTRODUCTION

The Infrared Interferometer Spectrometer (IRIS) is a Michaelson-type interferometer designed for spacecraft use; hence the basic optical principles employed are classical and well-known. A beam splitter is exposed to incoming radiation, and every radiative component is divided into two separate beams. These beams are directed along different paths of the optical system before being focused concurrently on the detector. The optical distance of one of the paths is constant; the other path is varied at a constant rate by means of a movable mirror. The resultant interference pattern, then, is a function of path difference, and the measured flux at the detector is known as the interferogram.

One of the advantages of the interferometer is the wide spectral range which can be obtained; however a distinct disadvantage is the fact that the spectral analysis must be performed in terms of the transformed interferogram. This is clear when it is recognized that every point of the sampled interferogram contains an amplitude contribution due to each spectral component involved. Thus, the study of many of the effects of varying design parameters, as well as the operational use of the data, must necessarily be oriented around the reconstructed spectral profile. The large number of calculations involved in this transformation process for a wide spectral range, and the desired spectral resolution, then,

make the use of a fast, large-scale computer a necessity.

The literature on the theory of interferometric spectroscopy is abundant, [1] - [5]; however most of the work in this field was done prior to the advent of the second-generation computers of today. As a result, many of the experimenters could not avail themselves of the advantages inherent in such a system as described here.

The purpose of the programs presented here is two-fold: (i) to provide a means of determining and verifying design parameters for IRIS; and (ii) to provide the basis for operational computer programs which will be needed to process and analyze the data from the actual interferometer. To satisfy (i), a "closed-loop feedback" system, consisting of (a) a simulation model of IRIS, and (b) a program to transform the resulting data, are required. If handled properly, requirement (ii) is then fulfilled automatically.

Any simulation model is, at best, only an approximation of certain events. However, these events are usually combined in complex fashion, even if the physical phenomenon to be simulated appears simple when viewed in terms of effect only. In most instances, it suffices to consider only those characteristics which most significantly affect the final result. Nevertheless, use of the model and iteration through the learning cycle usually indicate ways in which the model can be improved. The "closed-loop" method of synthesis/analysis then also be-

comes a means of refining and enhancing the model to whatever degree is desirable, as well as serving as an effective tool in the initial design stages.

The most difficult interferometer effect to simulate is the total instrument response, since it is made up of a composite of a number of individual effects. Conceivably, this response could even vary from instrument to instrument. The individual effects included in the IRIS simulation model are those due to (i) the finite solid angle of admission; (ii) the finite path difference(obtained as a direct result of the finite mirror travel distance); (iii) noise at the detector; and (iv) the digitizing process. The latter, however, is external to the instrument itself, and is not included in the instrument response. Nevertheless, digitizing has a very decided effect on the transformed spectral profile.

The programs were designed such that they could be used for the study of similar interferometer systems merely by control of the input parameters; however to avoid over-generalization, thus preserving simplicity, as well as computer memory, certain options and decisions have been left to the discretion of the user. The structure of the programs is modular and the various effects may be included, or omitted, at the user's option, by proper setting of program switches. This permits flexible use of the system as a research tool, and minimizes changes required in the event that program modification is desired.

2.0 MATHEMATICAL ANALYSIS

The analysis presented herein is intended for use in connection with the paper by Hanel and Chaney regarding IRIS, Ref. [1]. The presentation begins with a discussion of the "pure" interferogram, i.e., one without any instrumental effects which cause distortion of the data, followed by the inclusion of each of the distortion effects.

2.1 THE "PURE" INTERFEROGRAM AND ITS SYNTHESIS

The derivation of the equation for the "pure" interferogram may be readily understood by reference to Fig. 1, which is a simplified schematic of the interferometer optical system.

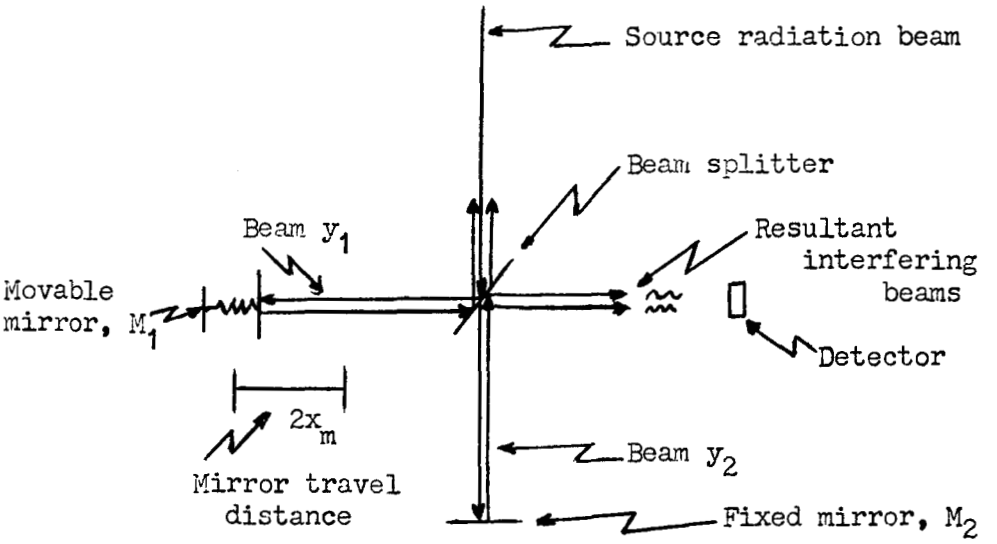

Fig. 1

Consider an incoming radiation beam of wave number, v_o. This beam is divided, by the beam splitter, into two beams,

y_1 and y_2. Beam y_1 is reflected to the movable mirror, M_1, and by M_1 back to the beam splitter, where it is again divided into two components. One of these components is reflected by the beam splitter back in the direction of the source, and the other is transmitted through the beam splitter toward the detector. Beam y_2 follows a path to the fixed mirror, M_2, and is also reflected back to the beam splitter, where it, also, is divided into two components. One of the latter is transmitted back toward the source, the other is reflected toward the detector. Interference is produced by the two beams arriving at the detector due to their respective optical path distances; when the traversed distances are equal, the beams are in phase. Thus, the state of interference at the detector is a fuction of path difference between the two interfering beams, and consequently, of the position of the movable mirror, M_1.

The superposition of two beams of constant amplitudes, a_1 and a_2, and the same angular frequency, w_o, yields a resultant of constant amplitude, A, and constant phase, φ, [5]. To see this, let y_1 and y_2 be given by

$$y_1(t) = a_1 \sin(w_o t - \alpha_1), \text{ and}$$
$$y_2(t) = a_2 \sin(w_o t - \alpha_2), \qquad (1)$$

where a_1, α_1 and a_2, α_2 are the amplitude and phase, respectively, for y_1 and y_2. Then, the resultant, y, is

$$y = y_1 + y_2$$
$$= a_1 \sin(w_o t - \alpha_1) + a_2 \sin(w_o t - \alpha_2)$$

$$= (a_1 \cos(\alpha_1) + a_2 \cos(\alpha_2)) \sin(w_o t)$$
$$- (a_1 \sin(\alpha_1) + a_2 \sin(\alpha_2)) \cos(w_o t)$$
$$= A \sin(w_o t - \varphi), \text{ where} \qquad (2)$$

$$A \cos(\varphi) = (a_1 \cos(\alpha_1) + a_2 \cos(\alpha_2)), \text{ and}$$
$$A \sin(\varphi) = (a_1 \sin(\alpha_1) + a_2 \sin(\alpha_2)). \qquad (3)$$

A can be found by squaring and adding equations (3):

$$A^2 = a_1^2 + a_2^2 + 2a_1 a_2 \cos(\alpha_1 - \alpha_2), \qquad (4)$$

and φ is found from

$$\tan(\varphi) = (a_1 \sin(\alpha_1) + a_2 \sin(\alpha_2))/(a_1 \cos(\alpha_1) + a_2 \cos(\alpha_2)). \qquad (5)$$

Thus, for a given w_o, it is seen that A and φ of equation (2) are constant, and can be found from equation (4) and (5), respectively.

If the incoming beam is split in half, i.e., if $a_1 = a_2 = a$, equation (4) becomes

$$A^2 = 2a^2(1 + \cos(\alpha_1 - \alpha_2)). \qquad (6)$$

Since the intensity, I', of the beam is proportional to the square of its amplitude, we can write

$$I' = A^2 = (B/2)(1 + \cos(\alpha_1 - \alpha_2)), \qquad (7)$$

where $B = 4a^2$.

The difference in phase of the two split beams, however, depends upon path difference, δ, and wave number, v_o. Consequently, equation (7) can be expressed as

$$I'(v_o, \delta) = (B/2)(1 + \cos(2\pi v_o \delta)), \qquad (8)$$

where B/2 is the intensity of the original beam.

Extending (8) over all positive wave numbers, v, and integrating with respect to v, equation (8) becomes

$$I'(\delta) = \tfrac{1}{2} \int_0^\infty B(v,T)(1 + \cos(2\pi v\delta))\, dv, \qquad (9)$$

where B is a function of wave number, v, and temperature, T. Hereafter, the constant component, $\frac{1}{2}\int_0^\infty B(v,T)\, dv$, is disregarded, and equation (9) is taken to be, [1] :

$$I(\delta) = \int_0^\infty B(v,T) \cos(2\pi v\delta)\, dv. \qquad (10)$$

Equation (10) is the equation of the "pure" interferogram, where B(v,T) is the spectral profile, and δ is defined over the range $(-\infty, \infty)$. Taking the range of path difference to be infinite is, of course, impossible, since the movable mirror must traverse a finite distance, $(-x_m, x_m)$; therefore, correspondingly, the effective path difference, δ, is restricted to the range $(-x_I, x_I)$. (The effect of this finite path difference limitation is discussed in 2.3.2.) Then, as δ varies from $-x_I$ to x_I, time, t, varies from $-\tau/2$ to $\tau/2$, and the distance traveled by the movable mirror is $2x_m$ (note that $x_I = 2x_m$). Thus, the effective optical path difference can be expressed as

$$\delta = V_I t = 2V_m t, \qquad (11)$$

where V_I and V_m are the constant velocities of the image and the mirror, respectively. Also,

$$\delta_{max} = V_I \tau/2 = V_m \tau = 2x_m = x_I, \quad -\tau/2 \leq t \leq \tau/2. \qquad (12)$$

Equation (10), then, becomes

$$I(t) = \int_0^\infty B(v,T) \cos(4\pi v V_m t)\, dv, \quad -\tau/2 \leq t \leq \tau/2. \qquad (13)$$

Now, let $B(v_i,T_k)$ be the function defined by

$$B(v_i,T_k) = \begin{cases} 0, & v_i < v_{min} \\ B(v_i,T_k), & v_{min} \leq v_i \leq v_{max} \\ 0, & v_{max} < v_i, \end{cases} \tag{14}$$

where $i = 0,1,2,\cdots, N$, and $B(v_i,T_k)$ is obtained for each temperature, T_k, $k = 1,2,\cdots,K$, by means of the Planck Blackbody Function:

$$B(v_i,T_k) = C_6 v_i^3 (\exp\{C_2 v_i/T_k\} - 1)^{-1}, \tag{15}$$

where $C_6 = 2hC_2 = 1.1909 \times 10^{-12}$ watt cm^2 $ster.^{-1}$; and $C_2 = hC/L = 1.4380$ cm ^oK; h is Planck's constant, L the Boltzman constant, C the velocity of light, T_k the temperature in degrees Kelvin, and v_i the wave number in cm^{-1}.

In order that the bias due to the instrument temperature be removed, the spectral profile is taken to be

$$B(v_i,T_k) = B_I(v_i,T_k) - B_{TG}(v_i,T_k), \tag{16}$$

where B_I is the blackbody intensity due to the instrument temperature, and B_{TG} is the target intensity..

Equation (13) can be approximated by the sum

$$I(t_j) = \Delta v \sum_{i=0}^{N} B(v_i,T_k) \cos(4\pi v_i V_m t_j), \tag{17}$$

where $v_i = v_{min} + i(\Delta v)$, for each

$$t_j = j(\Delta t),\ j = -M, -M+1,\cdots,0,1,\cdots,M.$$

Since (17) is symmetric about $t_j = 0$, $I(t_j)$ may be obtained by computing (17) for $j = 0,1,2,\cdots,M$, and reflecting $I(t_j)$, for all $j \neq 0$, to obtain $I(t_{-j})$. If, also, the time origin is translated such that the interferogram is defined over the

interval $t = (0,\tau)$, that is, if we let $t' = t + \tau/2$, or $t = t' - \tau/2$, then equation (17) becomes

$$I(t_j') = \Delta v \sum_{i=0}^{N} B(v_i,T_k) \cos(4\pi v_i V_m (t_j' - \tau/2)), \text{ or}$$

$$I(t_j') = \Delta v \sum_{i=0}^{N} B(v_i,T_k) \cos(4\pi v_i V_m t_j') \cos(4\pi v_i V_m \tau/2)$$

$$+ \Delta v \sum_{i=0}^{N} B(v_i,T_k) \sin(4\pi v_i V_m t_j') \sin(4\pi v_i V_m \tau/2). \quad (18)$$

Equation (18) is now the equation of the "pure" digital interferogram. However, for the purpose of detailed analysis and comparison with the transformed spectral profile below, it is helpful to carry the mathematical representation one step further.

The maximum resolution obtainable, due to the finite path difference, [3], [5], (see, also, 2.3.2.2) is

$$(\Delta v)' = 1/2x_I = 1/4x_m, \quad (19)$$

and the resolving power, R, obtainable for a given wave number, v_o, is

$$R = v_o/(\Delta v)'. \quad (20)$$

Thus, using equations (11), (12), and (19), the velocity of the mirror, V_m, can be written as

$$V_m = 2x_m/\tau = x_I/\tau = 1/2(\Delta v)'. \quad (21)$$

Substituting (21) into(18), the equation of the interferogram becomes

$$I(t_j') = \Delta v \sum_{i=0}^{N} B(v_i,T_k) \cos(2\pi v_i j/(\Delta v)'(2M+1)) \cos(\pi v_i/(\Delta v)')$$

$$+ \Delta v \sum_{i=0}^{N} B(v_i,T_k) \sin(2\pi v_i j/(\Delta v)'(2M+1)) \sin(\pi v_i/(\Delta v)'). \quad (22)$$

Clearly, when $v_i/(\Delta v)'$ is a positive integer, or zero, the sine terms vanish and (22) reduces to

$$I(t_j') = \pm \Delta v \sum_{i=0}^{N} B(v_i, T_k) \cos(2\pi v_i j/(\Delta v)'(2M+1)). \qquad (23)$$

This occurs when $(\Delta v)'$ divides both v_{min} and $i(\Delta v)$, since $v_i = v_{min} + i(\Delta v)$. It will become apparent in the sequel that this Diophantine relationship is important in the computational process, and further, that it imposes a restriction on the use of the simulation model and the subsequent analysis of the synthesized data.

2.2 ANALYSIS OF THE INTERFEROGRAM

The spectral profile, $B(v,T)$, is the Fourier cosine transform of (10):

$$B(v,T) = 2 \int_{-\infty}^{\infty} I(\delta) \cos(2\pi v \delta)\, d\delta. \qquad (24)$$

Taking δ over the finite range $(-x_I, x_I)$, and substituting $\delta = 2V_m t$, and $d\delta = 2V_m dt$ into (24), we obtain

$$B(v,T) = 4V_m \int_{-\tau/2}^{\tau/2} I(t) \cos(4\pi v V_m t)\, dt. \qquad (25)$$

Substituting (21) into (25), applying the time-origin transformation, $t = t' - \tau/2$, and writing the integrals as summations, equation (25) becomes

$$B(v_i,T_k) = (2/((\Delta v)'(2M+1))) \cos(\pi v_i/(\Delta v)') \sum_{j=0}^{2M} I(t_j') \cos(X)$$
$$+ (2/((\Delta v)'(2M+1))) \sin(\pi v_i/(\Delta v)') \sum_{j=0}^{2M} I(t_j') \sin(X), \qquad (26)$$

where the argument, $X = 2\pi v_i j/((\Delta v)'(2M+1))$.

Equation (26), then, is the Fourier transform of equation (22), and its form is adaptable to digital algorithmic solution.

For the simulated data, assuming no phase shift, it would be sufficient to analyze only half the interferogram, using the cosine transformation. However, in practice, it is difficult to determine exact zero path difference, because the sampled center point will probably not occur exactly at $\delta = 0$. Further, it is possible that the interferogram is not symmetric about zero path difference due to optical misallignment, and for other reasons. It is, therefore, desirable to use a sine and cosine analysis over all the 2M+1 points.

Then, the spectral amplitude, $B^c(v_{i_a},T_k)$, may be calculated from

$$B^c(v_{i_a},T_k) = (a_{i_a}^2 + b_{i_a}^2)^{\frac{1}{2}}, \text{ where} \tag{27}$$

$$a_{i_a} = 2/((\Delta v)'(2M+1)) \sum_{j=0}^{2M} I(t_j') \cos(2\pi i_a j/(2M+1)), \text{ and} \tag{28}$$

$$b_{i_a} = 2/((\Delta v)'(2M+1)) \sum_{j=0}^{2M} I(t_j') \sin(2\pi i_a j/(2M+1)), \tag{29}$$

and where $i_a = v_i/(\Delta v)'$.

Equations (28) and (29) hold only for integral values of i_a.

For some purposes, it is convenient to observe the transformed spectral profile in terms of temperature, T_k, as a function of wave number, v_{i_a}. To accomplish this, it is necessary to calculate the inverse Planck blackbody values. However, $B(v_{i_a},T_k)$ may be positive or negative, according as i_a is even or odd, and as the original $B(v_i,T_k)$ of the synthesis

is positive or negative. Since the cosine coefficients preserve this polarity, it is sufficient to carry the sign of a_{i_a} over to B^c. Then, the correctly-signed spectral values may be expressed as

$$(\text{SIGNUM}(a_{i_a}))\ B^c(v_{i_a},T_k). \tag{30}$$

The temperature, T_k, for each $k = 1,2,\cdots,K$, may now be obtained from

$$T_k = C_6 v_{i_a}/(\ln(C_2 v_{i_a}^3/((\text{SIGNUM}(a_{i_a}))\ B^c(v_{i_a},T_k)) + 1)). \tag{31}$$

2.3 DISTORTION EFFECTS

In section 2.1, the "pure" interferogram was developed. It is the purpose of this section to discuss those effects which produce the principal distortions in the data.

2.3.1 THE FINITE SOLID ANGLE

It can be shown, [2], [5], that the total flux on the detector due to a monochromatic source of wave number, v_o, is given by

$$I_1(v_o,\delta) = B(v_o,T)\ S\Omega(\sin(\pi v_o \delta\Omega/2\pi)/(\pi v_o \delta\Omega/2\pi))\ \cos(2\pi v_o \delta(1-\Omega/4\pi)), \tag{32}$$

where S is the useful aperture area, and Ω is the admissable solid angle.

The $(\sin X)/X$ factor and the $\Omega/4\pi$ term in the cosine argument are perturbations caused by the oblique rays due to the finite solid angle. The former represents an amplitude modulation; the latter takes the form of a slight phase shift in path difference and amplitude modulation.

For the purpose of the IRIS simulation, S was normalized to unity, and since Ω is small (= $\pi/200$ steradians), $\Omega/4\pi$ was neglected in comparison to unity. Equation (32) then becomes

$$I_2(v_o,\delta) = \Phi(v_o,\delta)\ B(v_o,T), \text{ where} \tag{33}$$

$$\Phi(v_o,\delta) = (\sin(\pi v_o \delta \Omega/2\pi)/(\pi v_o \delta \Omega/2\pi))\ \cos(2\pi v_o \delta). \tag{34}$$

Integrating (33) over all desired, finite values of wave number, the equation of the interferogram is now

$$I_3(\delta) = \int_{v_{min}}^{v_{max}} \psi(v,\delta)\ B(v,T)\ \cos(2\pi v\delta)\ dv, \tag{35}$$

$$\text{where } \psi(v,\delta) = \sin(\pi v \delta \Omega/2\pi)/(\pi v \delta \Omega/2\pi). \tag{36}$$

The effect of the finite solid angle, Ω, on the transformed spectral profile is discussed in sections 2.3.2.1 and 2.3.2.2.

2.3.2 THE LIMITING FUNCTION FOR FINITE PATH DIFFERENCE

As previously discussed (section 2.1), the restriction of mirror travel to the finite distance, $(-x_m, x_m)$, restricts δ to the finite range $(-x_I, x_I)$. In order to examine the effect on the transformed spectral profile due to this finiteness, it is convenient to define the rectangular function, $D(\delta)$, in such a way that, for a single wave number, v_o, equation (35) takes the form

$$I_4(v_o,\delta) = D(\delta)\ \psi(v_o,\delta)\ B(v_o,T)\ \cos(2\pi v_o \delta), \tag{37}$$

where $D(\delta)$ is the rectangular function defined by

$$D(\delta) = \begin{cases} 1, & -x_I \leq \delta \leq x_I \\ 0, & \text{elsewhere.} \end{cases} \tag{38}$$

The effect of this limiting function on the transformed spectral profile is discussed in sections 2.3.2.1 and 2.3.2.2.

2.3.2.1 THE INSTRUMENT FUNCTION

By definition, the instrument function is the Fourier transform of the interferogram resulting from a monochromatic source. An extended spectral range, then, defines a sequence of instrument functions of the same form but of varying magnitudes.

Consider equation (37). Let $T_c(f(x))$ denote the Fourier cosine transform of $f(x)$, and let $f(x) * g(x)$ be the convolution of $f(x)$ with $g(x)$. Then, the transformed spectral component, $B^c(v_o,T)$, is obtained from

$$\begin{aligned} B^c(v_o,T) &= T_c(I_4(v_o,\delta)) \\ &= T_c(D(\delta)\ \psi(v_o,\delta)\ B(v_o,T)\ \cos(2\pi v_o\delta)) \\ &= T_c(D(\delta)) * T_c(\psi(v_o,\delta)) * T_c(B(v_o,T)\ \cos(2\pi v_o\delta)) \\ &= T_c(D(\delta)) * T_c(\psi(v_o,\delta)) * T_c(I(v_o,\delta)) \\ &= T_c(D(\delta)) * T_c(\psi(v_o,\delta)) * T_c(T_c(B(v_o,T))) \\ &= T_c(D(\delta)) * T_c(\psi(v_o,\delta)) * B(v_o,T) \\ &= H(v_o,\delta) * B(v_o,T), \end{aligned} \tag{39}$$

where $H(v_o,\delta) = T_c(D(\delta)) * T_c(\psi(v_o,\delta))$, and $I(v,\delta)$ is given by equation (10).

Thus, the transformed spectral component, $B^c(v_o,T)$, is the convolution of the observed (source) spectral component, $B(v_o,T)$, and the function, $H(v_o,\delta)$. $H(v_o,\delta)$ is the instrument function, and is the convolution of the (sin X)/X function, $T_c(D(\delta))$, and the rectangular function, $T_c(\psi(v_o,\delta))$. It can be seen that there is no loss in generality in extending the monochromatic

source to the desired finite spectral interval. However, it is also apparent that the effect of the internal instrumentation on the data must be studied in terms of the instrument function for each spectral "component", where the spectral "component" is itself a very small spectral interval.

2.3.2.2 APODIZATION AND SPECTRAL RESOLUTION

The (sin X)/X function, $T_c(D(\delta))$, has a disturbing effect on the data for some applications. This is caused by the side lobes (secondary maxima) of the (sin X)/X function. The process of minimizing this effect is known as apodization.

It is not the purpose here to give a thorough treatment to the topic of apodization--this is a subject for extended work on this project. Nevertheless, several significant points are in order.

Apodization is performed at the expense of a loss in spectral resolution [2]. After linear (viz., triangular) apodization, the maximum resolution obtainable, due to the finite path difference, is no longer (ref. equation (19))

$(\Delta\nu)' = 1/2x_I = 1/4x_m$, but rather,

$$(\Delta\nu)' = 1/x_I = 1/2x_m. \qquad (40)$$

For example, with a mirror travel distance, $x_m = 0.2$ cm. (as is the case for IRIS), $(\Delta\nu)' = 2.5\ cm^{-1}$ without apodization, and $(\Delta\nu)' = 5\ cm^{-1}$ with apodization.

The finite solid angle, Ω, also imposes a limitation on the spectral resolution, [1], [2], which can be expressed in

the form

$$(\Delta\nu)' = \nu\Omega/2\pi. \tag{41}$$

Again using IRIS as an example, and taking $\nu_{max} = 2000\ cm^{-1}$ and $\Omega = \pi/200$ ster., it is seen that the maximum resolution obtainable for this particular wave number, due to the finiteness of Ω, is $5\ cm^{-1}$. Therefore, in this case, the limiting instrumental resolution factor is the finite solid angle, rather than the finite path difference. On the other hand, if ν is taken to be, say, $500\ cm^{-1}$, $(\Delta\nu)' = 5/4\ cm^{-1}$, and the limiting resolution is no longer due to the finite solid angle.

2.3.3 NOISE AT THE DETECTOR

The signal-to-noise ratio, S/N, used here, [1], is the ratio of the peak (zero path difference amplitude of the interferogram of a blackbody for the maximum expected temperature) signal to the RMS value of the noise. The noise is expressed as

$$N(t_j) = x_j(sA_{max}/RMS), \tag{42}$$

where s is a scaling constant; A_{max} is the peak amplitude; the x_j are normally-distributed (pseudo) random numbers; and

$$RMS = \left(\sum_{j=0}^{2M} (x_j - \bar{x})^2/(2M+1) \right)^{\frac{1}{2}}, \text{ with} \tag{43}$$

$$\bar{x} = \sum_{j=0}^{2M} x_j/(2M+1). \tag{44}$$

The equation of the interferogram now takes the form

$$I_5(\delta) = I_3(\delta) + N(t), \tag{45}$$

where I_3 and N are given by equations (35) and (42), respectively.

2.3.4 DIGITIZING

Each interferogram sample of IRIS is digitized into an information word of nine bits (eight bits plus a flag bit). The dynamic range of the amplitudes in the neighborhood of zero path difference is so great, compared to the rest of the interferogram, that the equal distribution of all amplitudes over this digitizing range would be extremely ineffecient. Consequently, a switch in telemetry voltage gain is instituted, which, in effect, produces a division of the interferogram amplitude by ten when the amplitude exceeds, in absolute value, one tenth of the peak value (A_{max} of equation (42)). The flag bit is used to indicate this switch in gain.

The net result of this digitizing process is a mapping which sends every possible intensity value (+, -, and 0) onto one of $255 + 2(115) = 485$ voltage levels, but with a greater density of levels (or sensitivity) in the $\pm$ neighborhood of zero intensity. Due to the way in which voltage levels are assigned, there are $(2^9 - 1) - 485 = 511 - 485 = 26$ counts which are not utilized out of the possible 511.

The digitizing system is exemplified by the contents of Table 2, 3.1.1.

3.0 PROGRAM ANALYSIS

The calculation procedure for each program is discussed separately in the following sections: 3.1, The Interferogram Synthesis Program; and 3.2, The Interferogram Analysis Program. The computational procedure for each is exemplified by the accompanying flow charts, and detailed in the explanations of those flow charts. Program listings are included in Appendix B. The plot programs are not included here; however plots of the results of the sample problem are included in Appendix A.

The programs are written in FORTRAN II for an IBM-7094 (Mod. 2)/1401 combination. The core memory capacity of the 7094 computer used is 32K words. The interferograms are plotted on an EAI magnetic tape-driven plotter, and the reconstructed spectral profiles are plotted on the IBM-1401 printer.

3.1 THE INTERFEROGRAM SYNTHESIS PROGRAM

The purpose of the Synthesis Program is to simulate the output of the interferometer in the form of both (i) a digital sampled interferogram (which, in turn, serves as input to the Analysis Program); and (ii) a graphical display (see 6.1) of the interferogram. The various effects (ref. section 2.0) are applied in the order of their natural occurrence. These effects, in their application, are independent of each other, and any combination of them, for a given run, is possible by means of proper specification of the input parameters. Program notation is defined in Table 1.

TABLE 1

DEFINITION OF NOTATION

Mathematical Notation	Program Notation	Explanation
v	NU	Wave number
Δv	DELNU	Integration interval
$(\Delta v)'$	DNU	Resolution
v_{min}	NUMIN	Minimum wave number in spectrum
v_{max}	NUTOP	Maximum wave number in spectrum
v_1	NUONE	Minimum wave number for each constant interval of input spectrum
v_2	NUTWO	Maximum wave number for each constant interval of input spectrum
i	I	Index on wave number
M	ITOP	Maximum value of i
t'	TKEP	Time
j	J	Index on time
$2M+1$	JTOP	Maximum value of j
dt'	DT	Time increment
TI	TI	Instrument temperature
TG,T	TT,TG, TEMP	Target temperature
$B(v_i,T)$	BNU(I)	Blackbody intensity for wave number, v_i, and temperature, T
----	TTNEW	Target temperature corresponding to each interval, (NUONE, NUTWO)
$I(t'_j)$	XINTEN(J)	Interferogram intensity (amplitude) as a function of time samples, t'_j
$B_{TI}(v_i,T)$	BTI(I)	Blackbody intensity due to the temperature of the instrument

TABLE 1

DEFINITION OF NOTATION

(continued)

Mathematical Notation	Program Notation	Explanation
$B_{TG}(v_i,T)$	BTT(I)	Blackbody intensity of the target
s	SCALE	S/N scaling factor
$N(t_j')$	XNOISE(J)	Calculated noise as a function of time
V_m	V	Mirror velocity
π	PI	3.14159265
Ω	OMEGA	Solid angle of admission
A_{max}	PEAK	Peak signal for noise computation
$\bar{x}$	XBAR	Mean value of the noise
RMS	RMS	RMS of the noise
----	PEAK2	Digitizing divide level (=1/10 PEAK)
ΔD	DELD	Interval between digitizing levels
----	SCA(J)	Digitized (scaled) interferogram values
F	F	Transformed spectral interval desired for Analysis Program
I_o	ZEROIN	D. C. component (= 0.0)
a_{i_a}	APRIME(I)	Transformed cosine coefficients
b_{i_a}	BPRIME(I)	Transformed sine coefficients
K - 1	KCARDS	Number of input cards which follow the "basic" parameter card

3.1.1 CALCULATION PROCEDURE AND EXPLANATION OF FLOW CHART

The calculation procedure for the Synthesis Program is summarized in the form of the following explanation of the Flow Chart, 3.1.1.1, pg. 22.

BOX 1

The card input parameters are: SW1, SW2, SW3, SW4, NUMIN, NUTOP, DELNU, ITOP, JTOP, DT, TI, TT, KCARDS, and SCALE. All of these appear on the first card. If KCARDS has a negative, or zero, value (see BOX 3 below), this is the only parameter card required for one interferogram (a simple, blackbody target). If additional spectral structure is required, KCARDS must specify the number of spectral components (in addition to the basic component specified on the first card) and consequently, the number of cards to follow the first card. Each of these latter cards must contain the target temperature, TTNEW, and the desired wave number interval, (NUONE, NUTWO), for each of the additonal spectral components. (See the sample problem for examples of the card images).

BOX 2

Necessary program initialization is performed.

BOX 3

The desired spectral profile, $B(\nu_i, T_k)$, is computed in accordance with the input parameters and equations (15) and (16). If more than a simple blackbody target is desired, one of the spectral intervals (usually, the longest, but not nec-

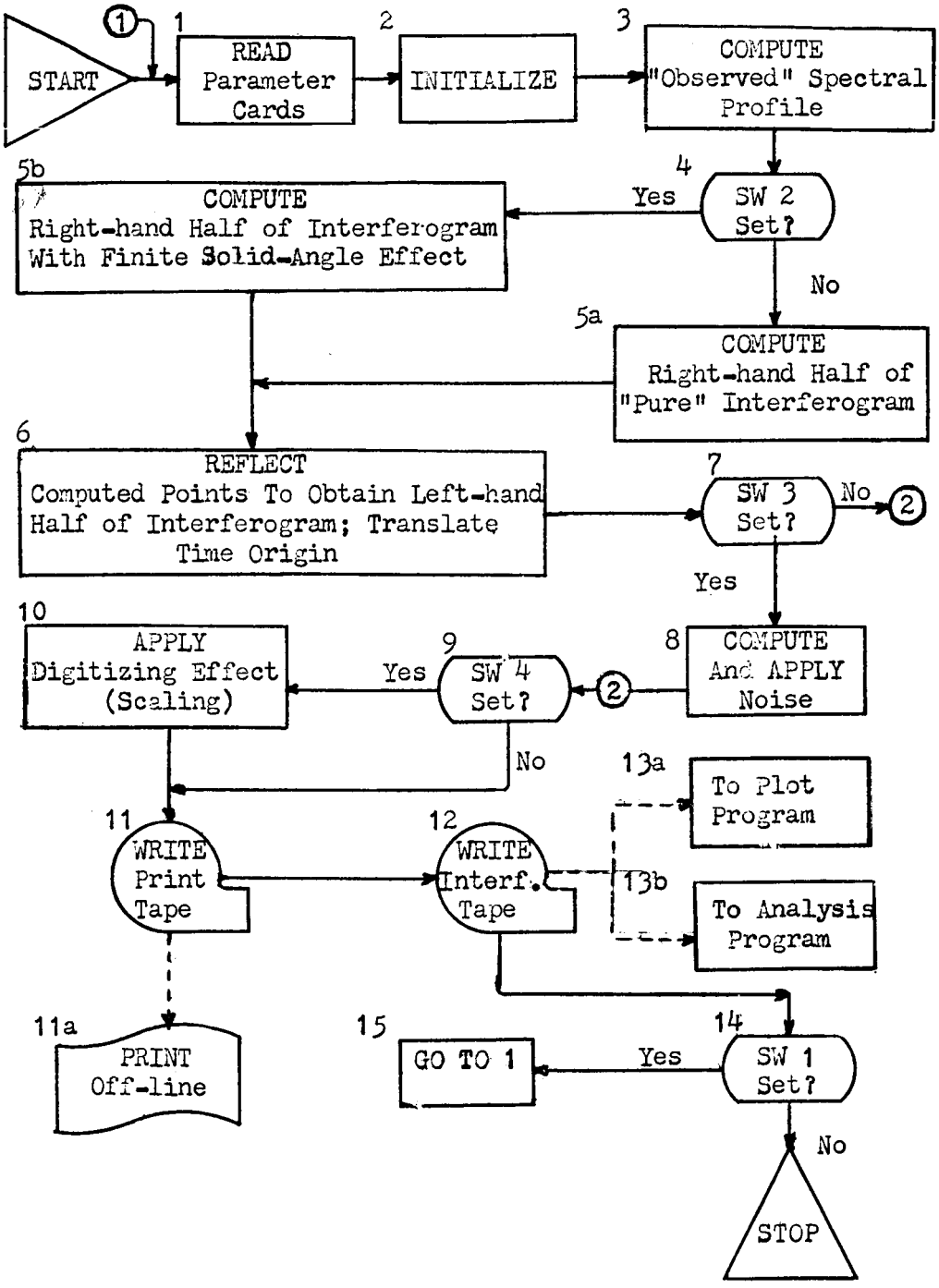

3.1.1.1 FLOW CHART, SYNTHESIS PROGRAM

essarily) and its corresponding target temperature, must be selected as the basic component over the entire spectral range, (NUMIN, NUTOP). This, then, is specified on the first parameter card. The remaining spectral components, determined by the contents of the KCARDS, are superimposed on the basic spectrum, prior to the calculation of the composite spectrum, by the program.

BOX 4

SW2 is the "(sin X)/X switch". If SW2 is a non-zero, positive value, the interferogram is computed with the Finite Aperture Effect included (BOX 5b). Otherwise, the "pure" interferogram is computed (BOX 5a).

BOX 5a

The "pure" interferogram is computed in accordance with equation (17), for $j = 0,1,2,\cdots,M$.

BOX 5b

The right-hand half of the interferogram, including the Finite Solid-Angle Effect, is computed (see equation (35)) according to the following:

$$I_3(t_j) = \Delta v \sum_{i=0}^{N} \psi(v_i,t_j)\, B(v_i,T_k) \cos(4\pi V_m v_i t_j), \qquad (46)$$

where the parameters are as previously defined.

BOX 6

The computed points of the right-hand half of the interferogram are reflected to produce the entire interferogram, which is symmetric about $t_j = 0$ (ref. pg. 8). Then, the time

origin is translated to the extreme left, such that t_j' is defined over the range $(0,\tau)$.

BOX 7

SW3 is the "noise" switch. If SW3 is set to a non-zero, positive value, noise at the detector is calculated and applied to each point of the interferogram (BOX 8). Otherwise, the program jumps the noise computations and proceeds to BOX 9.

BOX 8

Noise is calculated and applied in accordance with the procedures noted below and the equations of section 2.3.3. Rectangular (pseudo) random numbers, x_p', $p = 1,2,\cdots,P'$, are computed by means of the relationship

$$x_{p+1}' = Kx_p' \pmod{2^P}, \text{ where} \tag{47}$$

x_p' is the pth random number; x_{p+1} is the p+1 st random number; K is a constant(the largest power of five which will fit the computer's word length); and P is the number of bits per computer word.

It is known, [7], that the set of rectangular random numbers, $\{x_p'\}$, can be given a near-normal distribution by forming the set, $\{x_j\}$, where

$$x_j = \sum_{p=1}^{P'} x_p', \text{ for each } j. \tag{48}$$

For this simulation, P' is taken to be 10. Thus, each random number, x_j, of the normally-distributed set, $\{x_j\}$, is the sum of ten rectangular random numbers, x_p'. The generation of the set, $\{x_j\}$, is accomplished by a FAP subroutine. The remainder

of the noise calculations is performed in FORTRAN.

BOX 9

SW4 is the "digitizing switch". If SW4 is a non-zero, positive value, the digitizing effect is applied, as described below, BOX 10. Otherwise, the program proceeds directly to BOX 11.

BOX 10

Table 2, below, exemplifies the actual IRIS digitizing process. Since the telemetry data format has not yet (at the

TABLE 2

TM INFO. WORD

GAIN BIT	INFO. BITS	DECIMAL COUNT	TM VOLTAGE	APPROX. INTENSITY
1	00000000	0	Not Encoded	---------
1	00000001	1	+31.750	0.73×10^{-2}
⋮				
1	01110011	115	+ 3.200	0.73×10^{-3}
0	00000001	1	+ 3.175	( )
⋮				
0	01111111	127	+ 0.025	( )
0	10000000	128	0.0	0.0
⋮				
0	11111110	255	- 3.175	-0.73×10^{-3}
1	10001101	141	- 3.200	( )
⋮				
1	11111111	255	-31.750	-0.73×10^{-2}

DIGITIZING PROCESS

TABLE 2

time of this writing) been definitely specified, the mapping illustrated by Table 2 is not carried to its final form here.

The digitizing effect is applied as detailed below.

Let I(J) represent the calculated interferogram amplitudes (by whatever logical program path this point was reached). Then, for all J such that

$$|I(J)| > |PEAK2| \text{ , for PEAK2 = PEAK/10,} \tag{49}$$

the I(J) are converted to the new amplitudes, I(J)/10, and those points involved are flagged. Thus, PEAK2 is the "divide threshold". A new interferogram, I*(J), results, such that

$$I^*(J) \leq |PEAK2| \text{, for all J.} \tag{50}$$

It is now necessary to map each of the points, I*(J), onto its appropriate digitizing level in the range (-PEAK2, PEAK2). This is accomplished by computing and rounding to the nearest integral value the numbers, SCA(J), where

$$SCA(J) = I^*(J)/(\Delta D), \text{ and where} \tag{51}$$

$$\Delta D = PEAK2/127.$$

Therefore, each of the (scaled) amplitudes, SCA(J), of the digitized interferogram is one of the numbers:

-127,-126,•••,-1,0,1,•••,126,127.

BOX 11

The output tape for printing includes: (i) all input parameters; (ii) the source spectral profile, $B(v_i,T_k)$; (iii) noise, if calculated; and (iv) the final interferogram, versus time.

BOX 12

The resultant interferogram, versus time, is written to

tape. If the digitizing effect has not been applied, the amplitudes are in standard floating point format (the time array always is, in any case). If digitizing has been applied, the amplitudes are of the form noted in BOX 10. Then, each amplitude word is contained in one 7094 36-bit word according to the following format:

```
Bit
Pos.  35/ ...26/25/24/23/22/21/20/19/18/ ...1/0
       S  ...  F  x  x  x  x  x  x  x  x  ...
```

Bit positions 18-25, inclusive, are reserved for the binary count designating the digitizing level. Bit position 26 is the divide (voltage gain) flag; a 1 in this position indicates that the original amplitude was divided by ten. The sign bit is carried in bit position 35. Thus, only seven of the eight positions, 18-25, are required, but this format will allow for easy conversion to the final telemetry word format, when required. (Note that the other bit positions are ignored.)

Intensity and time are written to this tape as separate arrays.

BOX 13a

The output tape, BOX 12, from the Synthesis Program is used as input to the Analysis Program.

BOX 13b

The same output tape, BOX 12, from the Synthesis Program is used as input to the Interferogram Plot Program.

BOX 14

SW1 is used if more than one interferogram is desired in

the same computer run. Setting SW1 to a non-zero, positive value causes the program to return to BOX 1 and read the next set of parameters. Otherwise, the program halts.

BOX 15

Return to BOX 1 and begin the next interferogram.

3.2 THE INTERFEROGRAM ANALYSIS PROGRAM

The purpose of the Analysis Program is to accept a digital interferogram from magnetic tape, transform those amplitudes to obtain the calculated spectral profile, $B^c(v_{ia},T_k)$, and then output the results for printing and plotting. In addition, since this program and its calculation procedure will be used as a basis for the final reduction program, computational efficiency is of primary concern (as opposed to the Synthesis Program which, because of anticipated limited use, employs no special computational algorithms to improve the efficiency and running time). The calculation procedure is explained in 3.2.1 and exemplified by the Flow Charts, 3.2.1.1 and 3.2.1.2.

3.2.1 CALCULATION PROCEDURE AND EXPLANATION OF FLOW CHARTS

The calculation procedure for the Analysis Program is detailed in the following explanation to Flow Charts 3.2.1.1 and 3.2.1.2. The former outlines the gross processing logic, and the latter is the detailed computational procedure employed in the algorithmic solution which produces the calculated spectral profile. Thus, the second Flow Chart is a detailed version of part of BOX 5 and all of BOX 6 of 3.2.1.1.

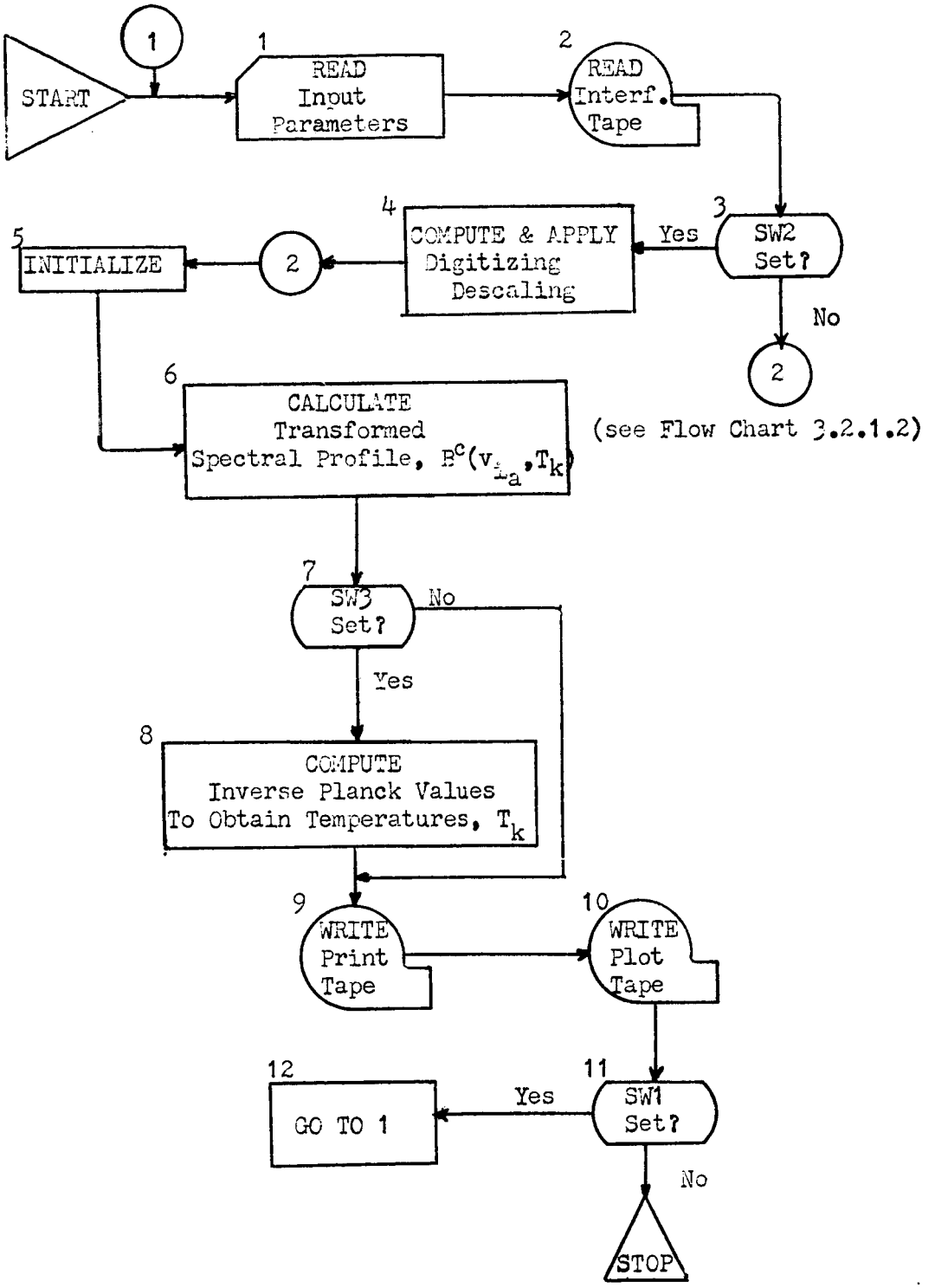

3.2.1.1 ANALYSIS PROGRAM FLOW CHART

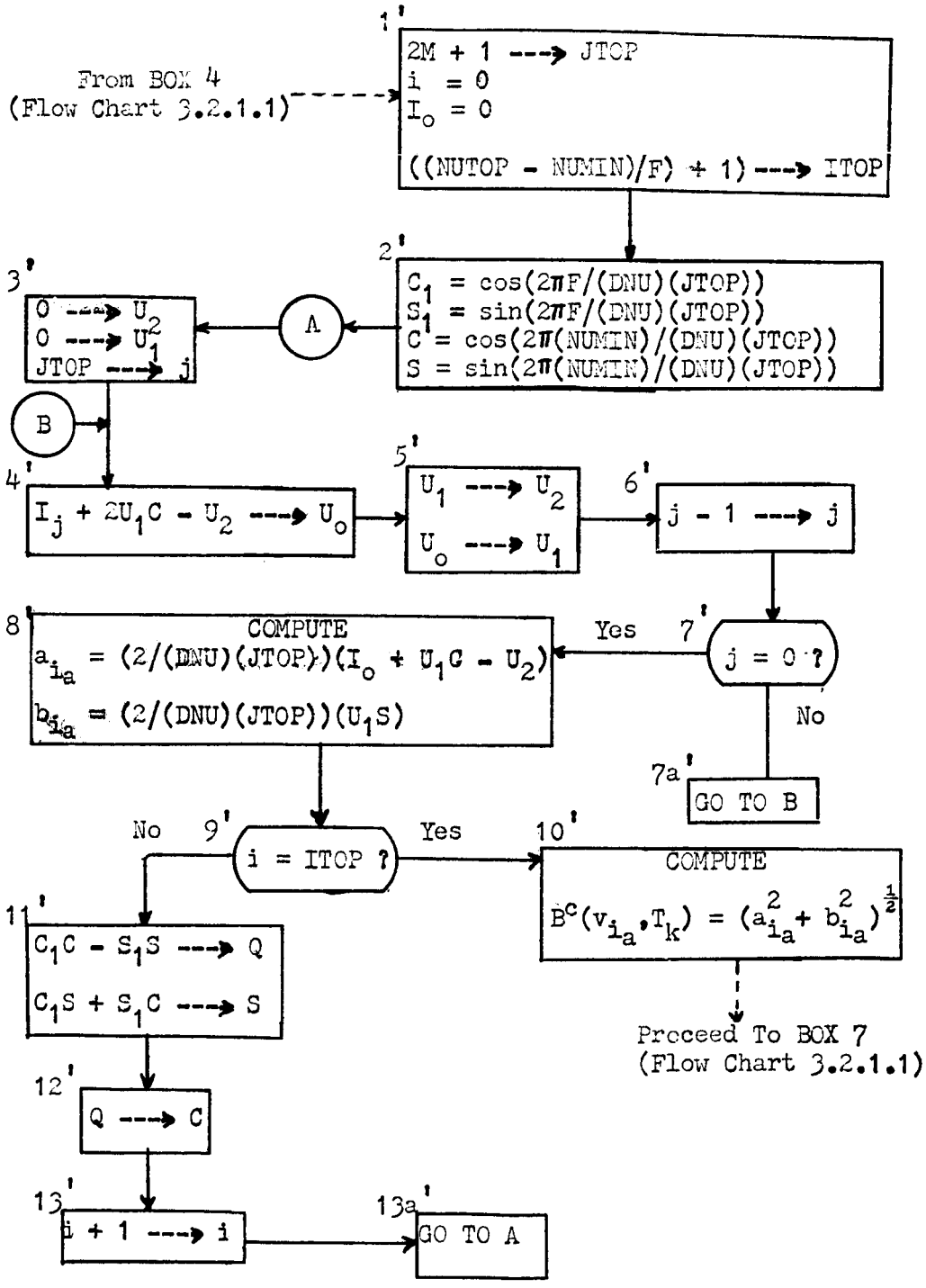

3.2.1.2 FOURIER TRANSFORMATION ALGORITHM FLOW CHART

BOX 1

The input parameters are: SW1, SW2, SW3, NUMIN, NUTOP, JTOP, DNU, F, and TI. (See the sample problem for examples of the card images.)

BOX 2

The digital interferogram is read into computer core memory from magnetic tape. This is the interferogram output tape of the Synthesis Program, and contains the time array, TKEP(J), as well as the array, I(J), (or XINTEN(J)). It should be noted that the time array, TKEP(J), is not required in the Analysis Program; however equivalent information is required, i.e., the total number of samples, 2M+1, and the time span, τ. TKEP(J) is put on the tape for the purpose of plotting time versus intensity. Operationally, of course, the time of each interferogram must be known in order to compute satellite position and instrument earth-coverage for each interferogram.

BOX 3

SW2 is the "digitizing descaling switch". That is, if the data have had the Digitizing Effect applied (setting of SW4 of the Synthesis Program), then SW2 of this program must be set to a non-zero, positive value to "descale" the data (BOX 4). Otherwise, the program proceeds directly to BOX 5.

BOX 4

Digitizing descaling consists of reconverting each of the numbers, SCA(J), (see 3.1.1, pg. 26) into an intensity

value by multiplying SCA(J) by ΔD, for each J, and then multiplying each of the flagged (indicating that a switch in gain, or divide by ten, was performed on that datum) values by ten. This procedure, as well as the conversion back to floating-point format, is accomplished by a FAP subroutine.

BOX 5,6

BOXES 5 and 6 accomplish the necessary initializtion and the sin/cos transformation which results in the calculated spectral profile. This procedure is detailed below and exemplified by Flow Chart 3.2.1.2.

A solution of equation (23) is sought in the form of equations (27), (28), and (29). It can be shown, [6], that this solution can be computed by means of the following algorithm:

$$a_{i_a} = (2/(\Delta v)'(2M+1))(I_o + U_{1i}\cos(2\pi i_a/(2M+1)) - U_{2i}), \qquad (52)$$

and

$$b_{i_a} = (2/(\Delta v)'(2M+1))(U_{1i}\sin(2\pi i_a/(2M+1))), \qquad (53)$$

where the U_{ji} are defined recursively by

$$U_{2M+2,i} = U_{2M+1,i} = 0$$
$$U_{ji} = I_j + 2U_{j+1,i}\cos(2\pi i_a/(2M+1)), \text{ for} \qquad (54)$$
$$j = 2M, 2M-1, \cdots, 1, 0, \text{ and } i = 0,1,2,\cdots,ITOP.$$

It is now possible to explain the previous statement (2.1, pg. 10) concerning the restriction on the use of the simulation model and the subsequent analysis of the data. Recall that (pg. 11) i_a was defined to be

$i_a = v_i/(\Delta v)' = (v_{min} + i(\Delta v))/(\Delta v)'$, for i = (0,N), and for those values of i only that produce integral values of i_a. The requirement that i_a be an integer is imposed by the time origin transformation, which resulted in equation (23), and by the Diophantine nature of the algorithm (54). Thus, for example, if it is desired to analyze the interferogram to a resolution of 2.5 cm^{-1}, the integration interval, Δv, cannot be chosen to be, say, $\Delta v = 1$ cm^{-1}. For then, $i(\Delta v)$ is not an integral multiple of $(\Delta v)'$ for every i = 0,1,2,•••,N. In this case, the minimum resolution which could be obtained from the Analysis Program would be 5 cm^{-1}.

It is now convenient to add one more refinement to the algorithm. In the event that the user does not wish to retrieve the spectral profile for every spectral component, in increments of the minimum resolution, the factor, F, is introduced. F is the "computational resolution", and must satisfy the condition that it is an integral multiple of $(\Delta v)'$. That is,

$$i_a = (v_{min} + i(\Delta v)F)/(\Delta v)' \qquad (55)$$

must still be an integer, for all i_a. The upper limit, ITOP, of the range of i (equations (54)), then, is determined by

$$ITOP = ((NUTOP - NUMIN)/F) + 1. \qquad (56)$$

It should be noted that the program, in iterating on i, employs the trigonometric identities for the sine and cosine of the sum of two angles, over the range of v = (NUMIN, NUTOP), in increments of F. That is, Δv of equation (55) is taken to

be unity, and the observance of the above restriction is left to the discretion of the user. Then, the ith iteration produces the sine and cosine of

$2\pi(v_{min} + iF)/(\Delta v)'(2M+1)$, $i = 0,1,2,\cdots,ITOP$,

$= (2\pi v_{min}/(\Delta v)'(2M+1)) + (2\pi iF/(\Delta v)'(2M+1))$

$=$ ARG1 + ARG2.

Therefore,

$\cos(ARG1 + ARG2) = \cos(ARG1)\cos(ARG2) - \sin(ARG1)\sin(ARG2)$,

and

$\sin(ARG1 + ARG2) = \sin(ARG1)\cos(ARG2) + \sin(ARG2)\cos(ARG1)$.

BOX 7

SW3 is the "amplitude-to-temperature-conversion switch". If SW3 is set to a non-zero, positive value, the amplitudes are converted to blackbody temperatures, T_k. Otherwise, the program proceeds directly to BOX 9. In either case, the amplitudes, $B^c(v_{i_a},T_k)$ are included in the printout, BOX 9.

BOX 8

The amplitudes, $SIGNUM(a_{i_a})\ B^c(v_{i_a},T_k)$, are converted to blackbody temperatures, T_k, by means of the inverse Planck Function, equation (31).

BOX 9

The output for printing on the IBM-1401 is written to magnetic tape. The printed output consists of: a listing of the received interferogram values, I(J), all input parameters (BOX 1), I, NU(I), BNU(I) (or B^c), BPRIME(I), APRIME(I), BTT(I), and TEMP(I) (or T).

BOX 10

The arrays, BNU(I) and TEMP(I), are written to magnetic tape to be used as input to the plot program which formats the plots of temperature versus wave number for subsequent plotting on the IBM-1401 printer.

BOX 11, 12

SW1 is used if more than one interferogram is desired in the same computer run. Setting SW1 to a non-zero, positive value causes the program to return to BOX 1 and read the next set of input parameters. Otherwise, the program halts.

4.0 SAMPLE PROBLEM

A number of computer runs, on artificial spectra, with varying parameters, have been made to date. One of these is presented here as an example. Runs were made, using the same artificial spectrum, of the following interferograms; (i) "pure"; (ii) finite solid-angle effect only; (iii) with noise only; (iv) with digitizing effect only; and (v) with all effects. All other input parameters were held constant for these five cases. The sampling rate used was slightly more than four times the highest frequency present (3415 samples for the 10-second interferogram). The sixth run was made to include all effects at approximately half the sampling rate used above (1707 samples). Thus, run (vi) is identical, with respect to input parameters, to (v), except for sampling rate. Both Synthesis and Analysis runs were made for these six cases,

and the plotted output for each is included in Appendix A. In addition, an interferogram plot (run (vii)) for a monochromatic source, v = 650, with all effects, is included to illustrate the effect of the (sin X)/X fuction on the interferogram (no analysis output is included for this case).

The input parameters for run (v) are listed in 6.1.1 of Appendix A. Except for switch settings, this input is also valid for (i) - (iv), inclusive. As noted above, run (vi) is identical to (v), except for sampling rate.

Interferogram plots for the above seven cases are presented in sections 6.1.3 - 6.1.9, respectively, of Appendix A.

The transformed spectral profile, in the form of plots of temperature versus wave number, of cases (i) - (vi), inclusive, are shown in 6.1.10 - 6.1.15, respectively. These plots are made with a temperature resolution of one degree, and a spectral resolution of five wave numbers. Also shown on each plot, for comparison purposes, is the original, "observed" source spectrum.

In every case, the spectral range is taken over the interval, v = (251, 2000); the interferogram has a duration of 10 seconds; the instrument temperature is 270 ^{o}K; the input spectral profile is unchanged (except for (vii)); and the peak signal-to-noise ratio, S/N, is 1428 : 1 (SCALE = 0.0007).

5.0 RESULTS AND CONCLUSIONS

Experience to date with the programs has verified their effectiveness in the determination of instrument design and in forming the basis for operational data reduction.

The plot of the "pure" interferogram, 6.1.3, illustrates the large dynamic range in amplitude inherent in the undigitized interferogram. Concern over this problem led to the switch in voltage gain (or "division by ten") and the resulting digitization system previously described herein and in [1]. The gross effect of the digitizing process on the interferogram can be seen in 6.1.6; the effect on the transformed spectrum is apparent upon examination of 6.1.13.

As expected, the effect due to the signal-to-noise ratio at the detector is about the same as the effect due to digitizing. The peak signal-to-noise(RMS) initially calculated, [1], was on the order of 1000:1 to 2000:1. Computer runs made with varying S/N indicate that 1000:1 is the minimal tolerable threshold. A ratio of 2000:1 would allow excellent results in the transformed data. Comparison of the transformed spectral profiles for the "pure" case, 6.1.10, and the case which includes noise only, 6.1.12, illustrates the effect due to noise for this level(as previously noted, 1428:1).

The effect on the transformed data due to the finite solid angle, 6.1.11, appears to be the least of those effects studied. However, since the total instrument response in not included in the simulation, more effects on the actual data, in

addition to the presently-simulated effect, may be anticipated.

It may be concluded, then, that any improvement to the hardware system, in terms of the above effects, should first be made in the signal-to-noise ratio.

The improvement in the transformed spectral profile due to the doubling of the sampling rate has resulted in establishing this design criterion at the faster rate. A comparison of the effects of the two rates may be made from the examination of 6.1.8 and 6.1.15. In effect, the increase in sampling rate results in an extension of the usable spectral range by approximately 150-200 cm^{-1}, depending upon the S/N, and assuming a maximum tolerable error of about $\pm$ 2-3°K. Nevertheless, additional computer runs, utilizing more realistic (and finely-structured) input spectra, should be made and analyzed.

Finally, since the ratio of operational data reduction time to real (spacecraft acquisition) time is significant, the Analysis Program execution timing is of interest. Of course, for either program, execution time is a function of a number of variables, hence execution time for only one example is given here. For case (vi), that is, the interferogram with all effects included for 3415 samples, the IBM-7094 Synthesis Program execution time is approximately 18 minutes. For the transformation by the Analysis Program of that same interferogram, to a 5 cm^{-1} resolution across the entire spectral range, the execution time is approximately 1.2 minutes.

These times do not include the time for printing or plotting, and further, it must be recognized that additional "house-keeping" programming must be added to the current Analysis program in order to produce the operational data reduction program.

5.1 REFERENCES

1. Hanel, R. A. and Chaney, L., "The Infrared Interferometer Spectrometer Experiment (IRIS)", NASA X-650-64-204 (1964)

2. Connes, J., Recherches sur la Spectroscopie par Transformation de Fourier, "Rev. d'Opt.", Vol. 40, pp. 45, 101, 157, 213, (1961)

3. Strong, J., and Vanesse, G. A., Interferometric Spectroscopy in The Far Infrared, "J. Opt. Soc. Amer.", Vol. 49, pp. 844 (1959)

4. Lowenstein, E. V., On the Correction of Phase Errors in Interferograms, "App. Optics", Vol. 2, pp. 491 (1963)

5. Rense, W. A., and Willson, R. C., "The Theory, Design, and Development of An Interferometric Spectrometer", AFCRL-63-688 (1963)

6. Ralston and Wilf, Mathematical Methods for Digital Computers, pp. 258, Wiley (1960)

7. Hammer, C., "Monte Carlo Methods", Invited Lecture Series, Sponsored by The Washington, D. C. Chapter of A.C.M., UNIVAC (1963)

6.0 APPENDICES

The Appendix consists of two sections: Appendix A, 6.1, and Appendix B, 6.2. The contents of the former are listed below, and of the latter under 6.2, page 57.

6.1 APPENDIX A

The contents of Appendix A are as follows:

CONTENTS

NUMIN	NUTOP	DELNU	ITOP	JTOP
251	2000	1.0	1750	3415

DT	TI	TT	SCALE
.29282577E-02	250.0	275.0	.000700

SW1	SW2	SW3	SW4
-1.0	1.0	1.0	1.0

TTNEW = 225. NUONE = 251 NUTWO = 300

TTNEW = 300. NUONE = 301 NUTWO = 500

TTNEW = 260. NUONE = 501 NUTWO = 600

TTNEW = 269. NUONE = 601 NUTWO = 649

TTNEW = 320. NUONE = 650 NUTWO = 650

TTNEW = 269. NUONE = 651 NUTWO = 700

TTNEW = 271. NUONE = 701 NUTWO = 750

TTNEW = 200. NUONE = 751 NUTWO = 900

TTNEW = 300. NUONE = 901 NUTWO = 1100

TTNEW = 280. NUONE = 1101 NUTWO = 1149

TTNEW = 320. NUONE = 1150 NUTWO = 1150

TTNEW = 280. NUONE = 1151 NUTWO = 1200

TTNEW = 260. NUONE = 1201 NUTWO = 1399

TTNEW = 320. NUONE = 1400 NUTWO = 1400

TTNEW = 200. NUONE = 1700 NUTWO = 1700

6.1.1 SYNTHESIS PROGRAM INPUT PARAMETERS FOR C.M.

```
CARD
NO.
 1  -1+1+1+1 2512000 1017503415 29282577E-02250275 15    7000
 2  225 251 300
 3  300 301 500                                  CARD COL. NO. 56
 4  260 501 600
 5  269 601 649
 6  320 650 650
 7  269 651 700
 8  271 701 750
 9  200 751 900
10  300 9011100
11  28011011149
12  32011501150
13  28011511200
14  26012011399
15  32014001400
16  20017001700
    ↑
    CARD COL. NO. 1
```

SYNTHESIS PROGRAM

```
CARD
NO.
 1  -1+1+1 25120003415 25   5 250
    ↑                          ↑
    CARD COL. NO. 1            CARD COL. NO. 28
```

ANALYSIS PROGRAM

6.1.2 INPUT PARAMETER CARD IMAGES FOR CASE (v)

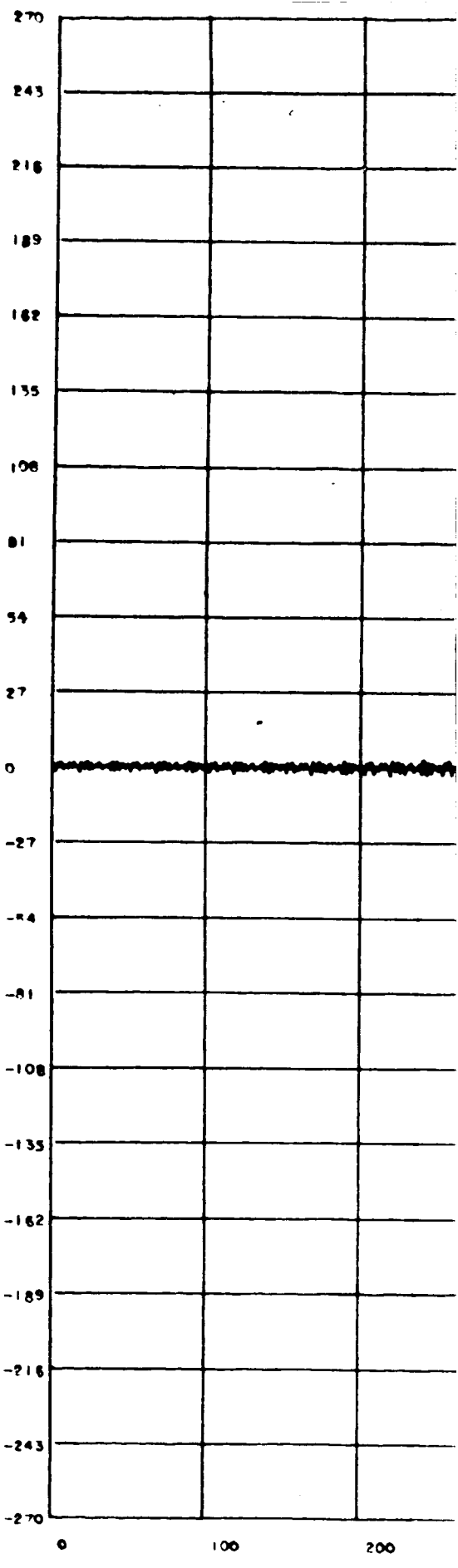
270
243
216
189
162
135
108
81
54
27
0
-27
-54
-81
-108
-135
-162
-189
-216
-243
-270
0
100
200

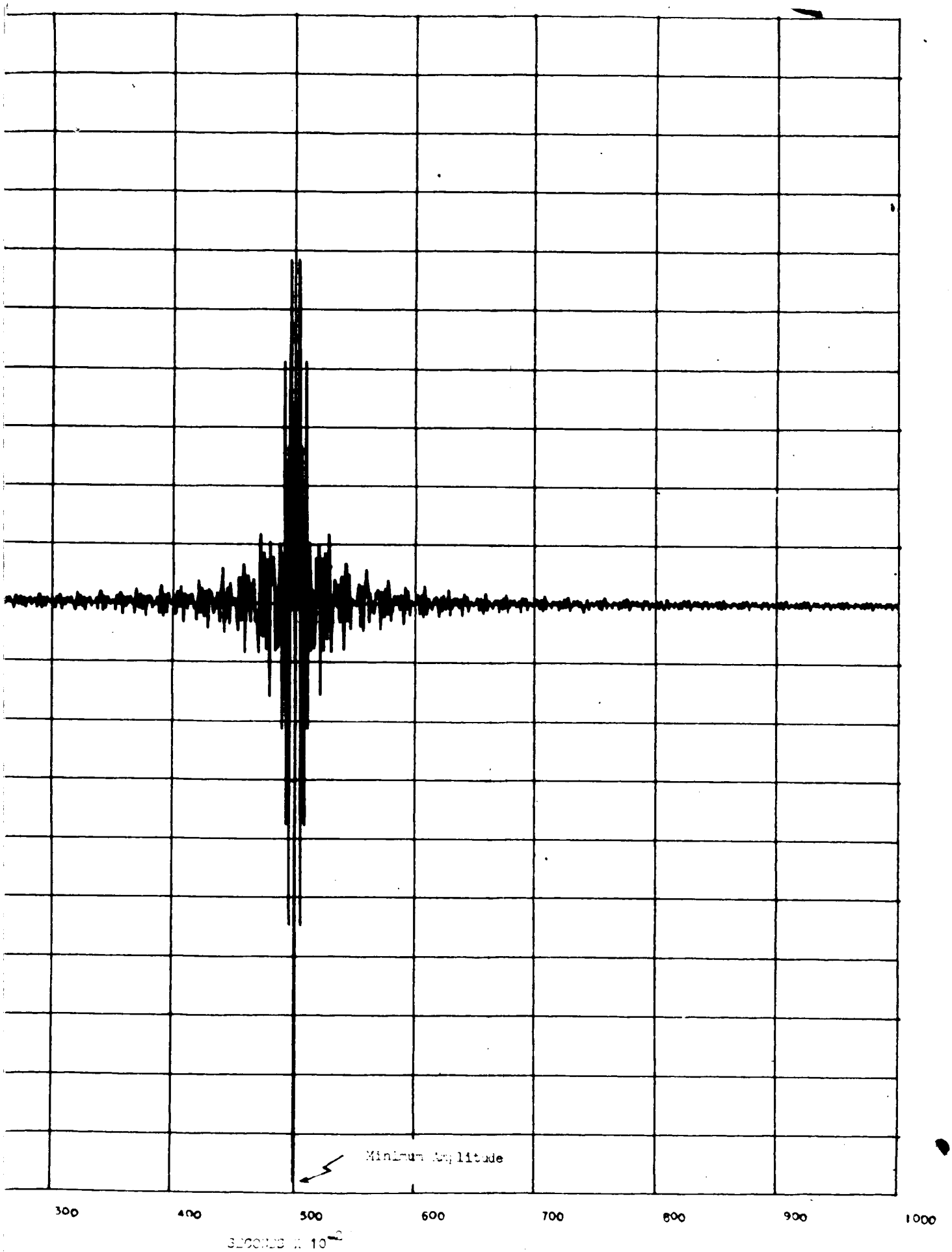

6.1.3 INTENSE NORM, CASE (1), ("PURE")

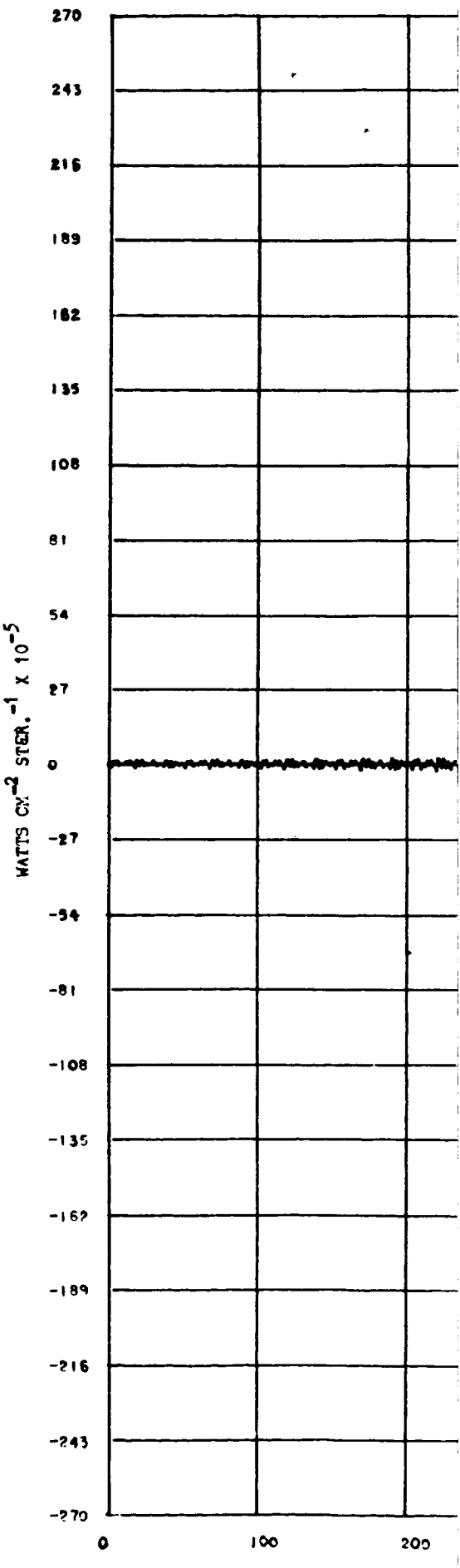
270
243
216
189
162
135
108
81
54
27
0
-27
-54
-81
-108
-135
-162
-189
-216
-243
-270
WATTS CM^{-2} STER.$^{-1}$ X 10^{-5}
0
100
200

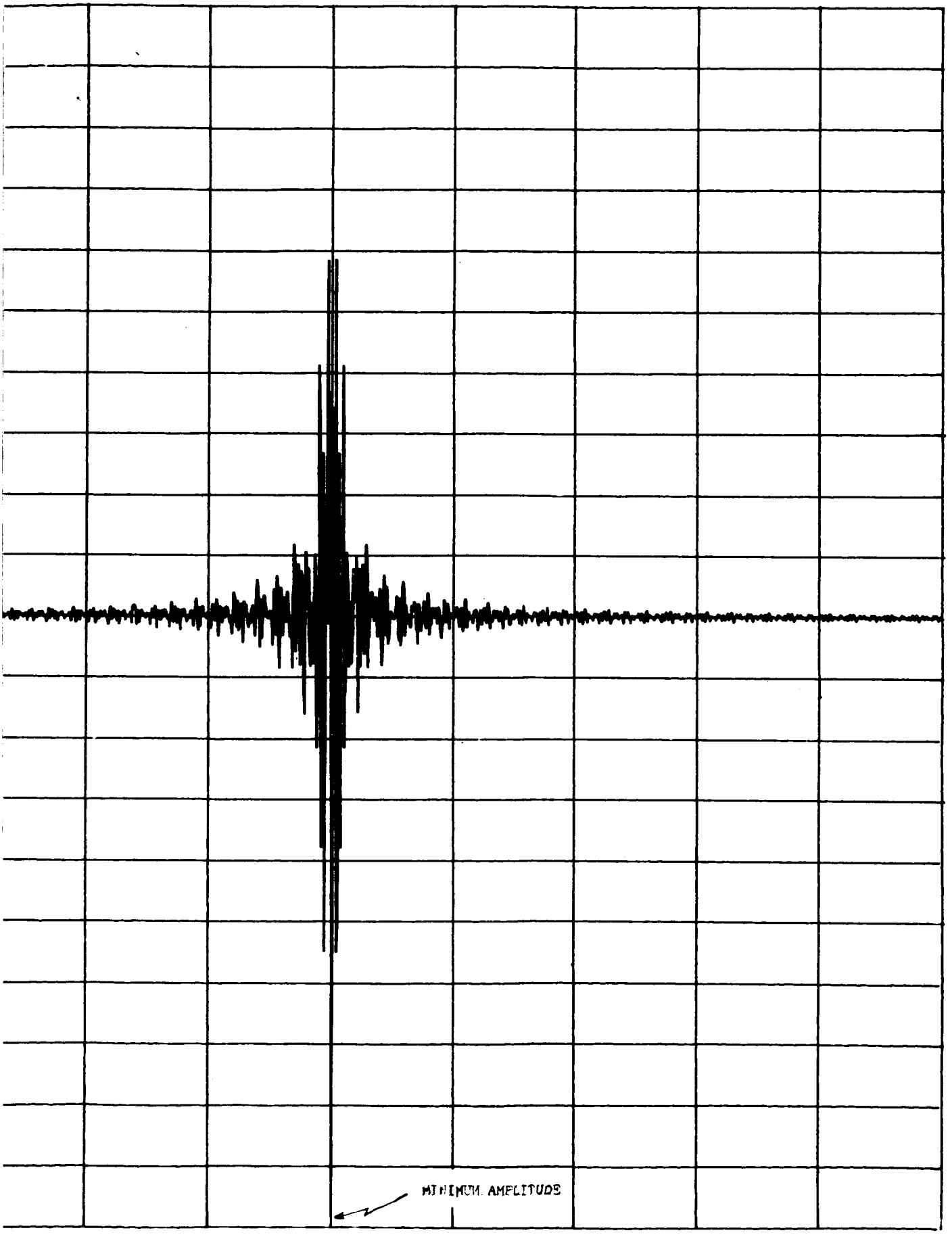

6.1.4 INTERFEROGRAM CASE (ii), (WITH FINITE SOLID ANGLE EFFECT)

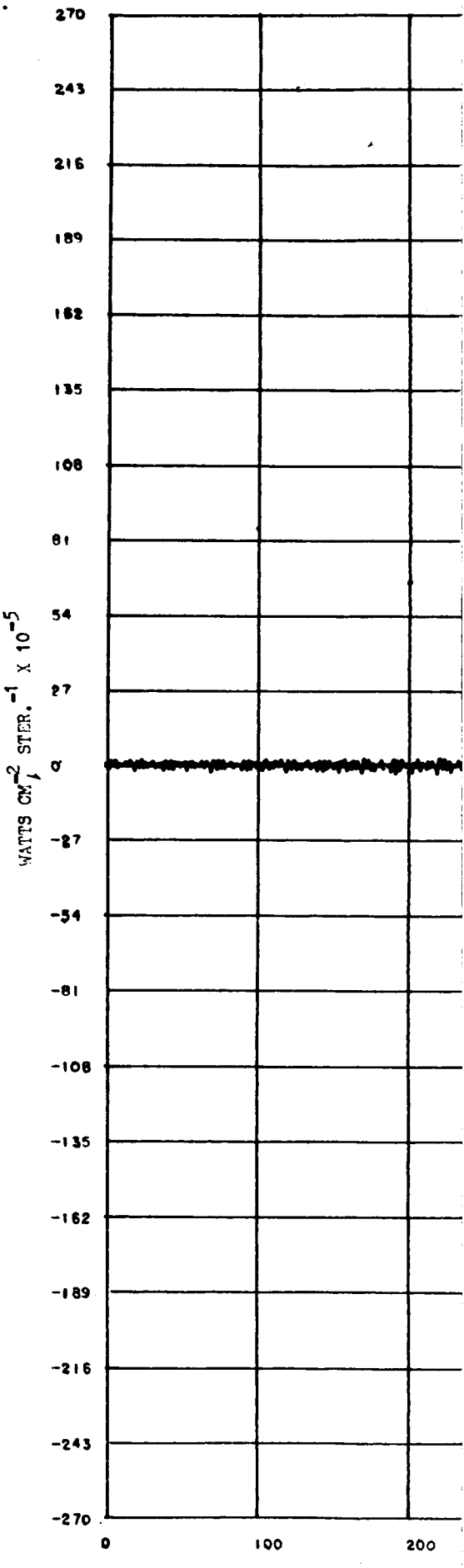
270
243
216
189
162
135
108
81
54
27
0
-27
-54
-81
-108
-135
-162
-189
-216
-243
-270
WATTS CM^{-2} STER.$^{-1}$ X 10^{-5}
0
100
200

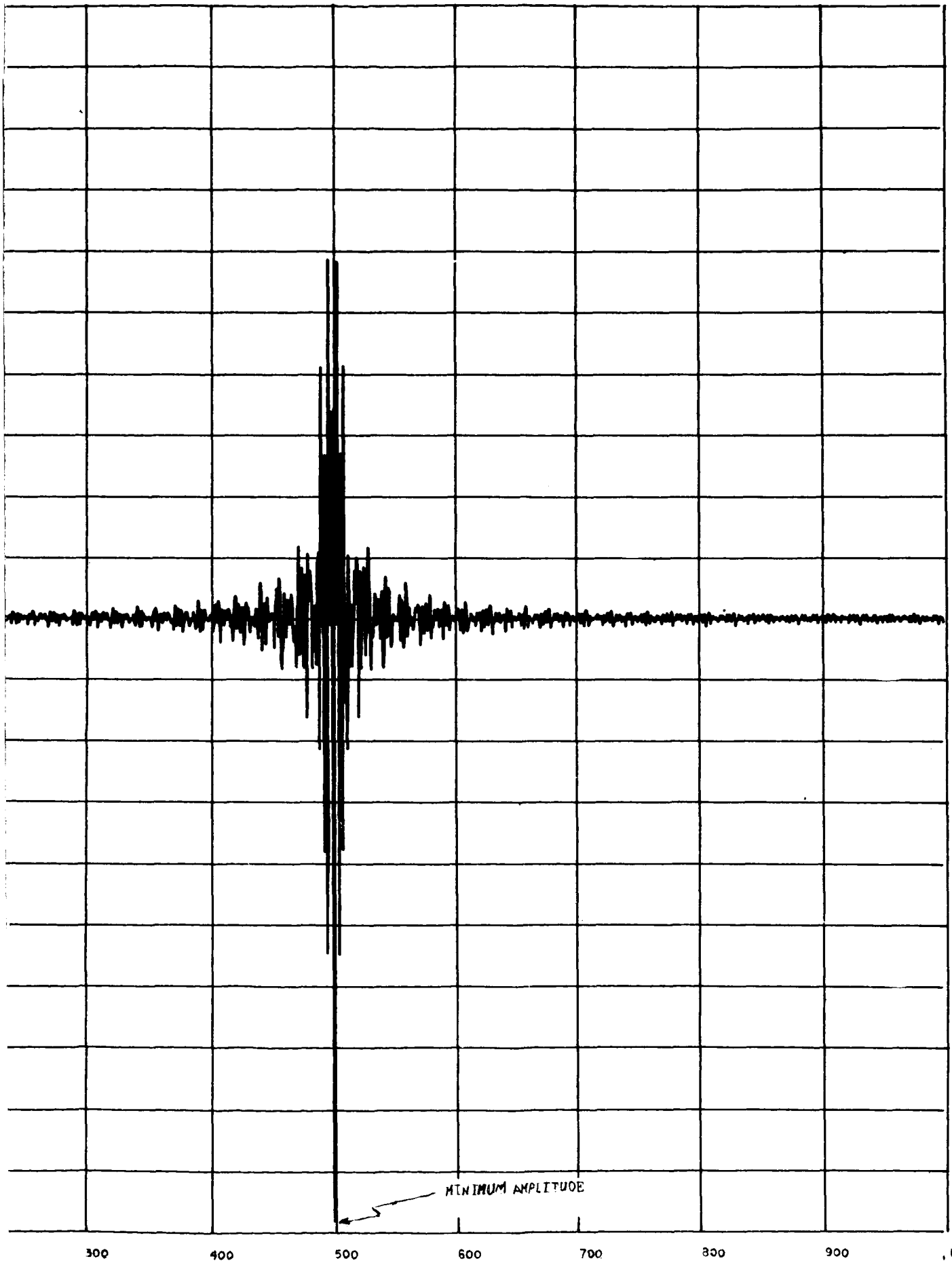

6.1.5 INTERFEROGRAM, CASE (iii), (WITH NOISE ONLY)

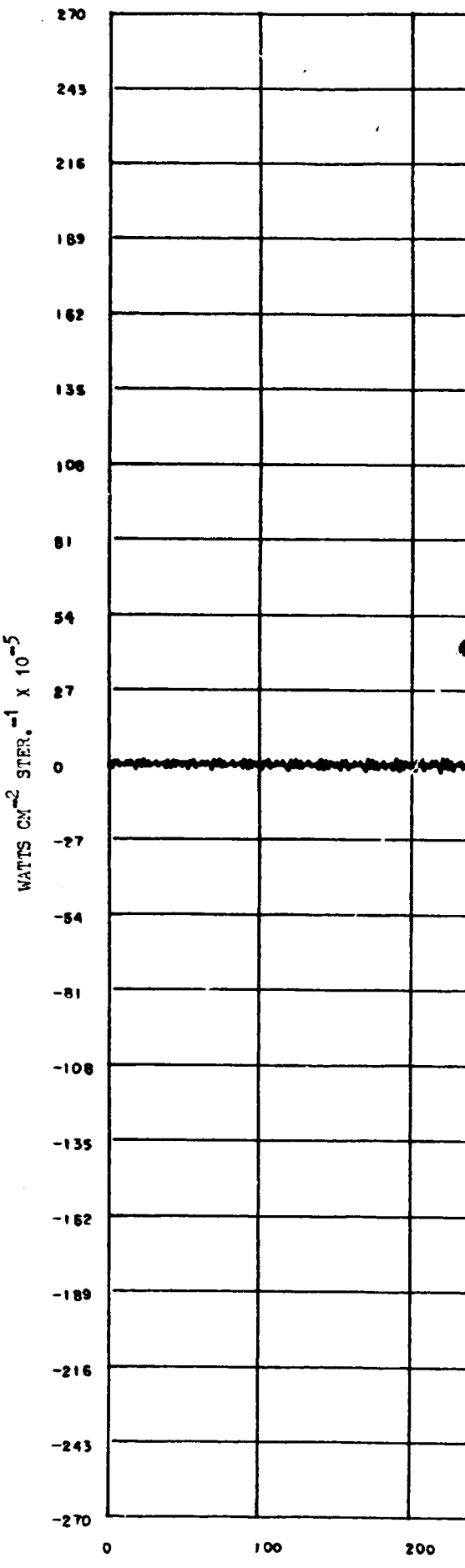
270
245
216
189
162
135
108
81
54
27
0
-27
-54
-81
-108
-135
-162
-189
-216
-243
-270
WATTS CM^{-2} STER.$^{-1}$ X 10^{-5}
0
100
200

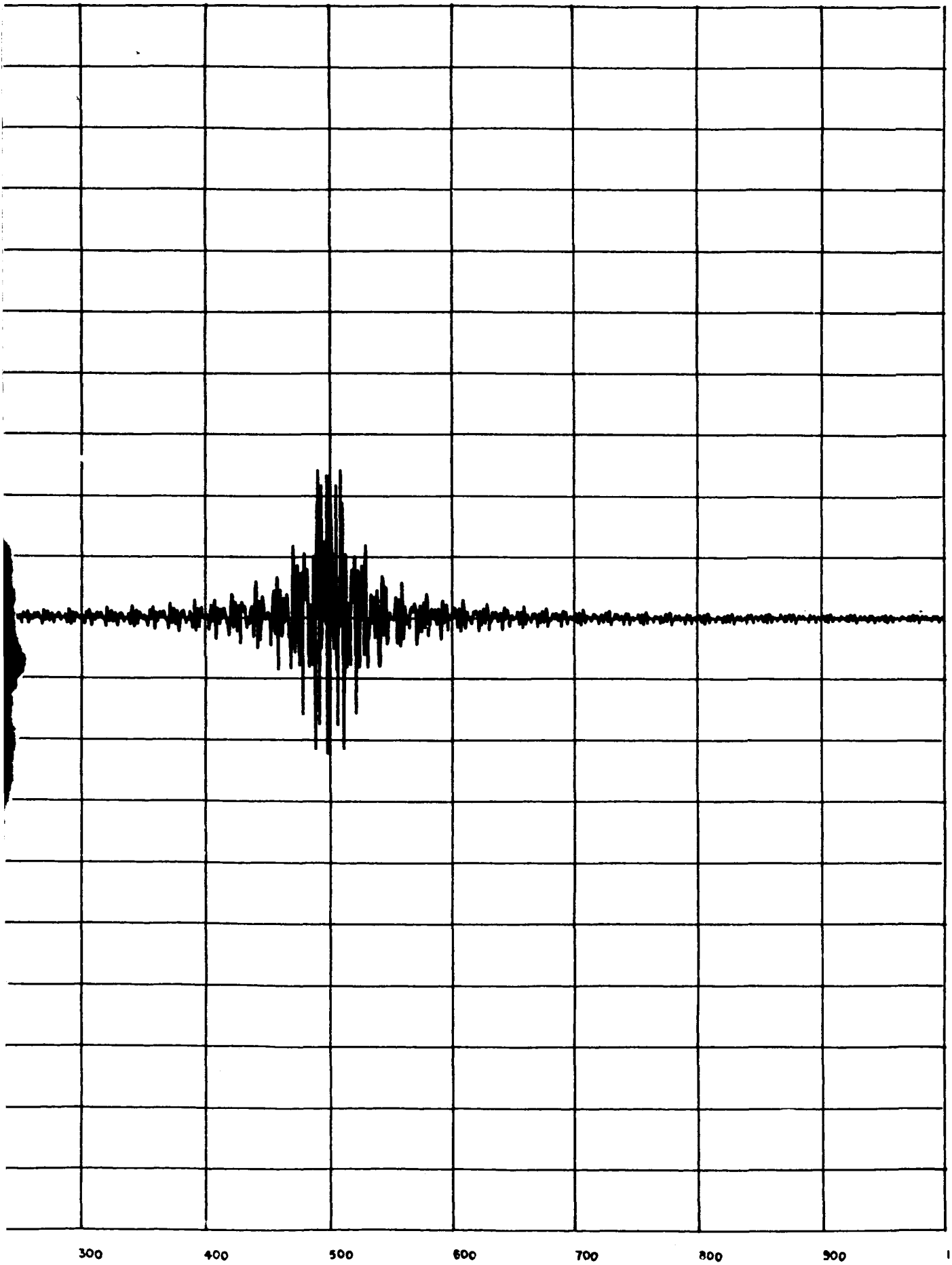

6.1.6 INTERFEROGRAM, CASE(iv), (DIGITIZING EFFECT ONLY)

270
243
216
189
162
135
108
81
54
27
0
-27
-81
-108
-135
-162
-189
-216
-243
-270
WATTS CM^{-2} STER.$^{-1}$ X 10^{-5}
0
100
200

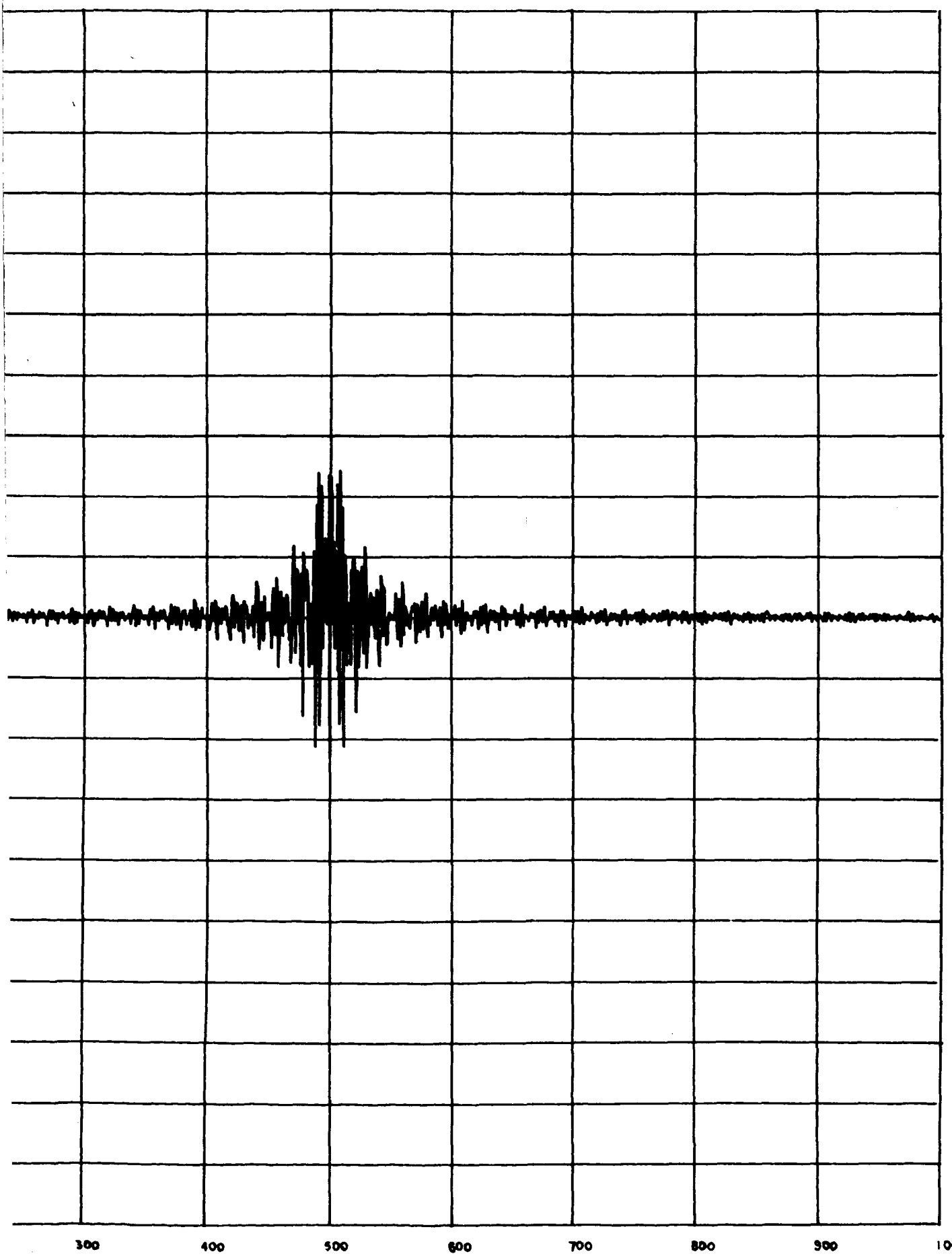

6.1.7 INTERFEROGRAM, CASE (v), (ALL EFFECTS)

2

270
243
216
189
162
135
108
81
54
27
0
-27
-54
-81
-108
-135
-162
-189
-216
-243
-270
WATTS CM^{-2} STER.$^{-1}$ X 10^{-5}
0
100
200

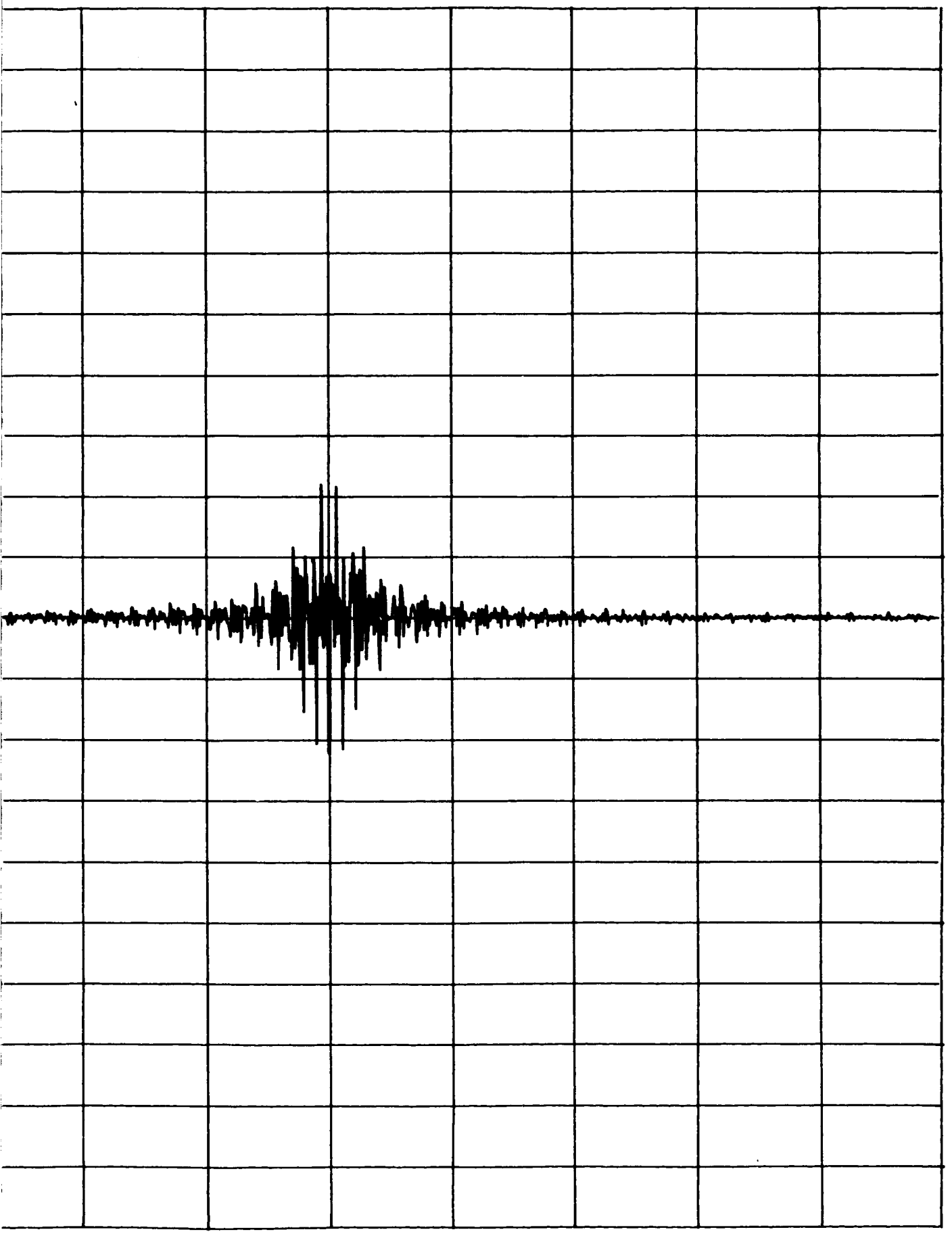

6.1.8 INTERFEROGRAM, CASE (vi), (ALL EFFECTS, SLOW SAMPLING RATE)

270
243
216
189
162
135
108
81
54
27
0
-27
-54
-81
-108
-135
-162
-189
-216
-243
-270
WATTS CM^{-2} STER.$^{-1}$ X 10^{-5}
0
100

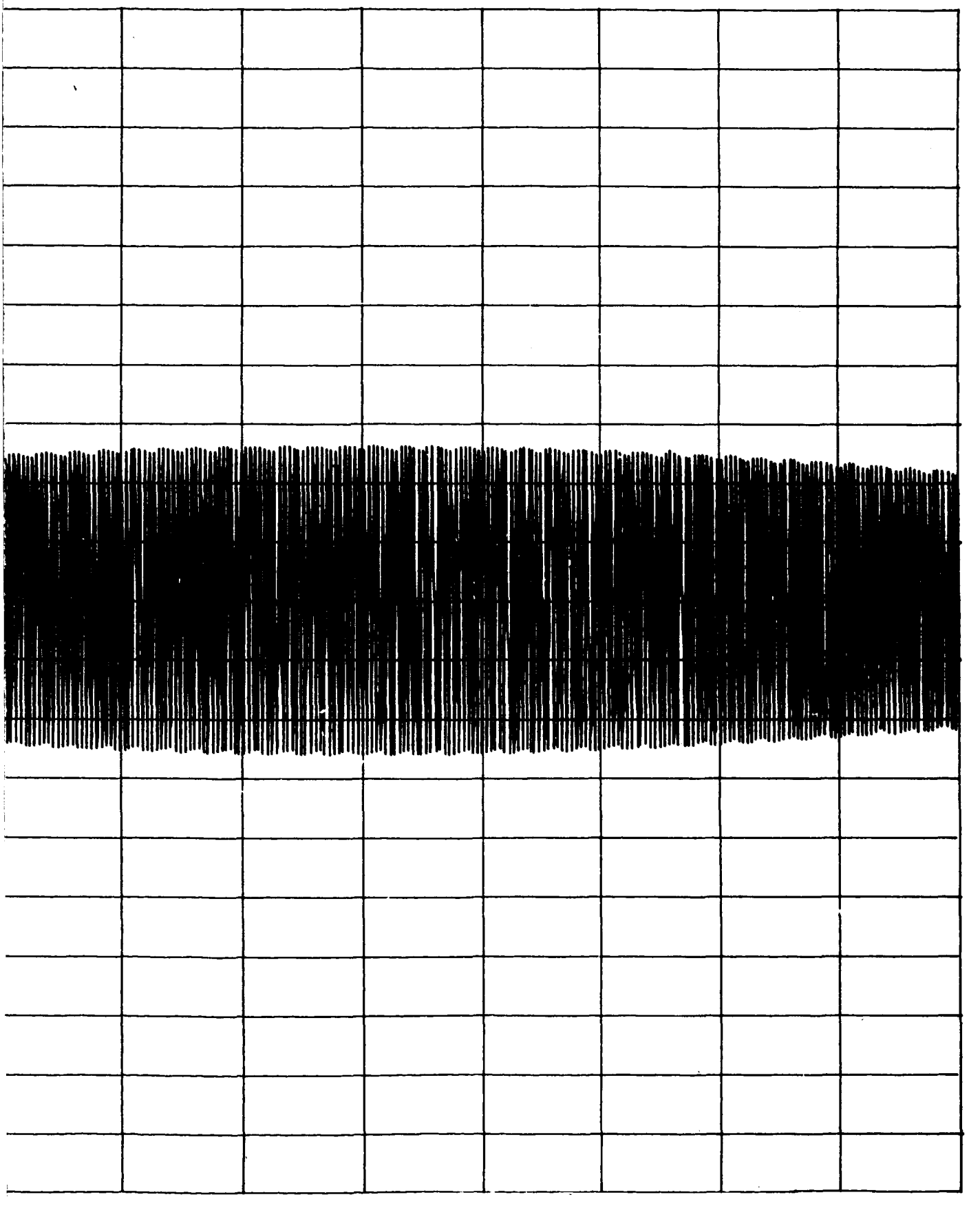

6.1.9 INTERFEROGRAM, CASE (vii), (FINITE SOLID-ANGLE EFFECT ONLY, $\nu = 650\ CM^{-1}$)

2000.00
1875.00

2

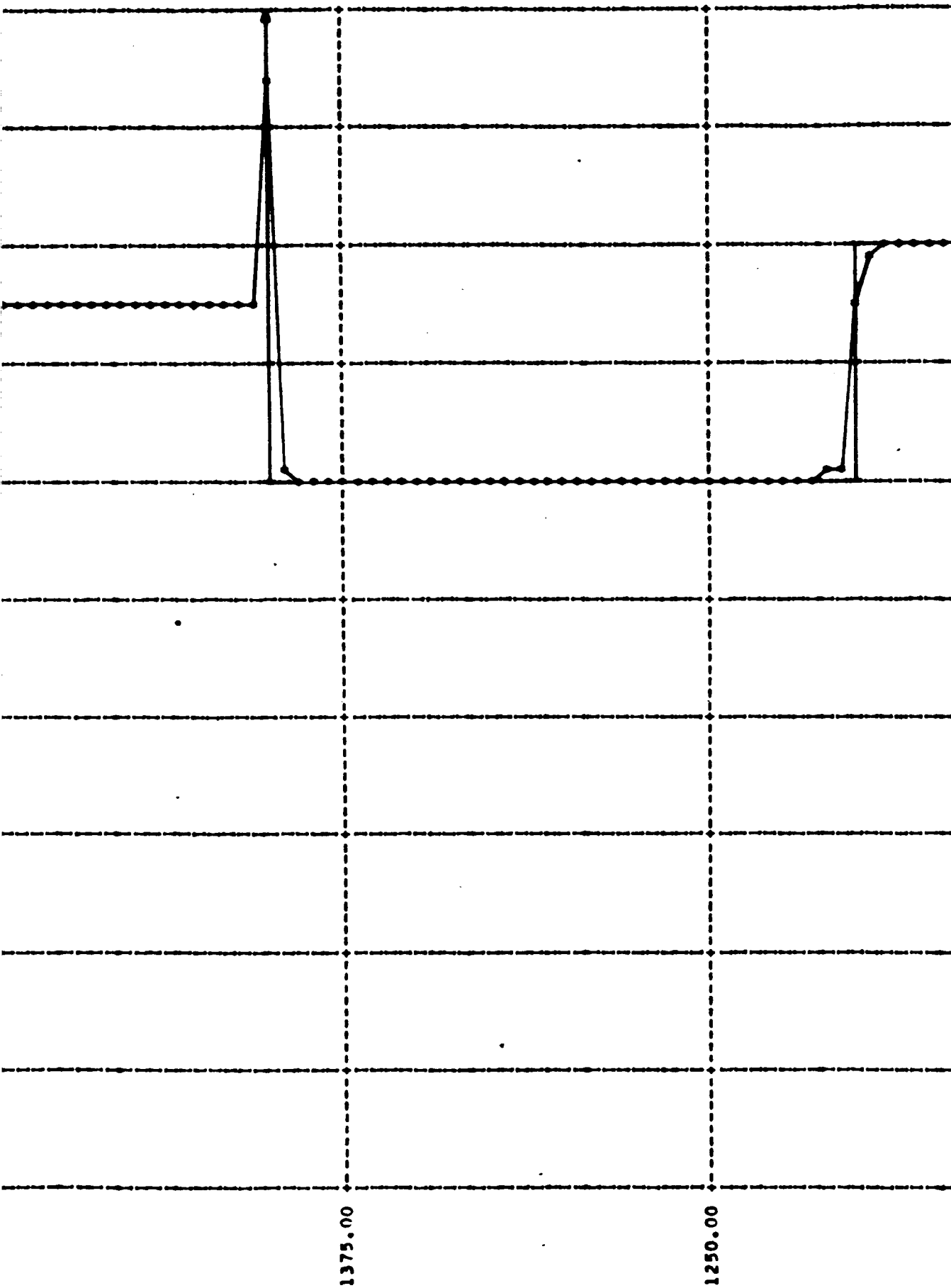
1375.00
1250.00

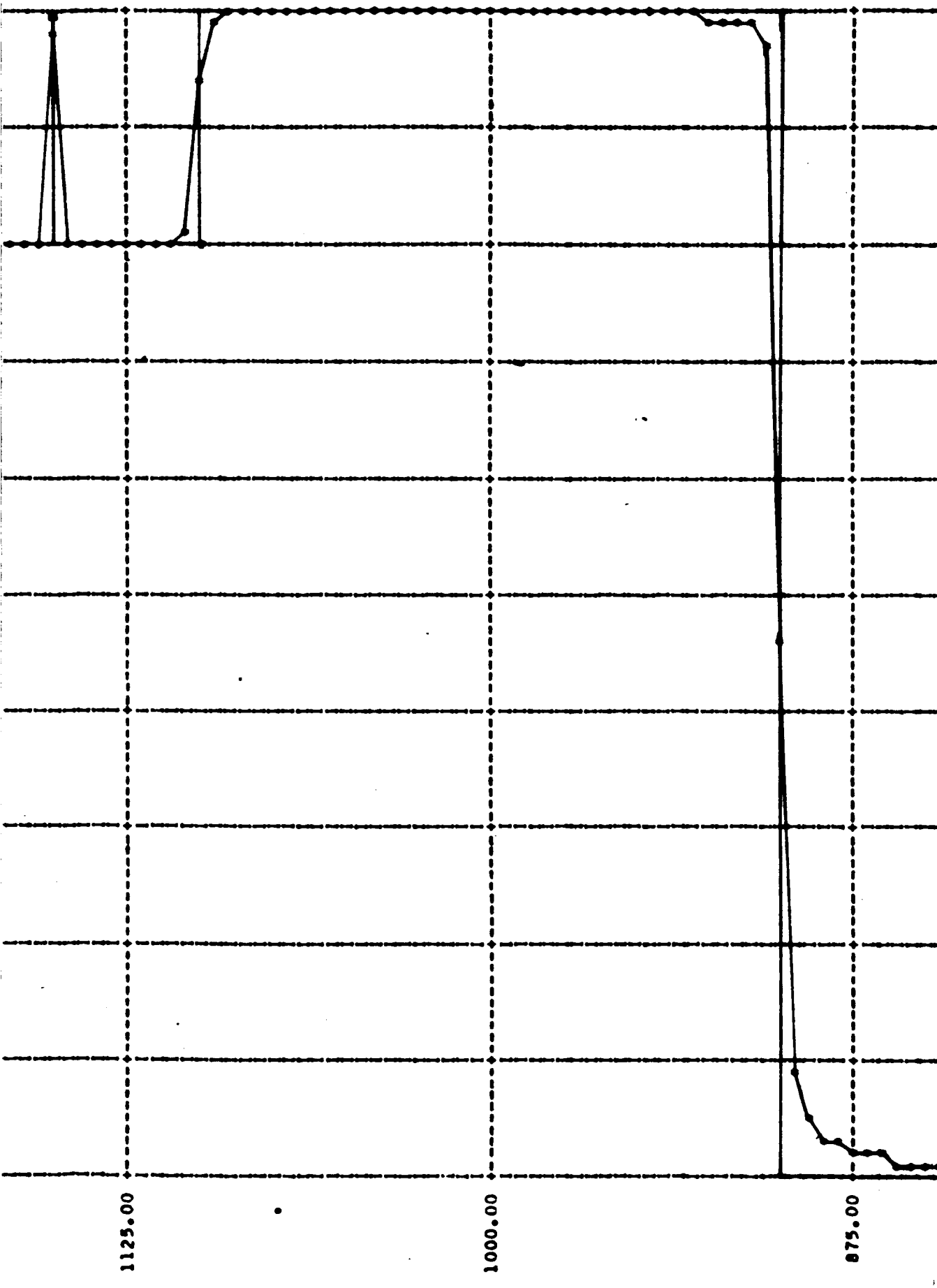
1125.00
1000.00
875.00

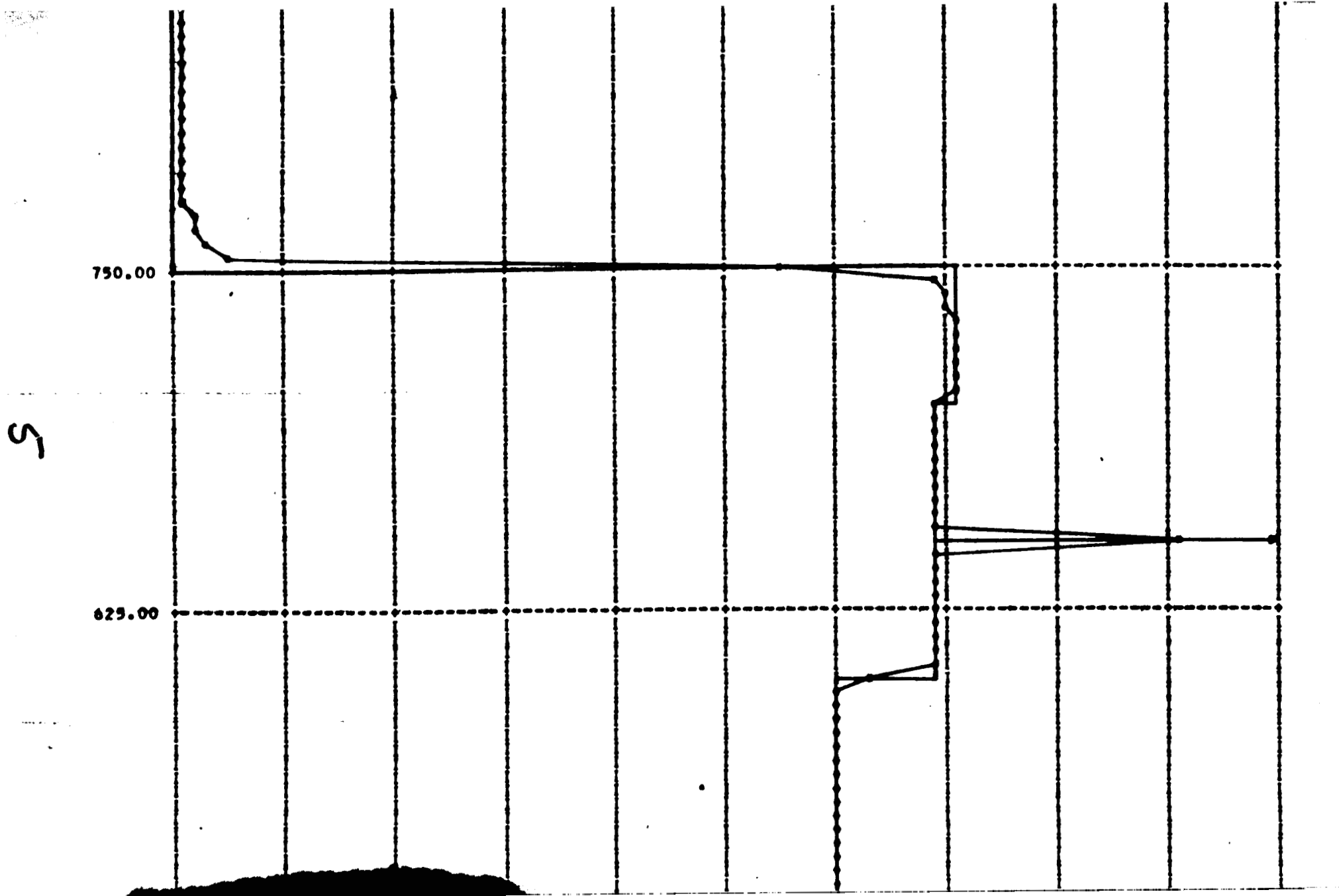
750.00
625.00

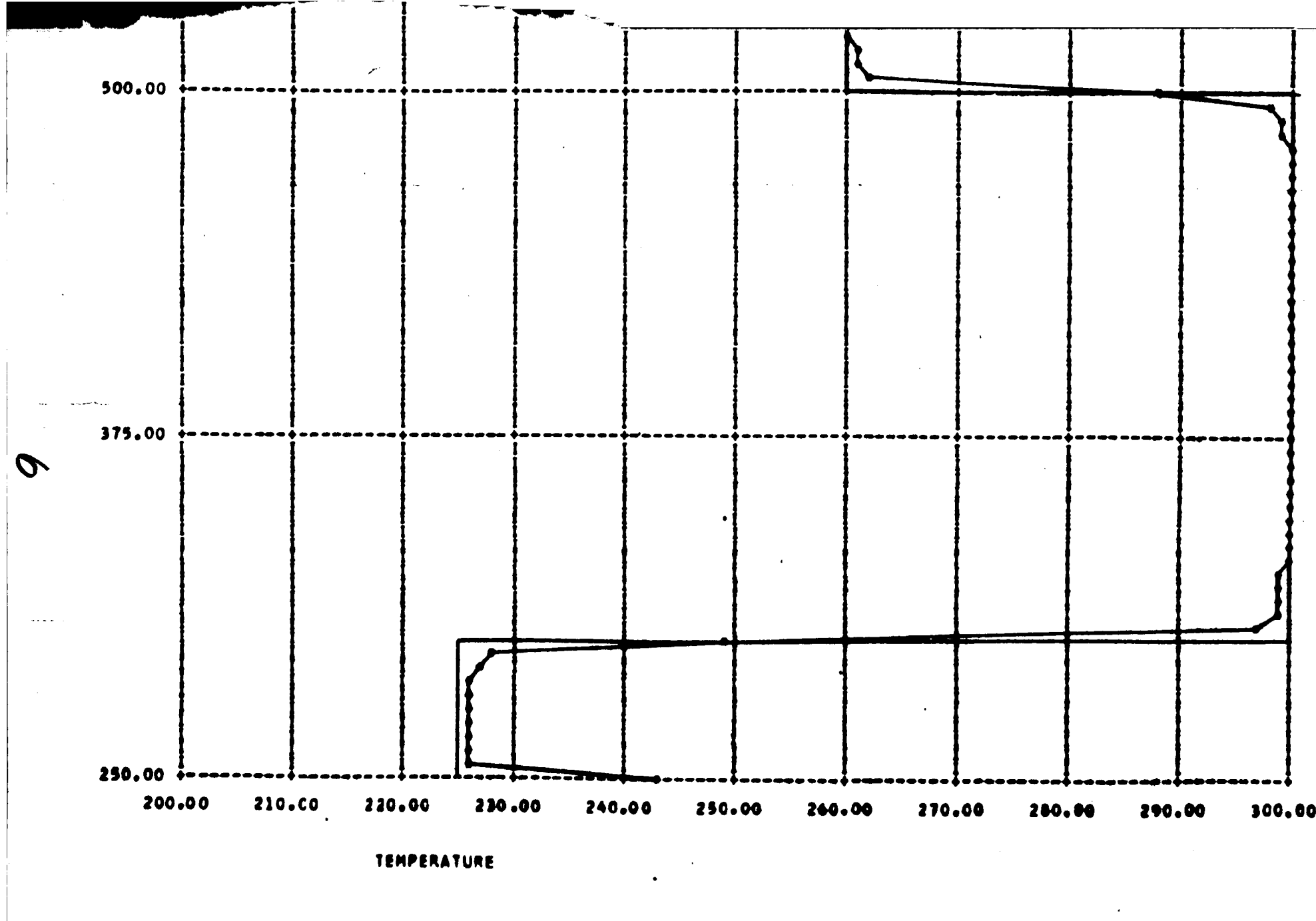
500.00
375.00
250.00
200.00
210.00
220.00
230.00
240.00
250.00
260.00
270.00
280.00
290.00
300.00
TEMPERATURE

[illegible] 2.1.11 TRANSFORMED SPECTRAL PROFILE

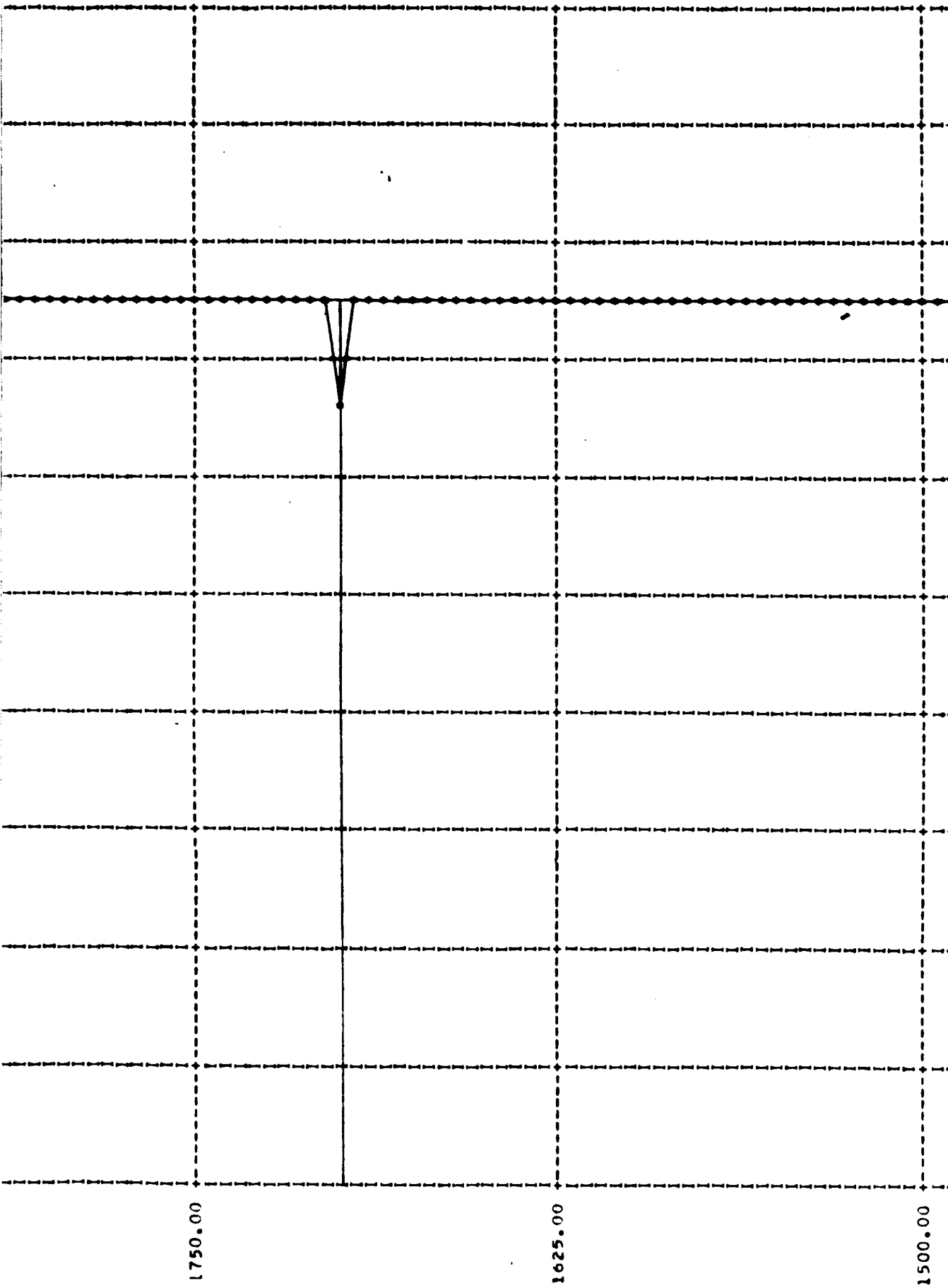

CASE (ii). (FINITE SOLID-ANGLE REFLECT ONLY)

2

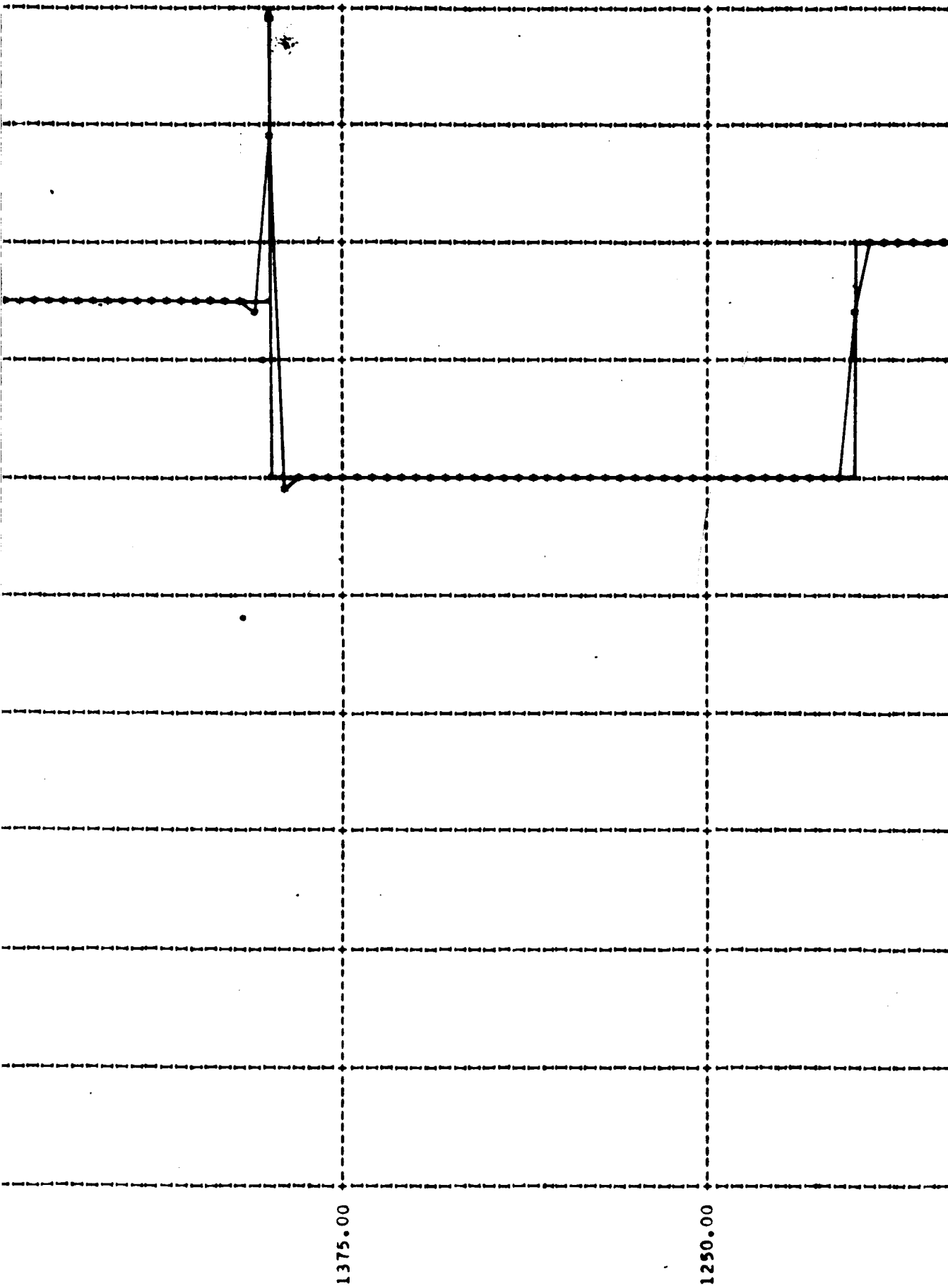
1375.00
1250.00

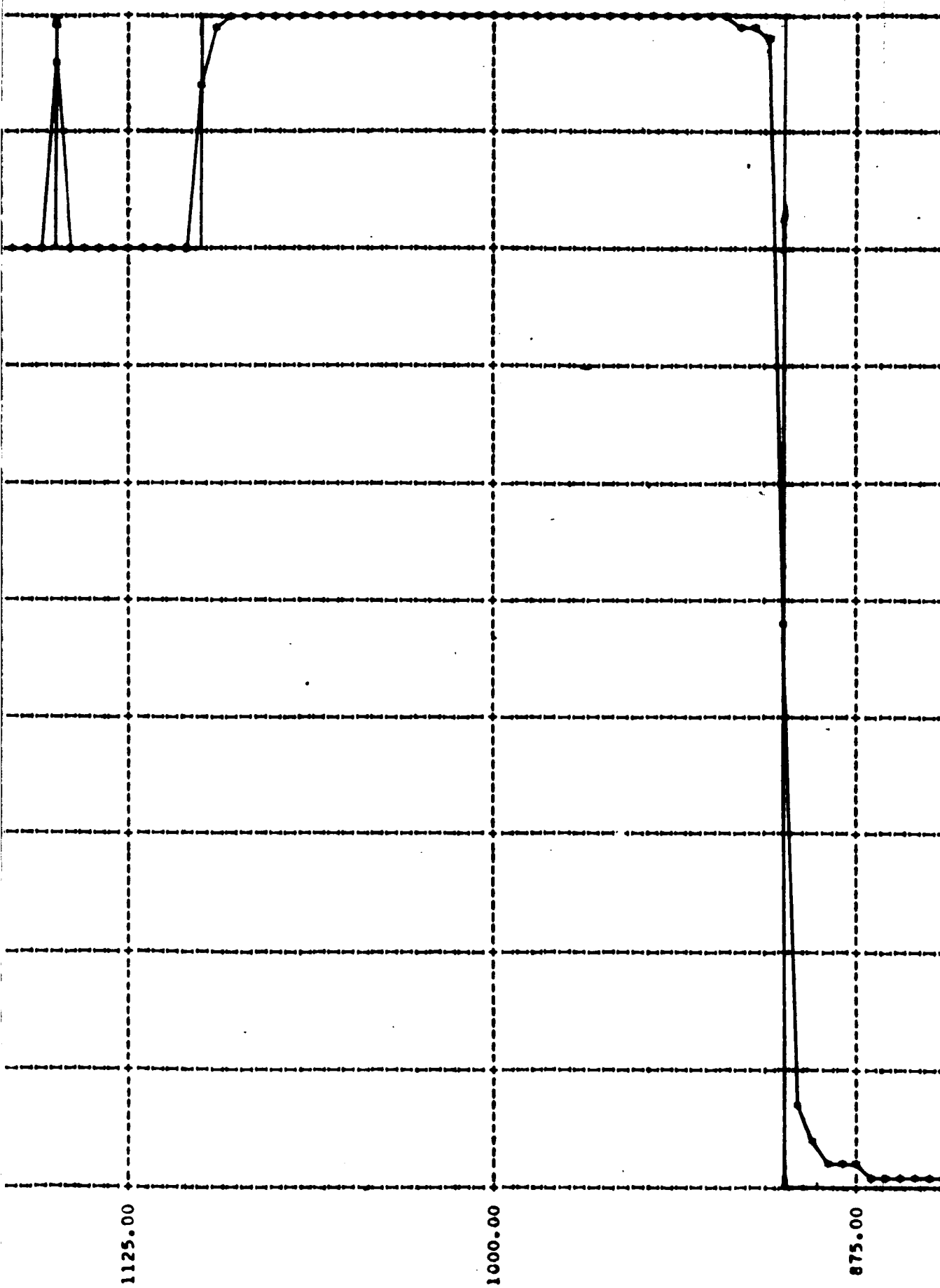
1125.00
1000.00
875.00

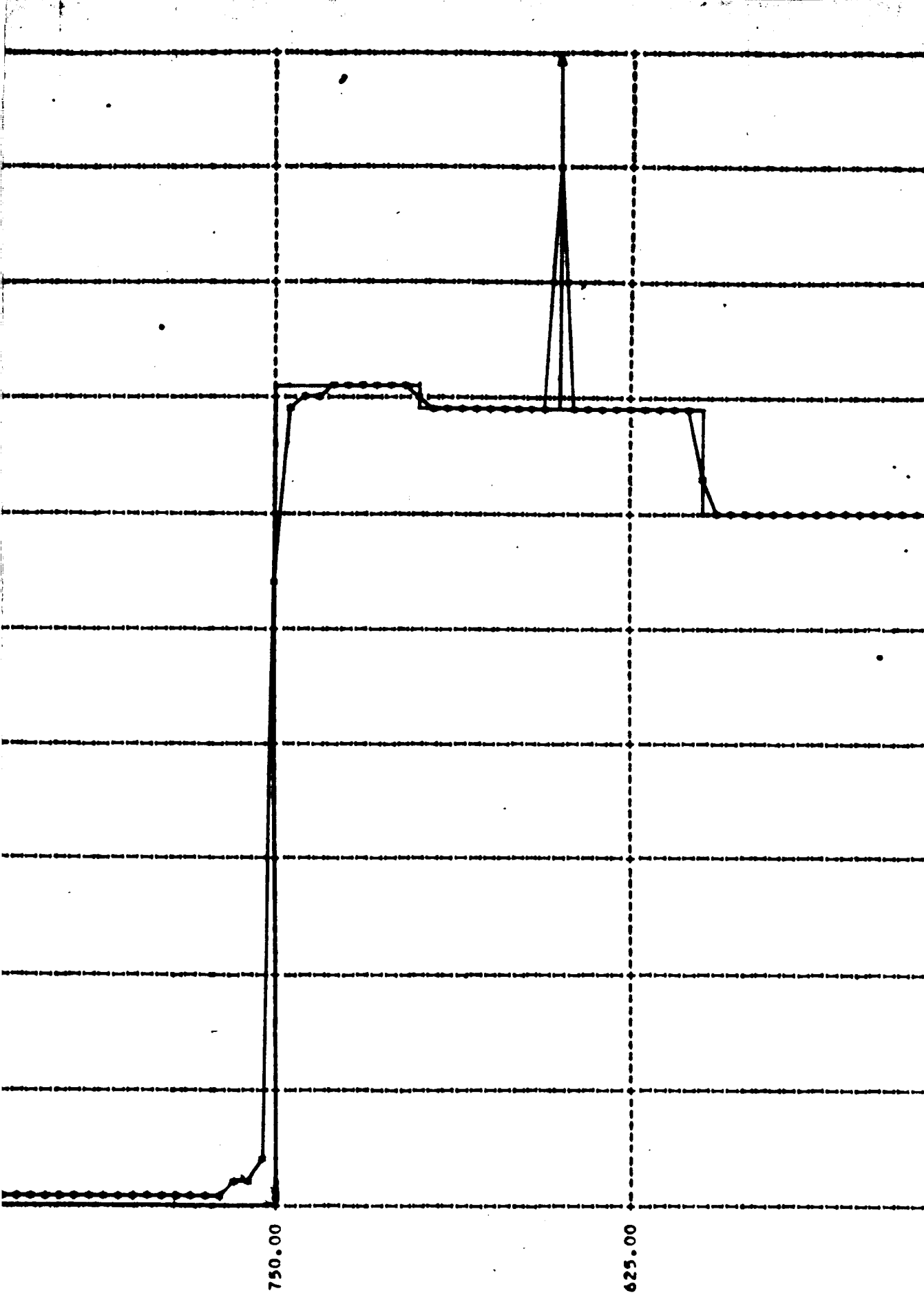
750.00
625.00

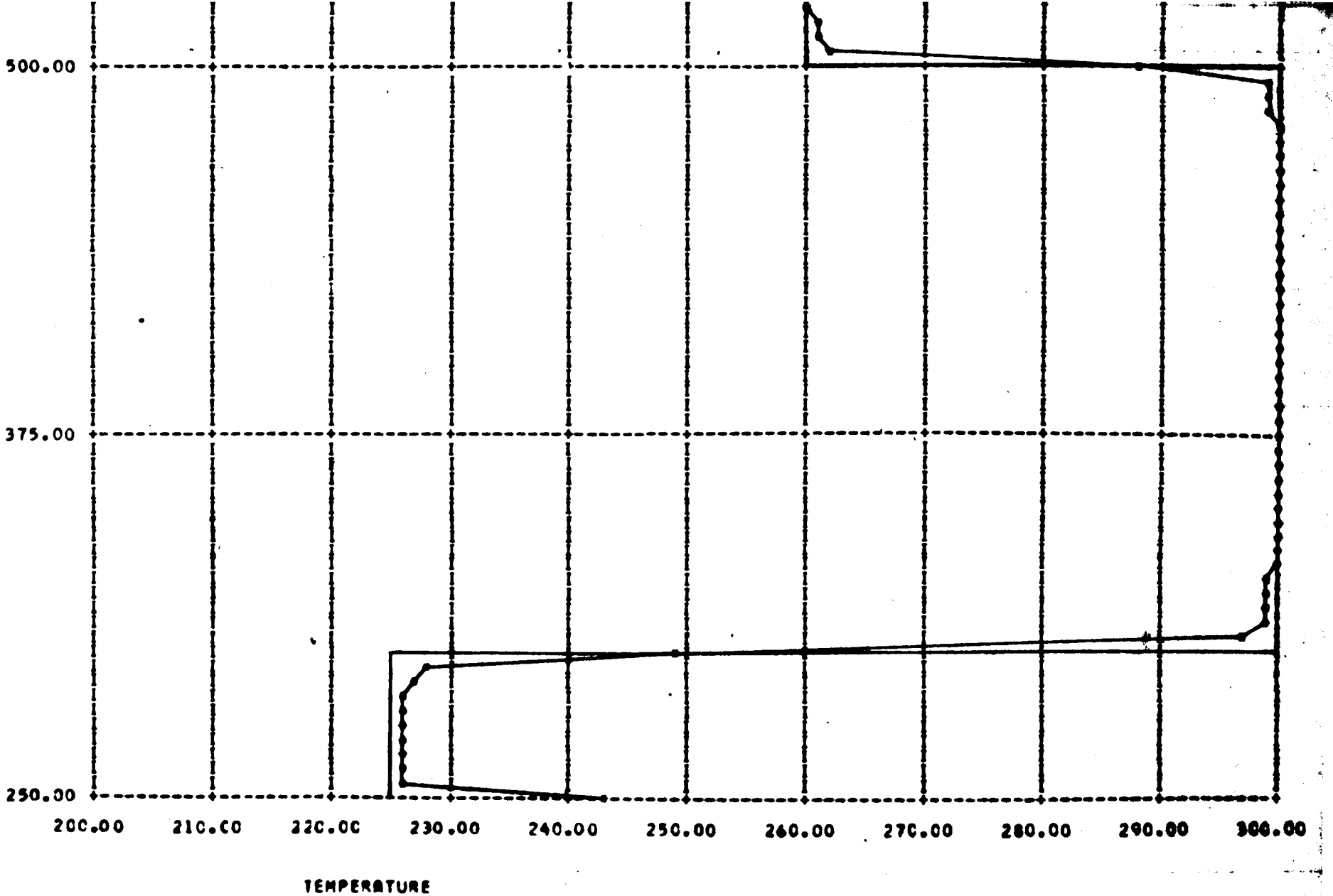
500.00
375.00
250.00
200.00
210.00
220.00
230.00
240.00
250.00
260.00
270.00
280.00
290.00
300.00
TEMPERATURE

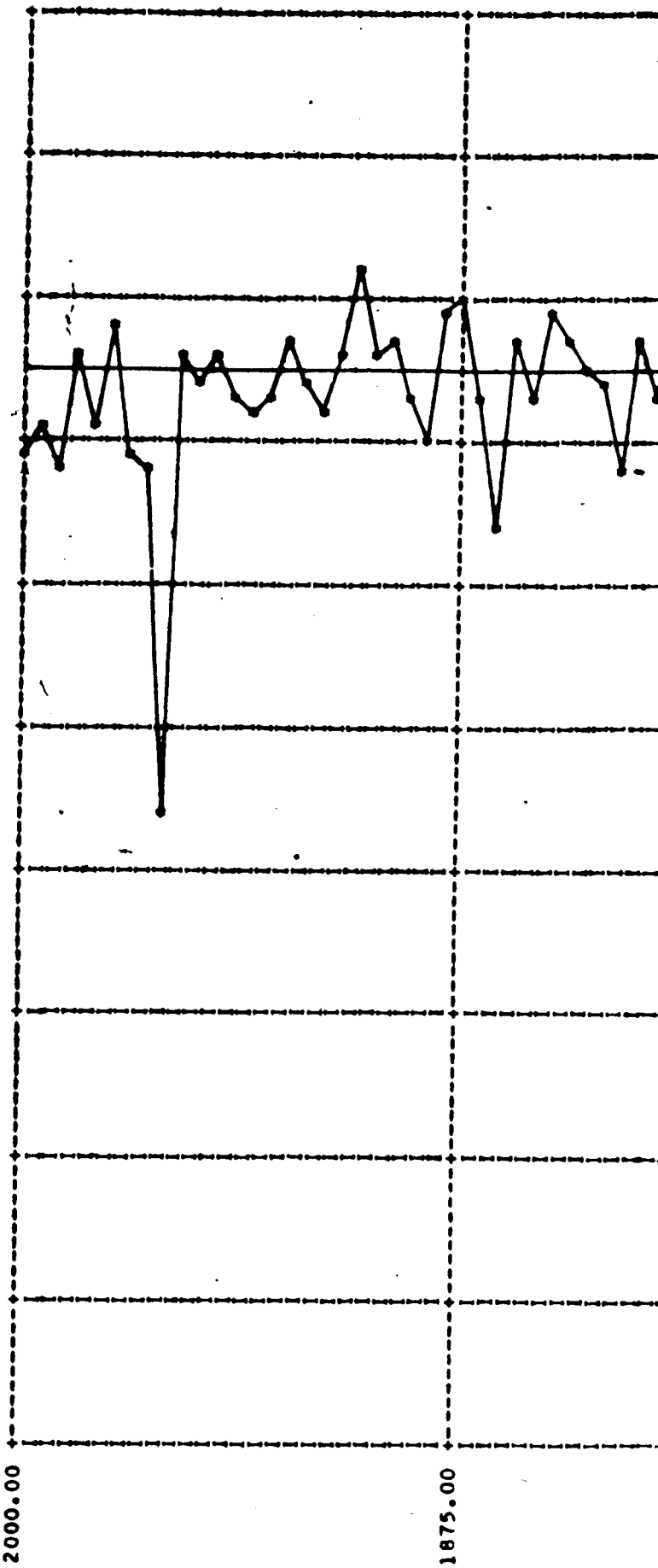

6.1.12 TRANSFORMED SPECTRAL PDF

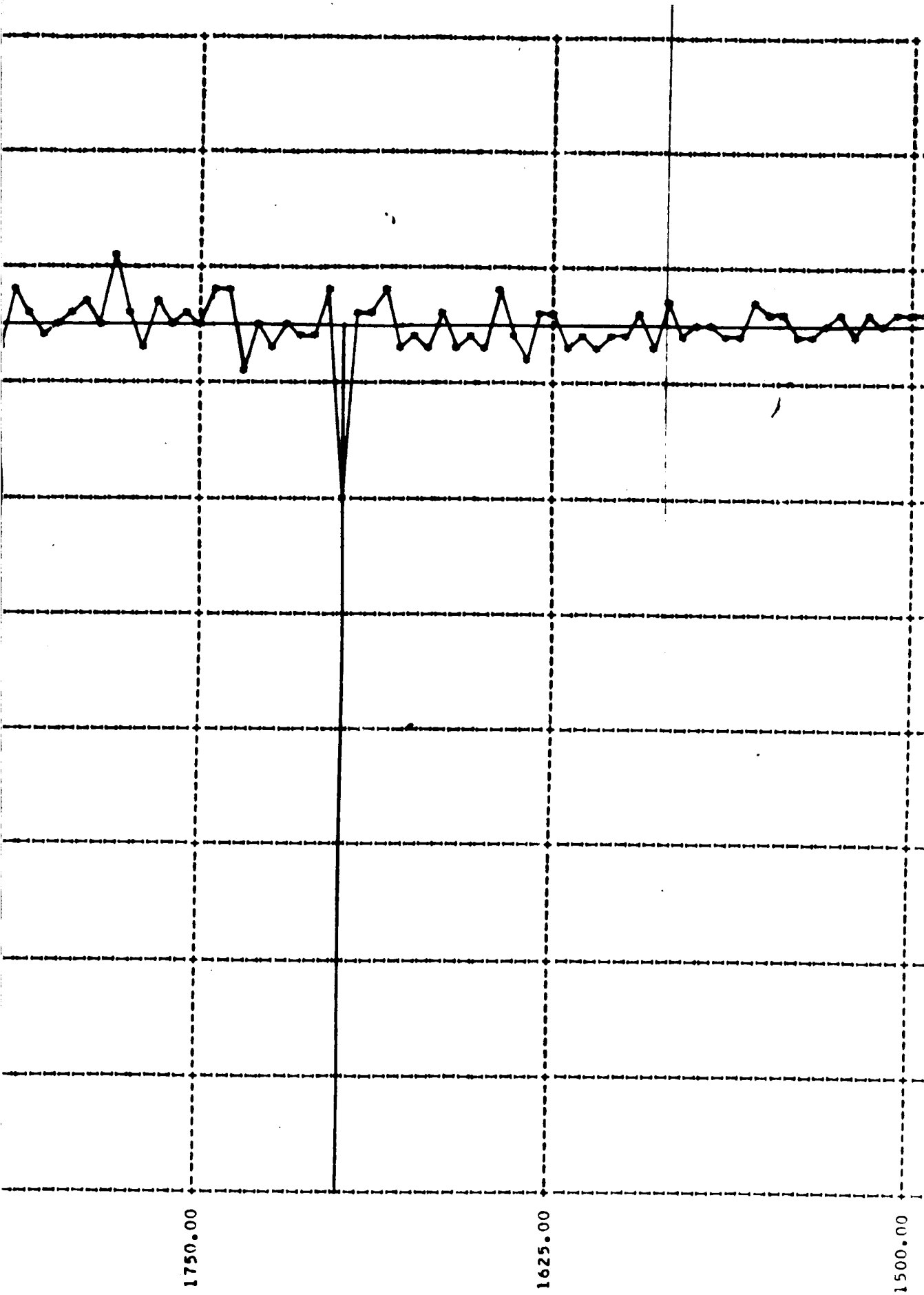

LB, CUST (111), (NOISE ONLY, S/N = 1428 : 1)

2

1375.00
1250.00

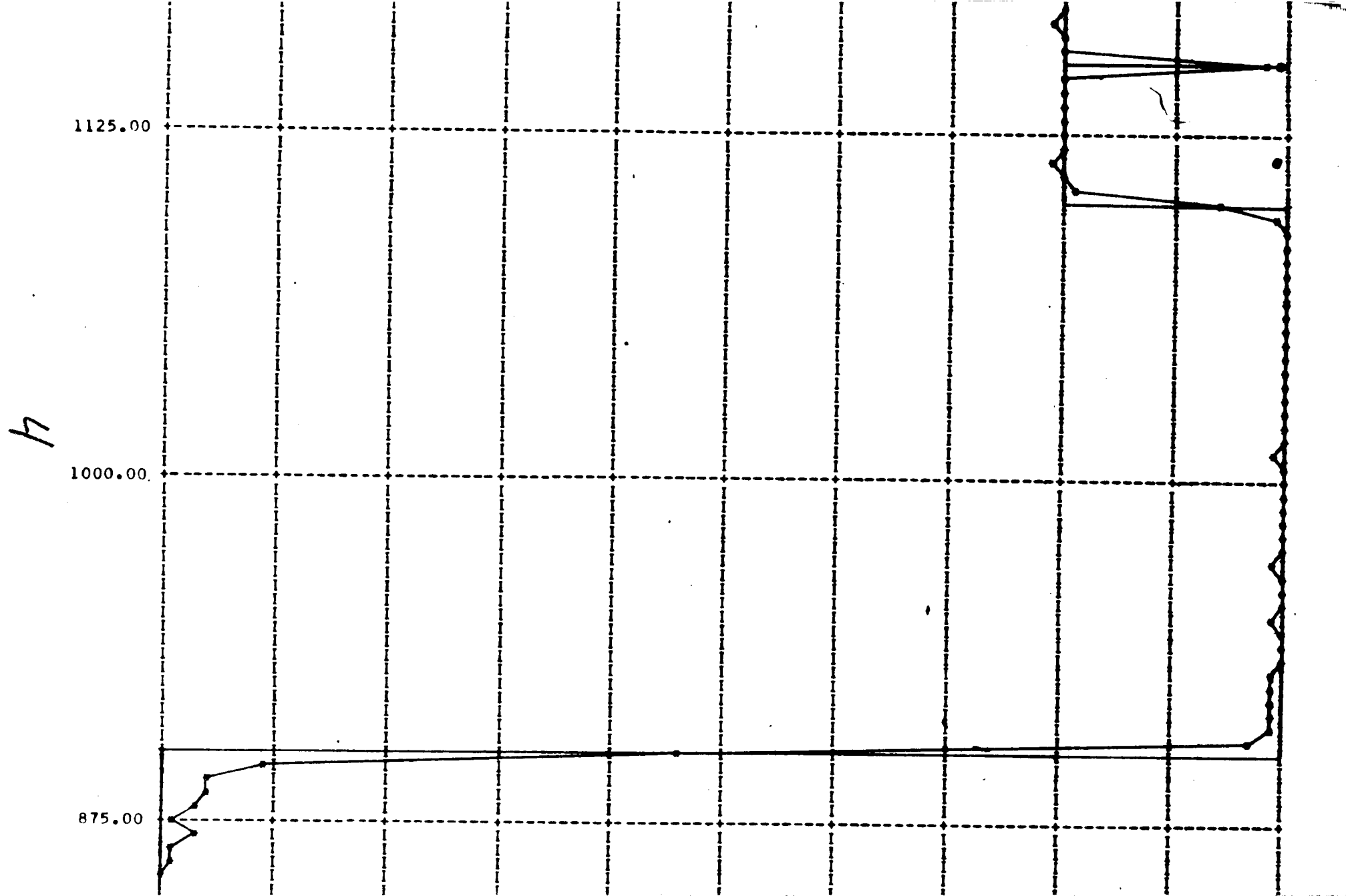
h
1125.00
1000.00
875.00

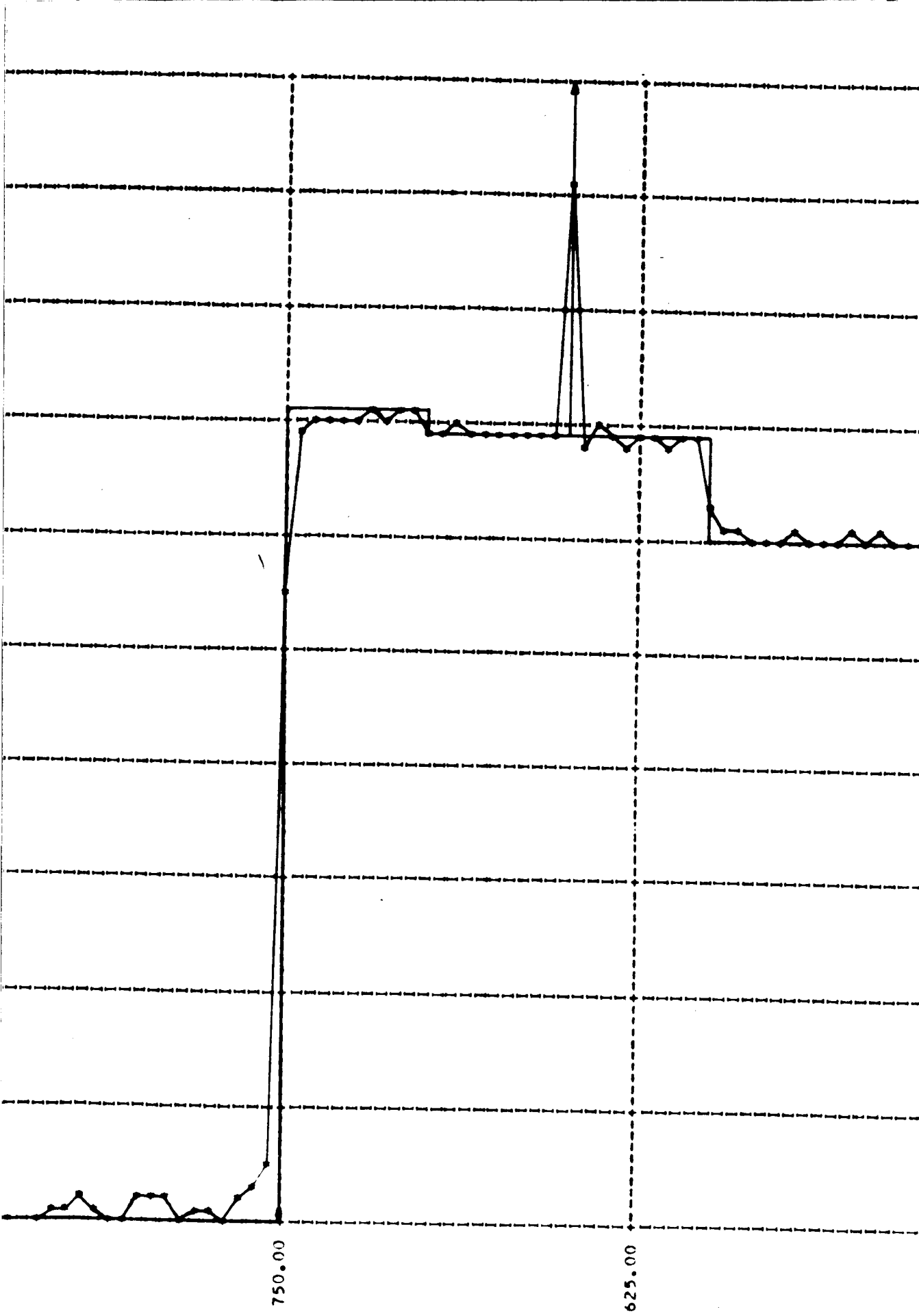
750.00
625.00

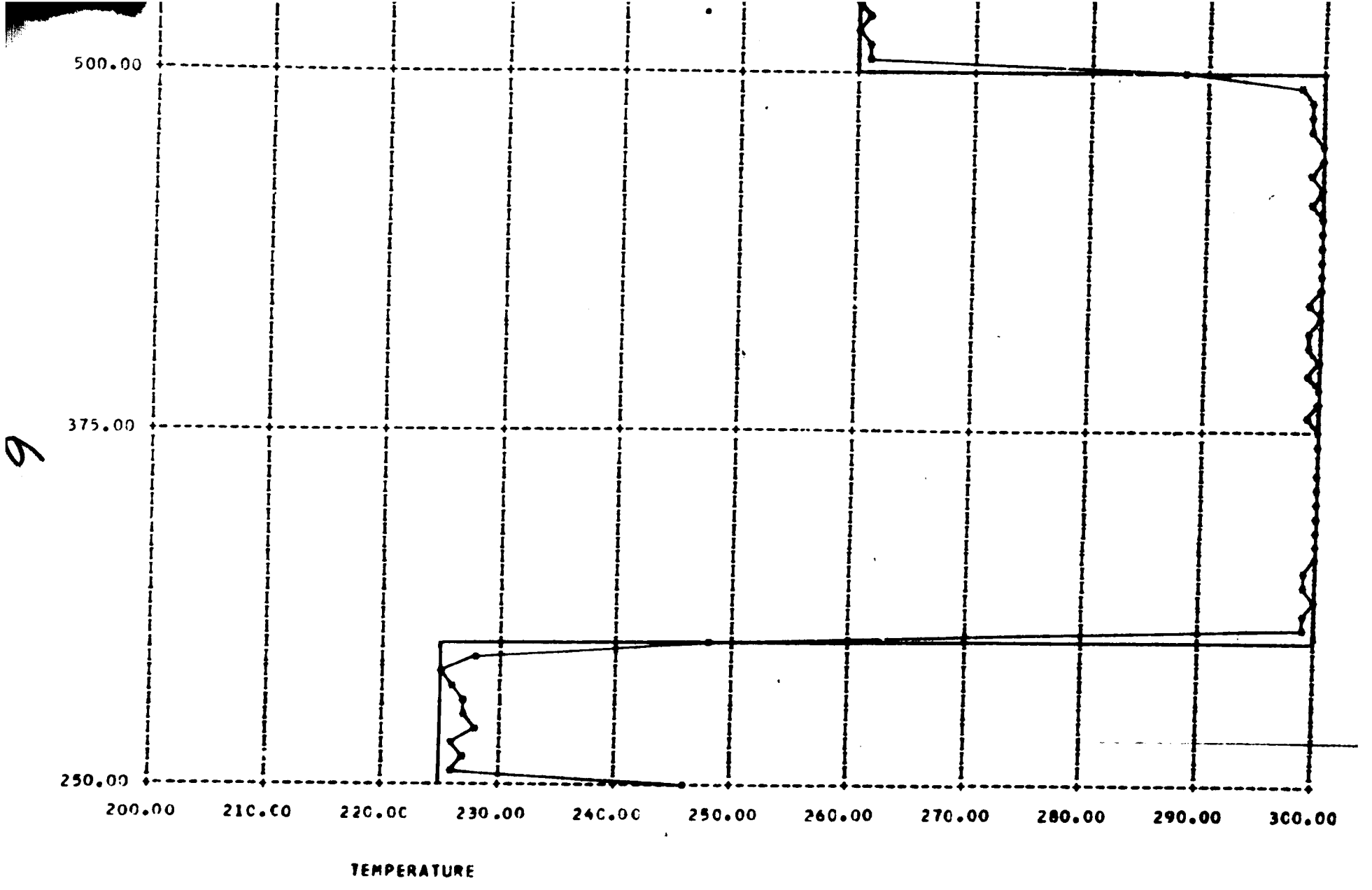
500.00
375.00
250.00
200.00
210.00
220.00
230.00
240.00
250.00
260.00
270.00
280.00
290.00
300.00
TEMPERATURE

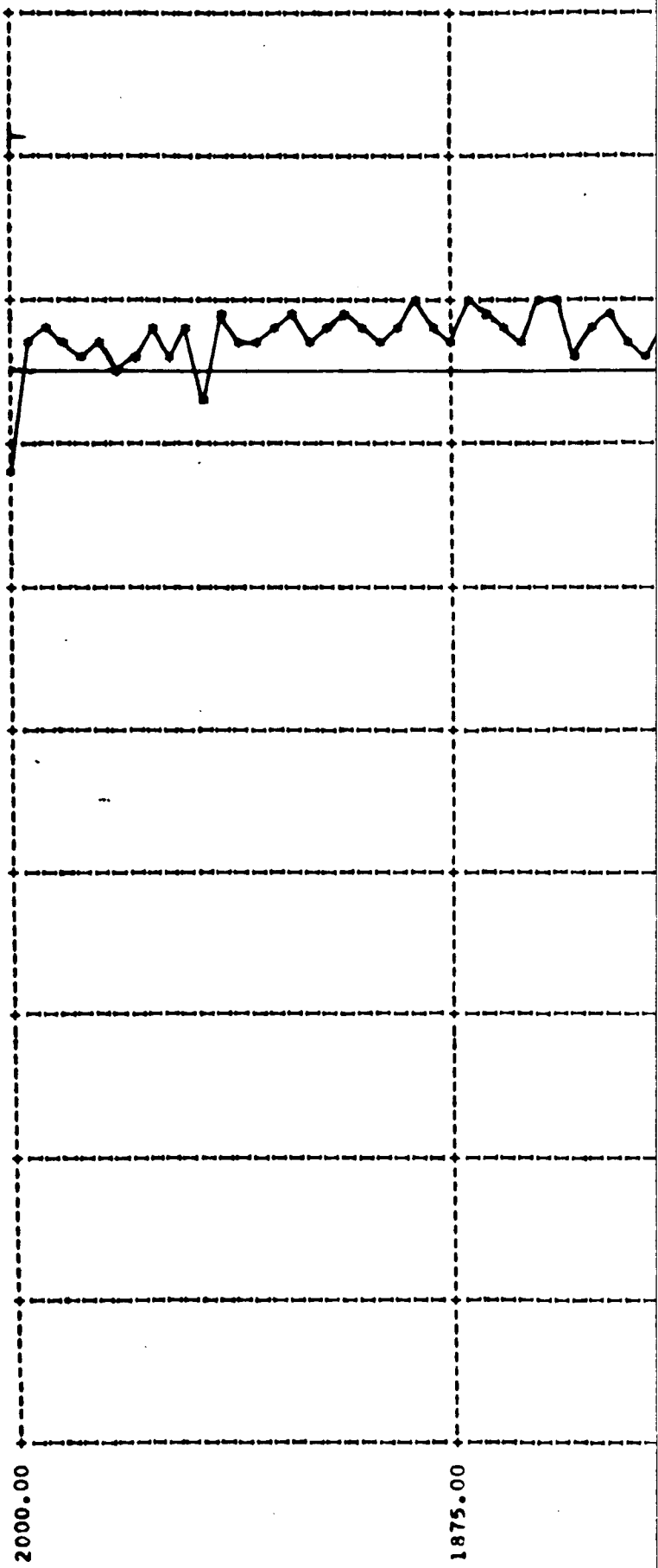

6.1.13

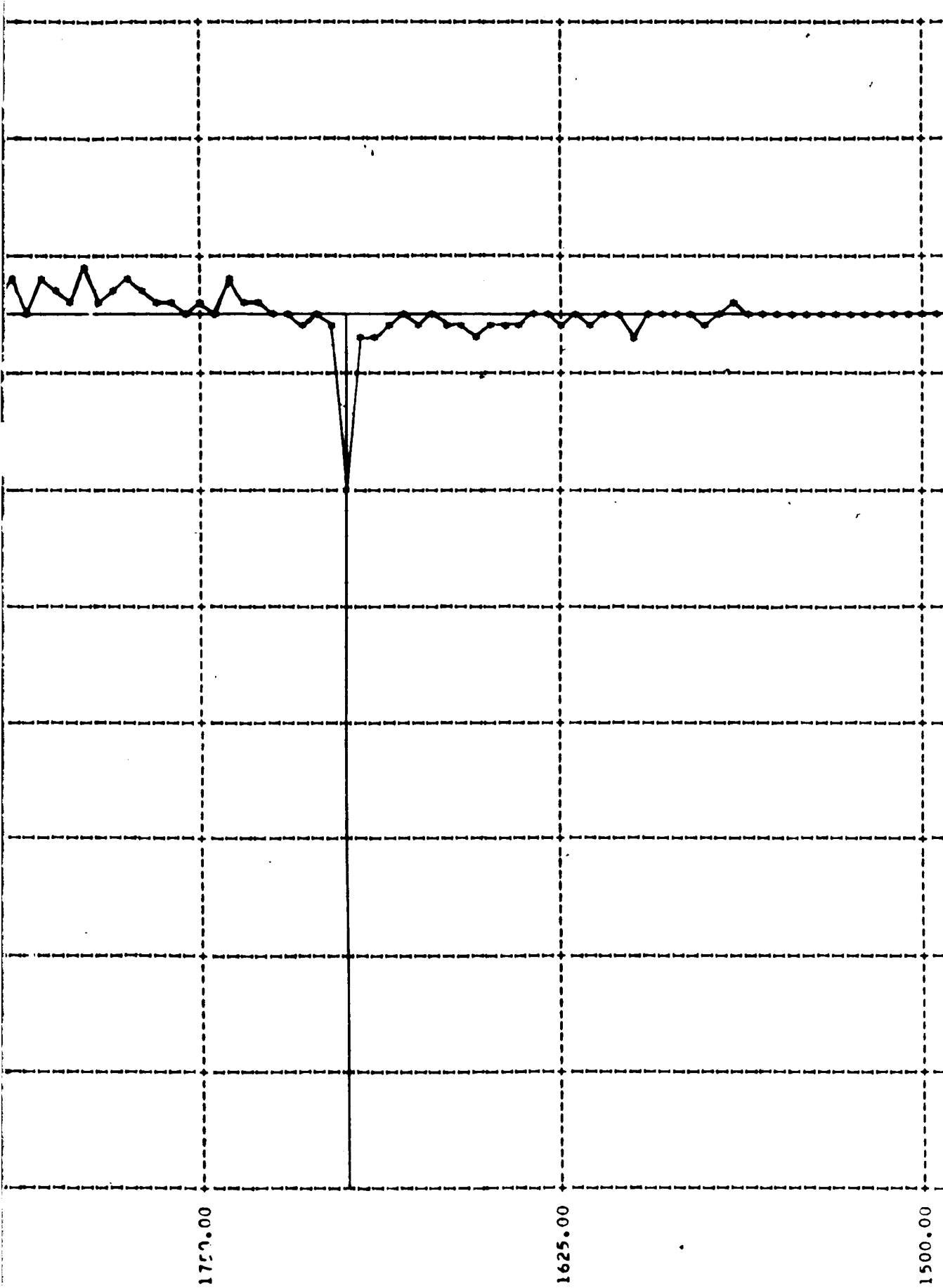

FILE, DIFF (dv), (DEBITING EFFECT ONLY)

2

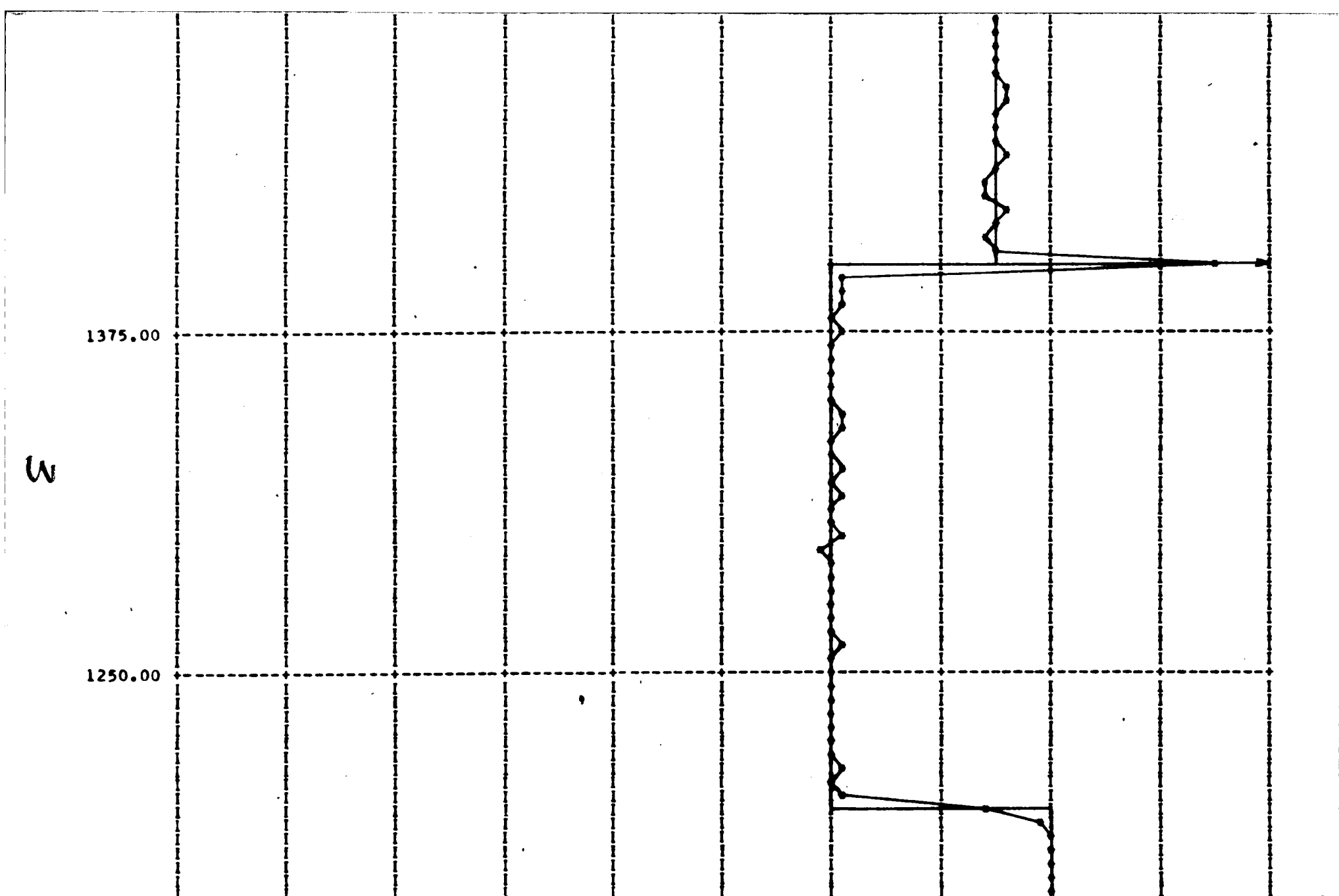
1375.00
1250.00
W

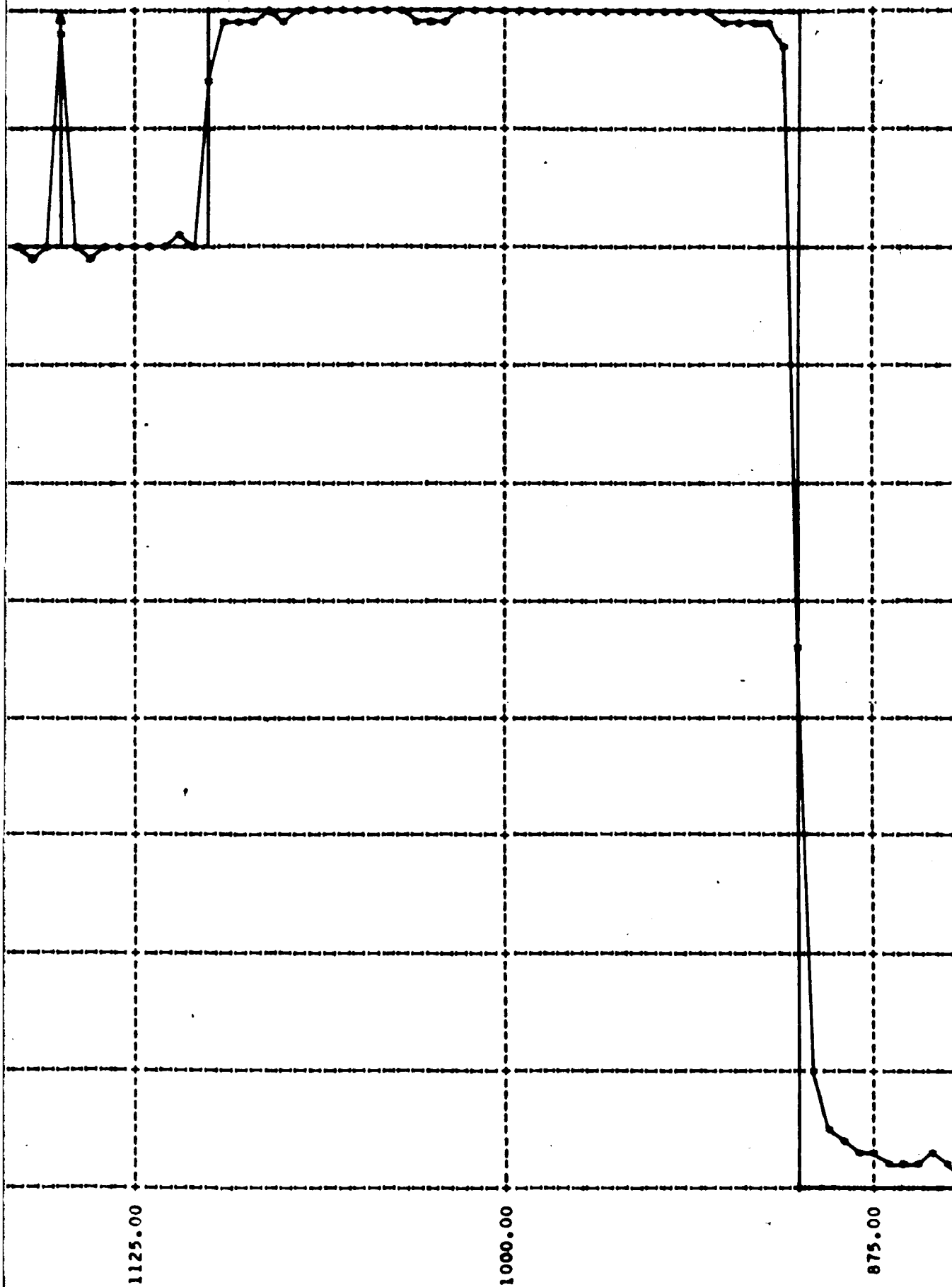
1125.00
1000.00
875.00

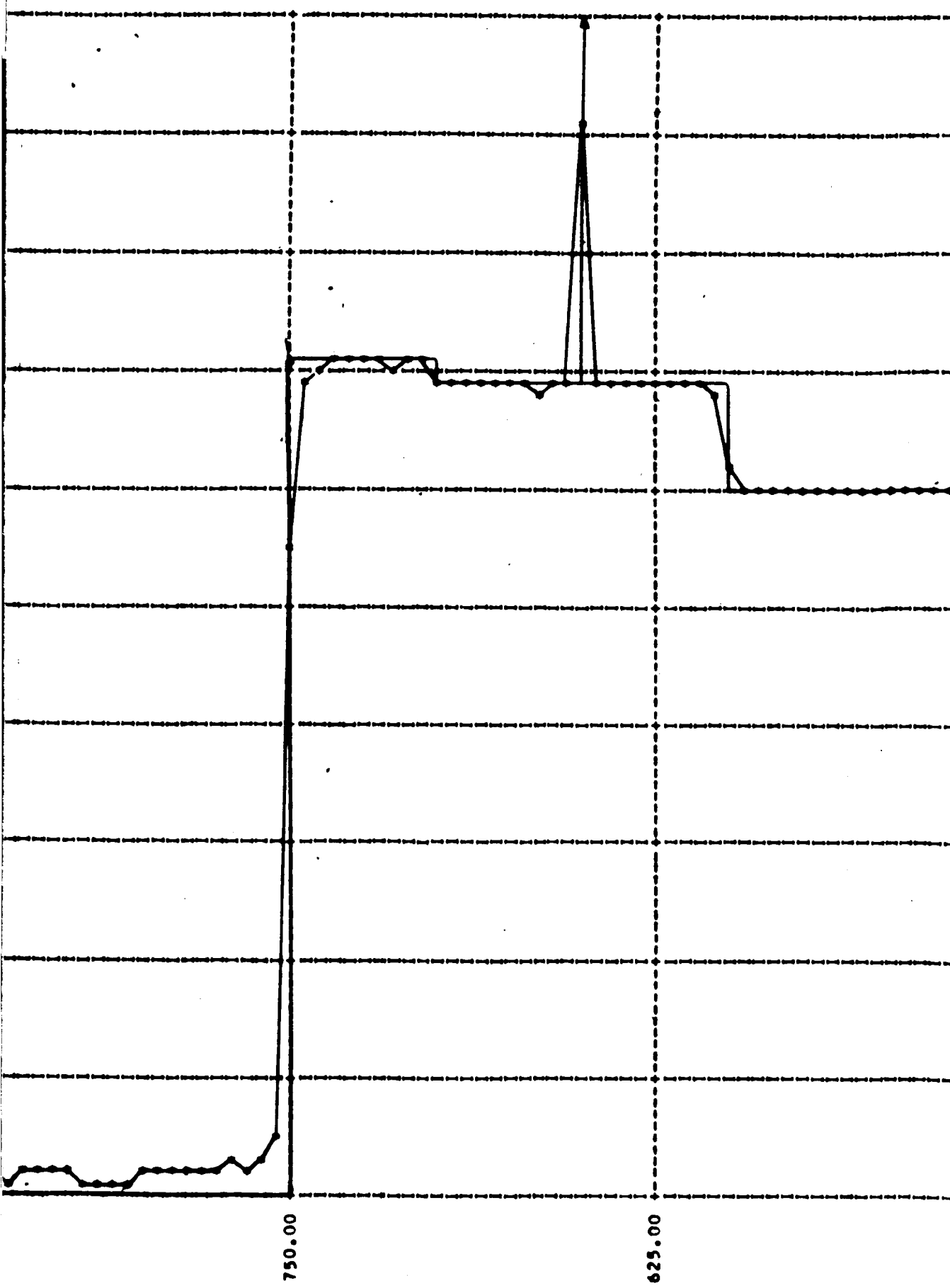
750.00
625.00

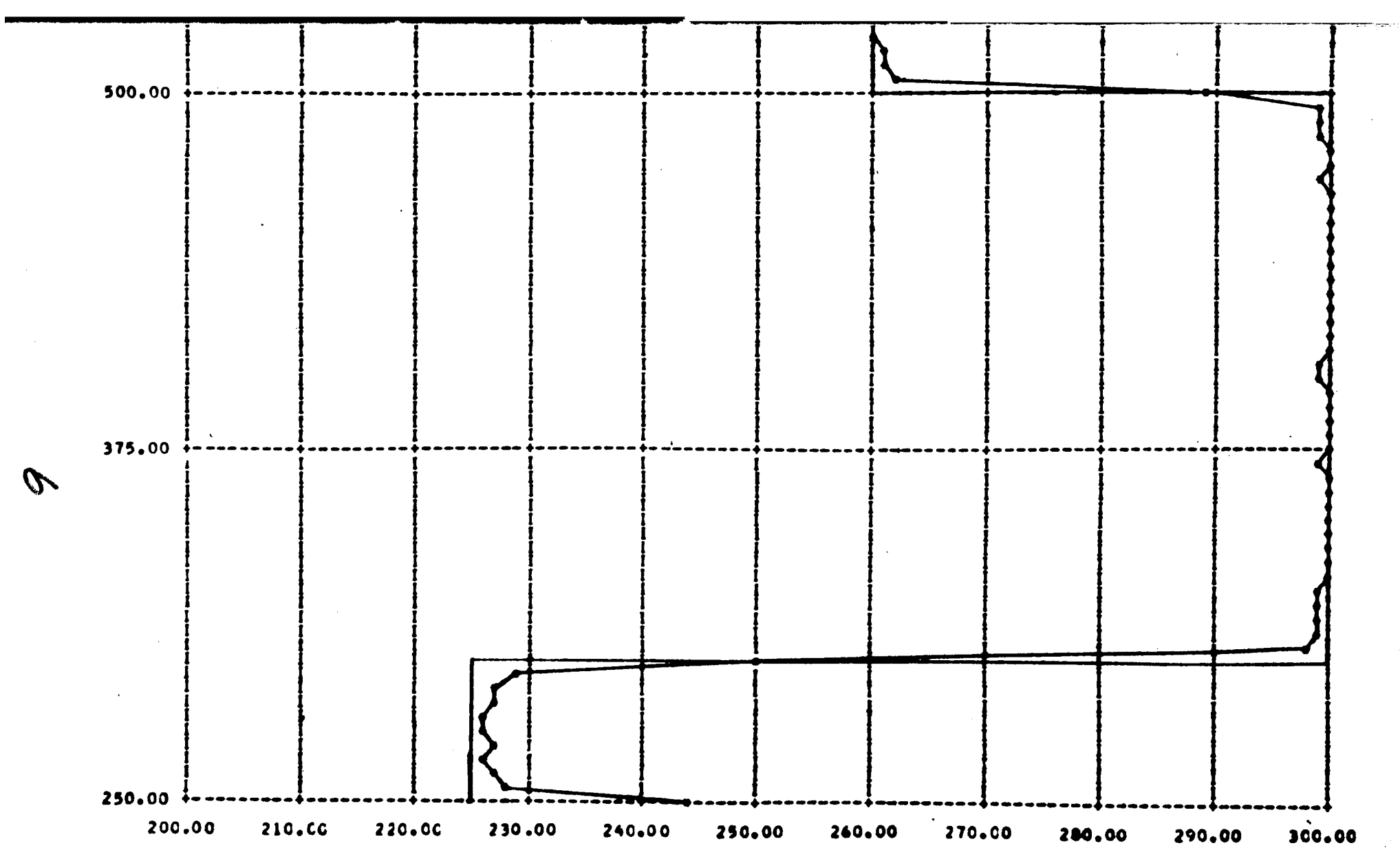
500.00
375.00
250.00
200.00
210.00
220.00
230.00
240.00
250.00
260.00
270.00
280.00
290.00
300.00
TEMPERATURE

6.1.14

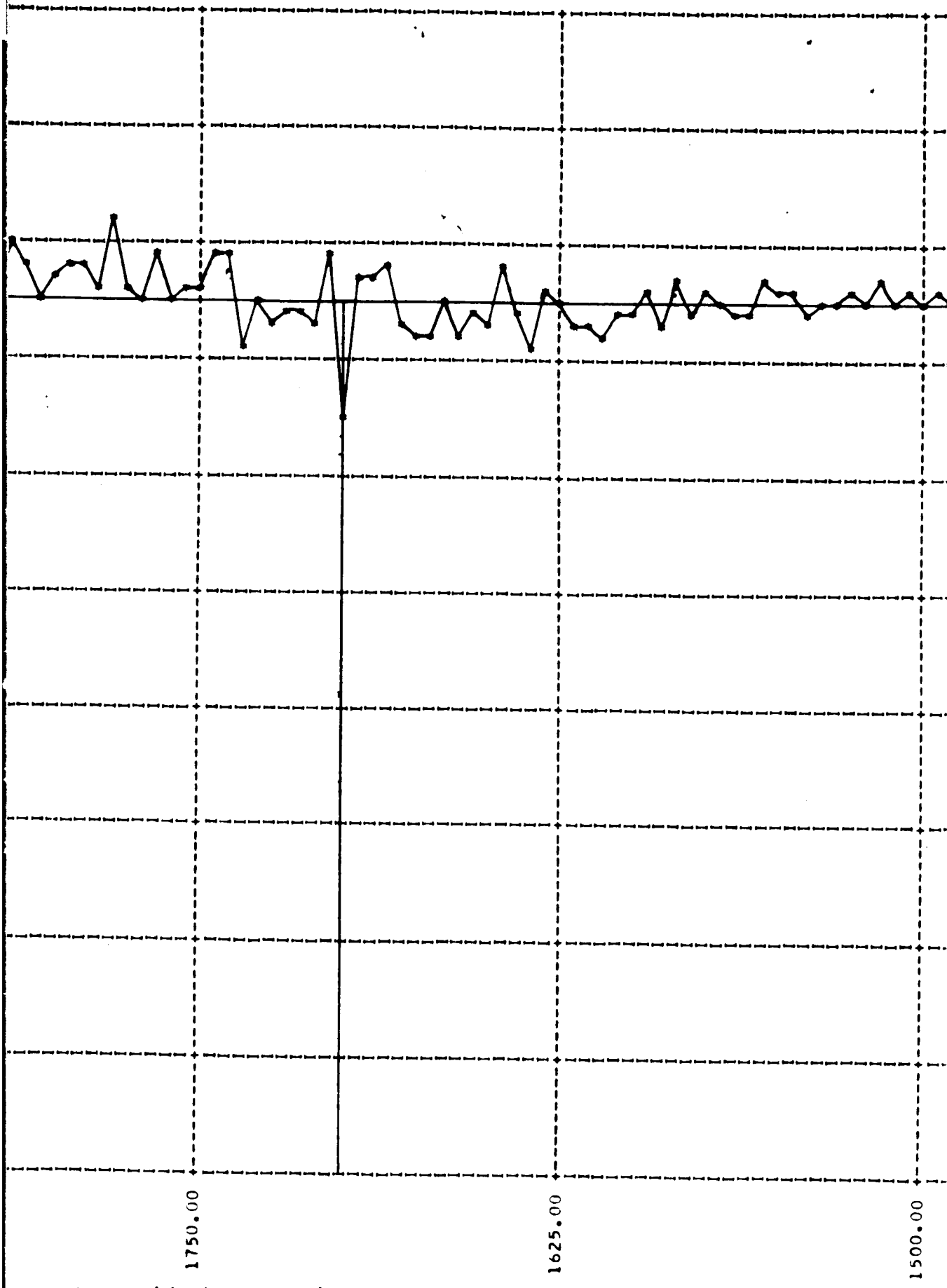

[illegible], SI E (v), (ALL PERIODS)

2

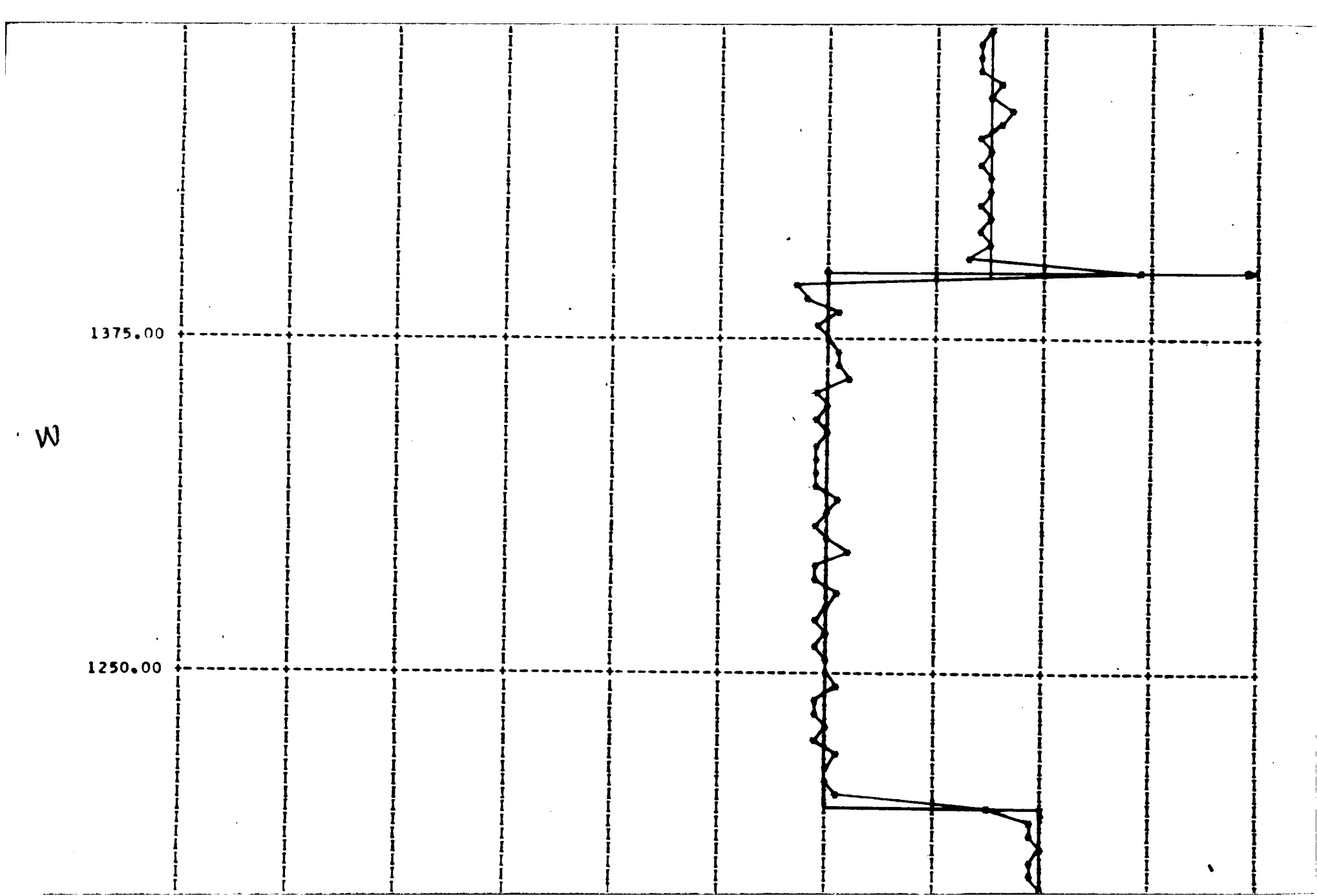
1375.00
1250.00
W

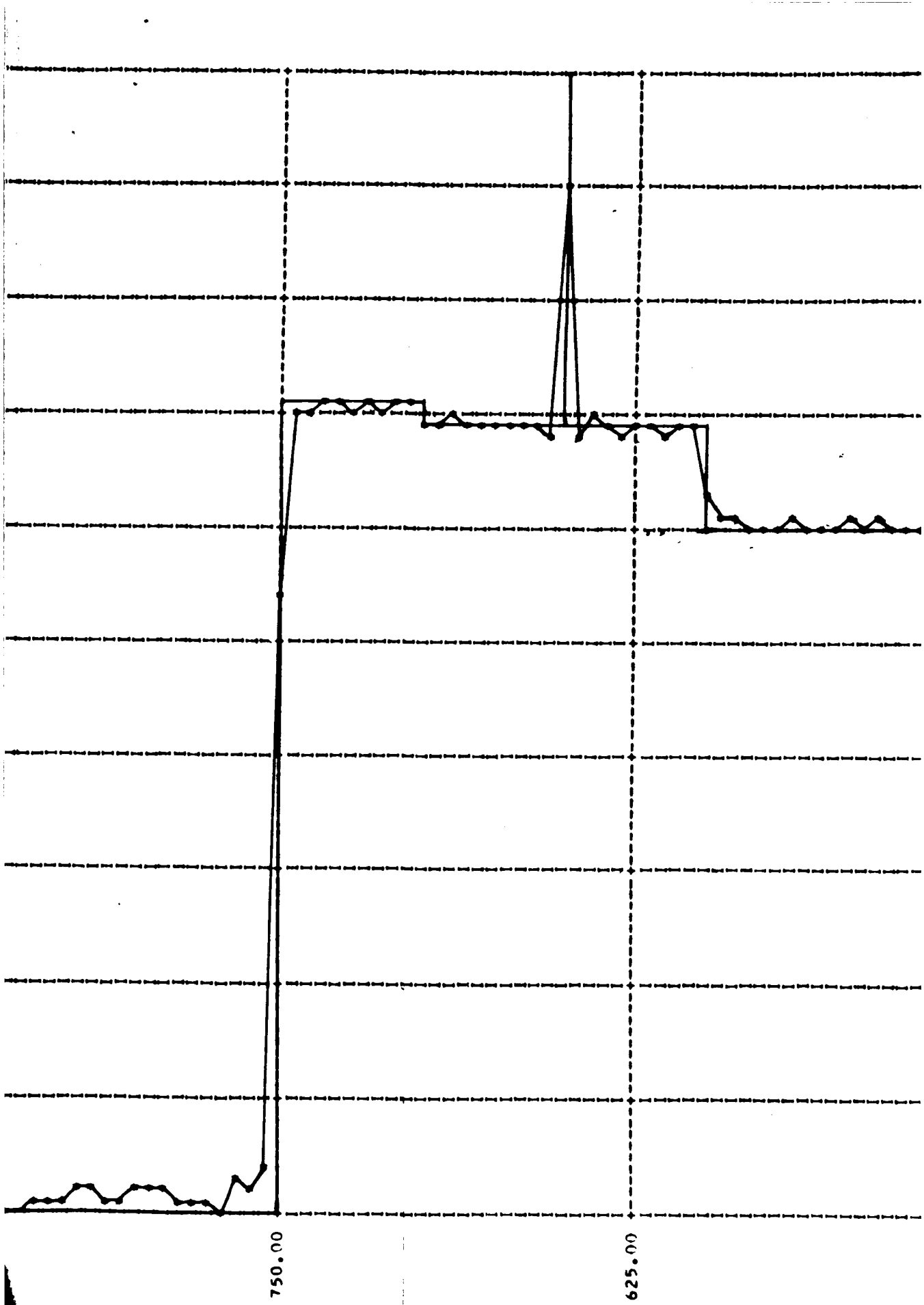
750.00
625.00

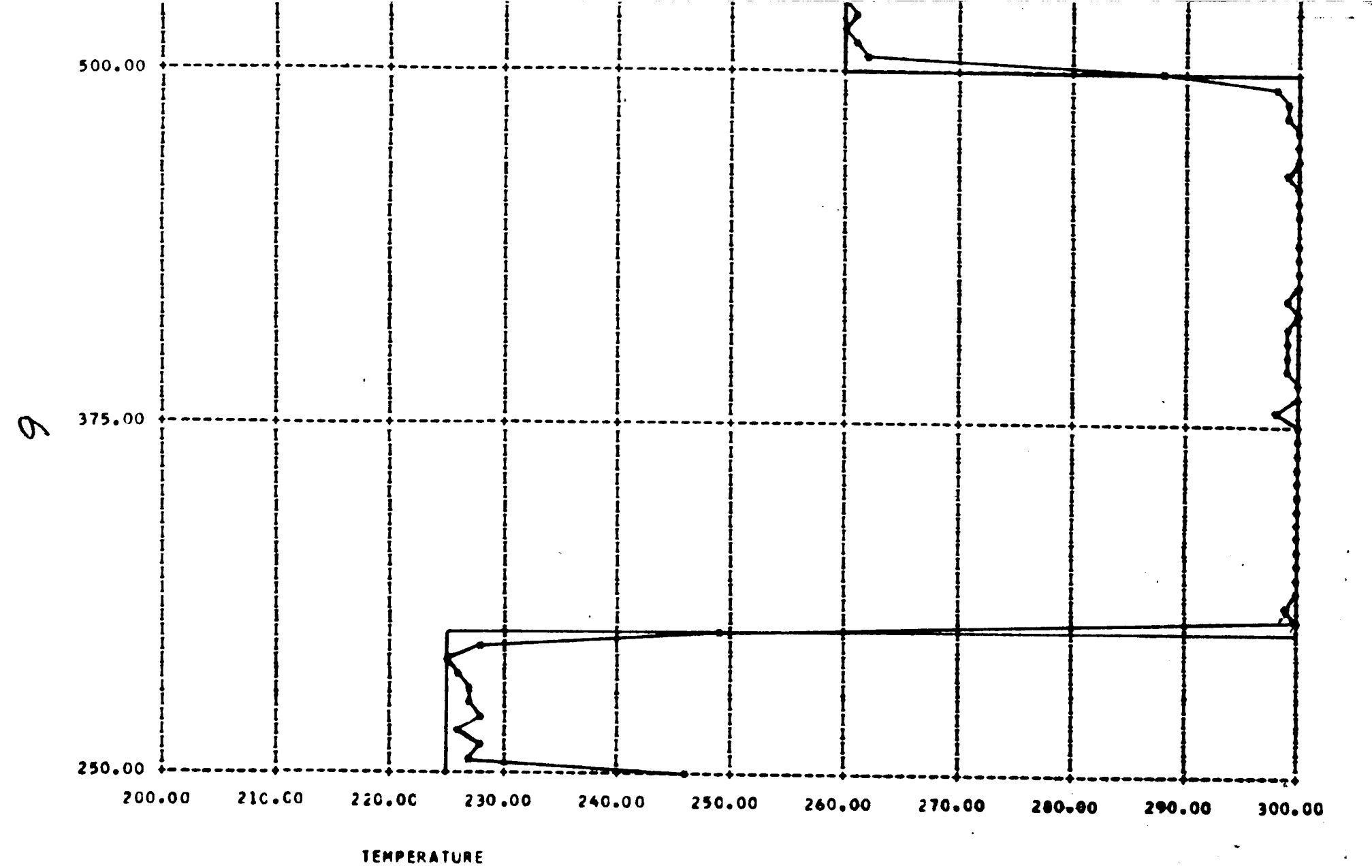
500.00
375.00
250.00
200.00
210.00
220.00
230.00
240.00
250.00
260.00
270.00
280.00
290.00
300.00
TEMPERATURE

6.1.15 TRANSFORMED SPECTRAL PROFILE

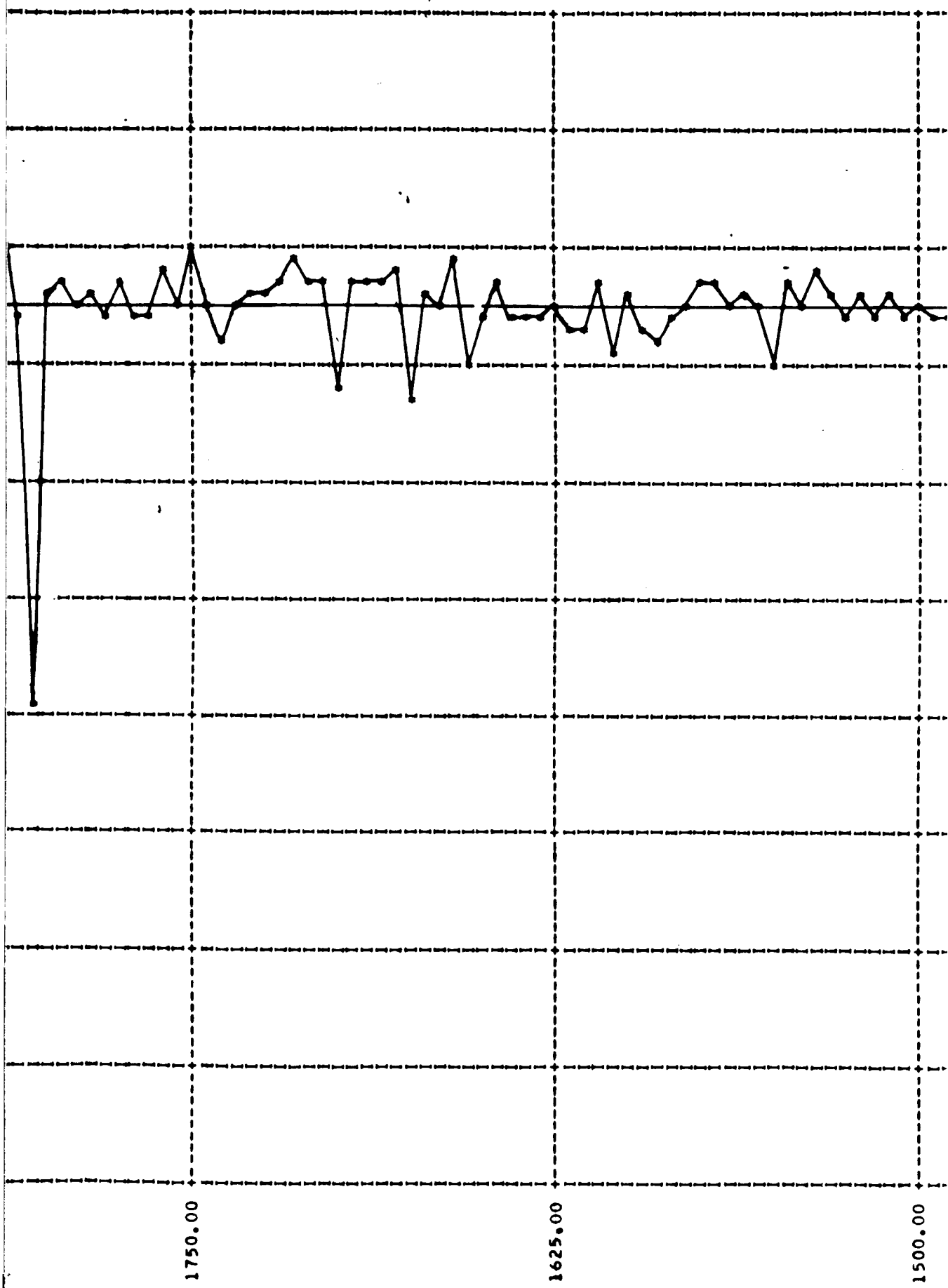

E, CASE (vi), (ALL EFFECTS, SLOW SAMPLING RATE)

2

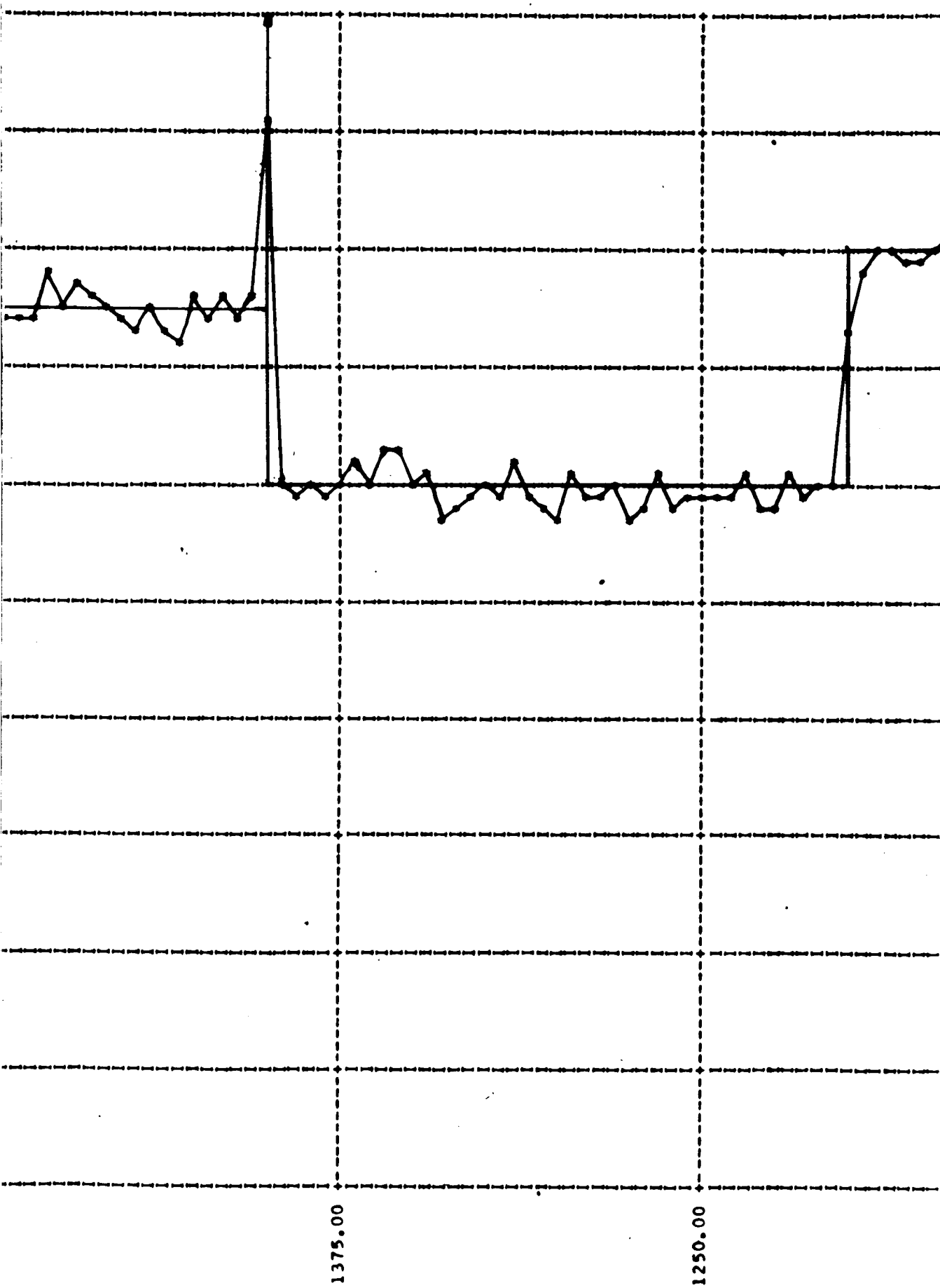
1375.00
1250.00

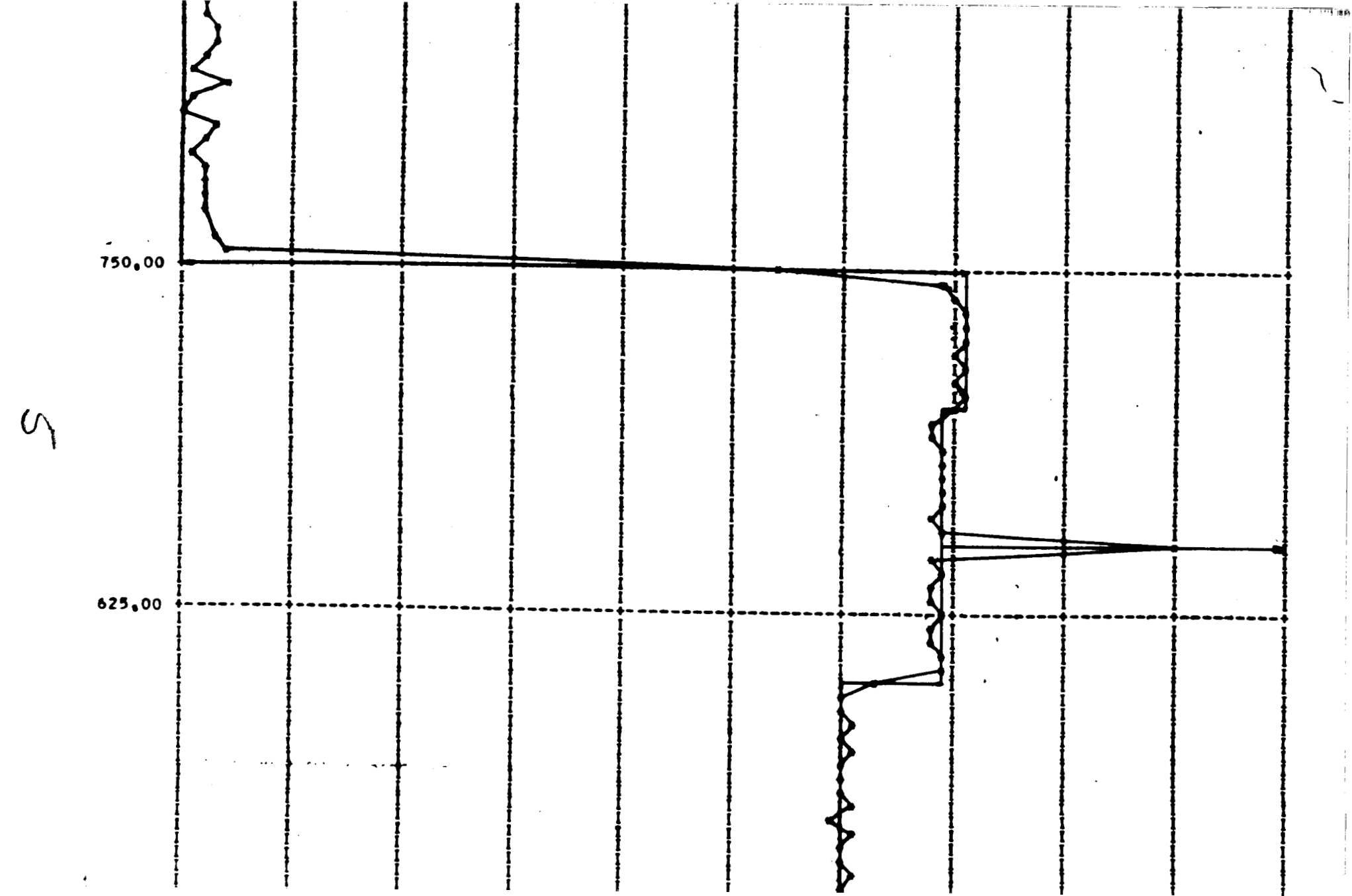
750.00
625.00

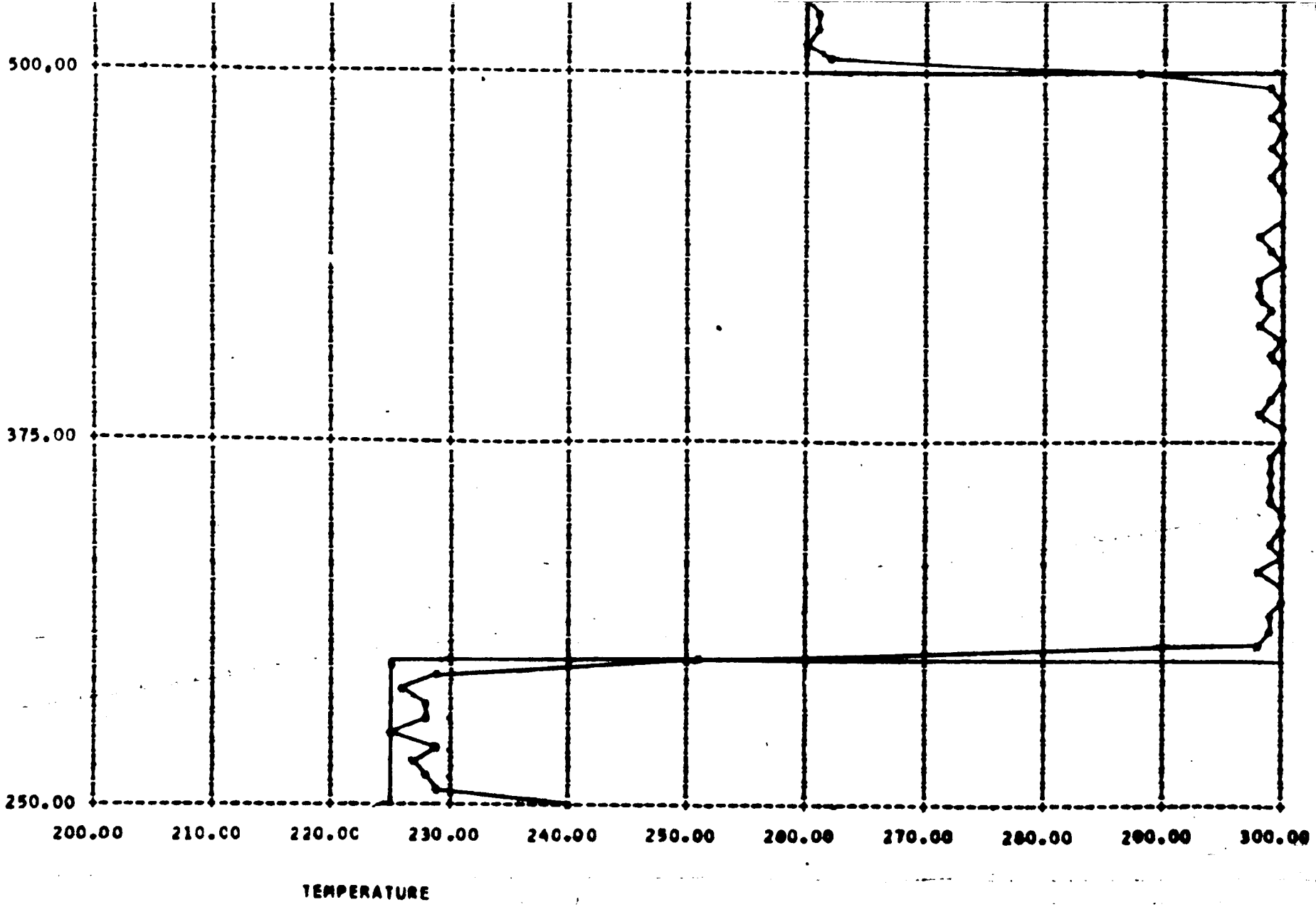
500.00
375.00
250.00
200.00
210.00
220.00
230.00
240.00
250.00
260.00
270.00
280.00
290.00
300.00
TEMPERATURE

6.2 APPENDIX B

The contents of Appendix B are as follows:

CONTENTS

```
      INTERFEROGRAM SYNTHESIS.

C           SETTING SW1 TO NON-ZERO POSITIVE VALUE CAUSES
C                 READ NEXT INPUT RECORD.
C           SETTING SW2 TO NON-ZERO POSITIVE VALUE CAUSES
C                 INCIDENT RAY EFFECT (SIN(X)/X).
C           SETTING SW3 TO NON-ZERO POSITIVE VALUE CAUSES
C                 ADDITION OF NOISE TO SIGNAL.
C           SETTING SW4 TO NON-ZERO POSITIVE VALUE CAUSES
C                 DIGITIZING EFFECT.
C           STORED PROGRAM CONSTANTS ARE...
C                 (1). PLANCK FUNCTION RADIATION CONSTANTS,
C                      C6 = 1.1909E-12
C                      C2 = 1.4380
C                 (2). MIRROR VELOCITY, V = 0.02 CM/SEC.
C                 (3). PI = 3.14159265
C                 (4). SOLID ANGLE OF ADMISSION,
C                         OMEGA =  PI/200.0 RADIANS.
C                 (5). MAXIMUM AMPLITUDE FOR BLACKBODY OF 300 DEGREES K,
C                       PEAK = 0.72210E-02
C
      DIMENSION TTNEW(100),NUONE(100),NUTWO(100),
     1TG(2000),BTI(2000),BTT(2000),BNU(2000),
     2XINTEN(3425),XNOISE(3425),TKEP(3425),IT(2000),SCA(3425)
    1 CONTINUE
      READ INPUT TAPE 2,2,SW1,SW2,SW3,SW4,NUMIN,NUTOP,DELNU,
     1ITOP,JTOP,DT,TI,TT,KCARDS,SCALE
    2 FORMAT(4F2.0,2I4,F3.1,2I4,E13.8,2F3.0,I3,F7.7)
    3 CONTINUE
      XNUMIN = NUMIN
      V =.02
      XJTOP = JTOP
      XITOP = ITOP
      XLMAX = (XJTOP - 1.0) / 2.0  + 1.0
      LMAX = XLMAX
      IF(KCARDS) 7,7,4
    4 CONTINUE
      DO 6 I = 1,KCARDS
      READ INPUT TAPE 2,5,TTNEW(I),NUONE(I),NUTWO(I)
    5 FORMAT(F3.0,2I4)
    6 CONTINUE
      GO TO 9
    7 CONTINUE
      DO 8 I = 1,ITOP
      TG(I) = TT
    8 CONTINUE
      GO TO 12
    9 DO 10 I = 1,ITOP
      TG(I) = TT
   10 CONTINUE
      DO 11 K = 1,KCARDS
      K1 = NUONE(K) - NUMIN + 1
      K2 = NUTWO(K) - NUMIN + 1
      T2 = TTNEW(K)
      DO 11 L = K1,K2
      TG(L) = T2
   11 CONTINUE
```

6.2.1 SYNTHESIS PROGRAM LISTING

```
   12 CONTINUE
C
C      BEGIN PLANCK FUNCTIONS.
C
       XNU = NUMIN
       C6 = 1.1909E-12
       C2 = 1.4380
       DO 13 I = 1,ITOP
       EA = EXPF(C2 * XNU/TI) - 1.0
       BTI(I) = C6 * (XNU ** 3.0) /EA
       EB = EXPF(C2 * XNU/TG(I)) - 1.0
       BTT(I) = C6 * (XNU ** 3.0)/EB
       BNU(I) = BTI(I) - BTT(I)
       IT(I) = I + (NUMIN - 1)
       XNU = XNU + DELNU
   13 CONTINUE
C
C      END OF PLANCK FUNCTIONS
        WRITE OUTPUT TAPE 3,14,NUMIN,NUTOP,DELNU,ITOP,JTOP,DT,TI,TT,
     1SCALE,SW1,SW2,SW3,SW4
   14 FORMAT(34H1 NUMIN   NUTOP  DELNU  ITOP  JTOP,8X,2HDT,10X,2HTI,6X,2
     1HTT,5X,5HSCALE/I6,5X,I4,3X,F4.1,2X,I4,2X,I4,3X,E13.8,3X,F5.1,3X,F5
     2.1,2X,F7.6//                                                26H  SW1    S
     3W2    SW3    SW4/1X,F4.1,3X,F4.1,3X,F4.1,3X,F4.1//)
        WRITE OUTPUT TAPE 3,140,(TTNEW(I),NUONE(I),NUTWO(I),I=1,KCARDS)
  140 FORMAT(20X,8HTTNEW = F4.0,5X,8HNUONE = I4,5X,8HNUTWO = I4//)
       WRITE OUTPUT TAPE 3,151
  151 FORMAT(6H1   NU,10X,3HBNU,12X,2HNU,10X,3HBNU,12X,2HNU,10X,3HBNU,12
     1X,2HNU,10X,3HBNU,12X,2HNU,10X,3HBNU///)
       I1 = 1
       I2 = 5
       K9 = ITOP/5
       DO 150 K = 1,K9
       WRITE OUTPUT TAPE 3,15,(IT(I),BNU(I),I = I1,I2)
       I1 = I1 + 5
       I2 = I2 + 5
  150 CONTINUE
   15 FORMAT(I7,5X,E12.5,4(5X,I4,5X,E12.5))
C
       PI = 3.14159265
       OMEGA = PI/200.0
       F4 = 4.0 * PI * V
       SLOOP = V * OMEGA
       TJ = 0.0
       DO 20 J = LMAX,JTOP
       XNU = XNUMIN
       XINTEN(J) = 0.0
       DO 19 I = 1,ITOP
       IF(SW2) 17,17,16
   16 SZ = SINF(SLOOP * XNU * TJ)/(SLOOP * XNU * TJ)
       IF(TJ) 17,17,18
   17 SZ = 1.0
   18 XINTEN(J) = DELNU * SZ * BNU(I)*COSF(F4*XNU  * TJ) + XINTEN(J)
       XNU = XNU + DELNU
   19 CONTINUE
       TJ =  TJ + DT
```

```
   20 CONTINUE
C
C      BEGIN REFLECTION.
C
       J2 = JTOP
       J3 = LMAX -1
       DO 21 J = 1, J3
       XINTEN(J) = XINTEN(J2)
       J2 = J2 - 1
   21 CONTINUE
C
C      END REFLECTION.
C
       PEAK = .72210E-02
       IF(SW3) 250,250,22
   22 CONTINUE
       CALL RANDOM(XNOISE(1),JTOP)
       XBAR = 0.0
       DO 23 J = 1,JTOP
       XBAR = XBAR + XNOISE(J)
   23 CONTINUE
       SUM = 0.0
       XBAR = XBAR / XJTOP
       DO 24 J = 1,JTOP
       XNOISE(J) = XNOISE(J) - XBAR
       SUM = SUM + XNOISE(J) ** 2.0
   24 CONTINUE
       RMS = (SUM/XJTOP) ** .5
       FNAGLE =(PEAK * SCALE) / RMS
       DO 25 J = 1,JTOP
       XNOISE(J) = XNOISE(J) * FNAGLE
       XINTEN(J) = XINTEN(J) + XNOISE(J)
   25 CONTINUE
  250 CONTINUE
66     FORMAT(1H1,14H RANDOM NOISE.//)
       WRITE OUTPUT TAPE 3,66
       WRITE OUTPUT TAPE 3,67,(XNOISE(J),J = 1,JTOP)
67     FORMAT(1X,10E13.5)
C
C      END NOISE COMPUTATION
C
       WRITE OUTPUT TAPE 3,26
   26 FORMAT(7H1XINTEN//)
       TJ = 0.0
       DO 27 J = 1,JTOP
       TKEP(J) = TJ
       TJ = TJ + DT
   27 CONTINUE
       K4 = JTOP/10 + 1
       K1 = 1
       K2 = 10
       DO 30 K3 = 1,K4
       WRITE OUTPUT TAPE 3,28,(TKEP(L),L = K1,K2)
       WRITE OUTPUT TAPE 3,29,(XINTEN(L),L = K1,K2)
   28 FORMAT(1X,10E13.5)
   29 FORMAT(1X,10E13.5//)
```

```
      K1 = K1 +10
      K2 = K2 + 10
   30 CONTINUE
      IF(SW4) 36,36,31
   31 CONTINUE
      PEAK2 = PEAK/10.0
      DELD = PEAK2/127.0
      CALL SCAL (XINTEN(1),JTOP,PEAK2,DELD,SCA(1))
      WRITE OUTPUT TAPE 3,32
   32 FORMAT(15H1XINTEN SCALED//)
      K1 = 1
      K2 = 10
      DO 34 K3 = 1,K4
      WRITE OUTPUT TAPE 3,28,(TKEP(L),L = K1,K2)
      WRITE OUTPUT TAPE 3,29,(SCA(L),L = K1,K2)
   33 FORMAT(1X,10013//)
      K1 = K1 + 10
      K2 = K2 + 10
   34 CONTINUE
   36 CONTINUE
      CALL WRITEA(XINTEN(3425))
      CALL WRITEA(TKEP(3425))
      IF(SW1) 35,35,1
   35 PAUSE 7
      END(1,1,0,0,0,0,1,1,0,1,0,0,0,0,0)
```

```
*       SIMMONS WRITEA..
*       CARDS COLUMN
*       FAP

                    00000           ENTRY   WRITEA
00000   0500 00 4   00001   WRITEA  CLA     1,4
00001   0621 00 0   00014           STA     CMD
00002   0766 00 0   01230           WTBA    8
00003   0540 00 0   00014           RCHA    CMD
00004   0060 00 0   00004           TCOA    *
00005   0022 00 0   00007           TRCA    *+2
00006   0020 00 0   00012           TRA     CLAM
00007   0764 00 0   01210           BSRA    8
00010   0060 00 0   00010           TCOA    *
00011   0020 00 0   00000           TRA     WRITEA
00012   0761 00 0   00000   CLAM    NOP
00013   0020 00 4   00002           TRA     2,4
00014   3 06541 0   00000   CMD     IORT    **,,3425
                                    END
```

```
*       SIMMONS RANDOM GENERATOR...
*       CARDS COLUMN
*       FAP


                        00000           ENTRY   RANDOM
00000   0020 00 0 00007 RANDOM  TRA     *+7
00001   0774 00 4 00000         AXT     0,4
00002   0774 00 2 00000         AXT     0,2
00003   0774 00 1 00CC0         AXT     0,1
00004   0441 00 0 00006         LDI     *+2
00005   0020 00 4 00003         TRA     3,4
00006   0 00000 0 00000         PZE     0
00007   0604 00 0 00006         STI     *-1
00010   0634 00 1 00003         SXA     *-5,1
00011   0634 00 2 00002         SXA     *-7,2
00012   0634 00 4 00001         SXA     *-9,4
00013   0500 00 4 00001         CLA     1,4
00014   0400 00 0 00372         ADD     =1
00015   0621 00 0 00367         STA     CAT
00016   0500 00 0 00370         CLA     RANDA
00017   0601 00 0 00371         STO     RANDB
00020   0500 60 4 00002         CLA*    2,4
00021  -0734 00 2 00000         PDX     ,2
00022   0774 00 4 00310         AXT     200,4
00023   0560 00 0 00370 SUE     LDQ     RANDA
00024   0200 00 0 00371         MPY     RANDB
00025  -0600 00 0 00371         STQ     RANDB
00026   0765 00 0 00004         LRS     4
00027  -0754 00 0 00000         PXD     0,,0
00030   0221 00 0 00373         DVP     =1000
00031   0400 00 0 00372         ADD     =1
00032   0601 00 4 00367         STO     DOG+200,4
00033   2 00001 4 00023         TIX     SUE,4,1
00034   0774 00 1 00310         AXT     200,1
00035   0500 00 1 00367 ROPE    CLA     DOG+200,1
00036   0400 00 1 00370         ADD     DOG+201,1
00037   0400 00 1 00371         ADD     DOG+202,1
00040   0400 00 1 00372         ADD     DOG+203,1
00041   0400 00 1 00373         ADD     DOG+204,1
00042   0400 00 1 00374         ADD     DOG+205,1
00043   0400 00 1 00375         ADD     DOG+206,1
00044   0400 00 1 00376         ADD     DOG+207,1
00045   0400 00 1 00377         ADD     DOG+208,1
00046   0400 00 1 00400         ADD     DOG+209,1
00047  -0501 00 0 00374         ORA     =0233000000000
00050   0300 00 0 00374         FAD     =0233000000000
00051   0601 60 0 00367         STO*    CAT
00052   2 00001 2 00054         TIX     RAG,2,1
00053   0020 00 0 00056         TRA     OUT
00054   2 00012 1 00035 RAG     TIX     ROPE,1,10
00055   0020 00 0 00022         TRA     SUE-1
00056   0020 00 0 00001 OUT     TRA     RANDOM+1
00057                   DOG     BSS     200
00367   0 00000 2 00000 CAT     PZE     0,2
00370  +343277244615    RANDA   OCT     343277244615
00371  +343277244615    RANDB   OCT     343277244615
                                END
```

```
*       SIMMONS  SCALE..
*       CARDS COLUMN
*       FAP


                      00000          ENTRY    SCAL
00000   0774 00 2 00000  SCAL   AXT      0,2
00001   0500 00 4 00001         CLA      1,4
00002   0621 00 0 00050         STA      CAT
00003   0500 00 4 00005         CLA      5,4
00004   0621 00 0 00051         STA      KAT
00005   0500 60 4 00002         CLA*     2,4
00006   0622 00 0 00046         STD      TRAP+2
00007   0500 60 0 00050  DEALIT CLA*     CAT
00010   0760 00 0 00003  MINUS  SSP
00011   0302 60 4 00003         FSB*     3,4
00012  -0120 00 0 00041         TMI      NOSCAL
00013   0500 60 0 00050         CLA*     CAT
00014   0241 00 0 00057         FDP      =10.0
00015   0131 00 0 00000         XCA
00016   0241 60 4 00004  GOL    FDP*     4,4
00017   0131 00 0 00000         XCA
00020  -0300 00 0 00061         UFA      =0233000000000  SPLITS NUMBER INTO WHOLE AND FRACTION.
00021   0760 00 0 00011         FRN
00022   0300 00 0 00061         FAD      =0233000000000
00023   0601 00 0 00053         STO      MAL
00024   0560 60 4 00004         LDQ*     4,4
00025   0260 00 0 00053         FMP      MAL
00026   0601 60 0 00051         STO*     KAT
00027   0601 60 0 00050         STO*     CAT
00030   0500 00 0 00053         CLA      MAL
00031  -0300 00 0 00060         UFA      =0211000000000
00032   0765 00 0 00000         LRS      0
00033  -0320 00 0 00056         ANA      =0000777777777
00034   0763 00 0 00000         LLS      0
00035  -0520 00 0 00054         NZT      SWIT
00036  -0501 00 0 00055         ORA      =0000400000000
00037   0601 60 0 00050         STO*     CAT
00040   0020 00 0 00044         TRA      TRAP
00041  -0625 00 0 00054  NOSCAL STL      SWIT
00042   0500 60 0 00050         CLA*     CAT
00043   0020 00 0 00016         TRA      GOL
00044   0600 00 0 00054  TRAP   STZ      SWIT
00045   1 00001 2 00046         TXI      *+1,2,1
00046  -3 00000 2 00007         TXL      DEALIT,2,**
00047   0020 00 4 00006         TRA      6,4
00050   0 00000 2 00000  CAT    PZE      0,2
00051   0 00000 2 00000  KAT    PZE      0,2
00052                    SWITCH BSS      1
00053                    MAL    BSS      1
00054                    SWIT   BSS      1
                                END
```

```
      INTERFEROGRAM ANALYSIS

C     SETTING SW1 TO NON-ZERO POSITIVE VALUE CAUSES READ NEXT RECORD.
C     SETTING SW2 TO NON-ZERO POSITIVE VALUE EFFECTS DIGITIZING SCALING.
C     SETTING SW3 TO NON-ZERO POSITIVE VALUE TRANSFORMS A(I)'S TO TEMPS.
C     DNU IS INTEFEROMETER RESOLUTION.  F IS FREQUENCY CONTROL,WHERE
C          WAVE NOS. COMPUTED ARE GIVEN BY...
C          NU(I) = NUMIN + F(I-1),FOR I=1,2,...,((NUMAX-NUMIN)/F)-1.
C     STORED PROGRAM CONSTANTS ARE...
C          (1).  PI = 3.14159265
C          (2).  C-C COMPONENT, ZEROIN = 0.0
C          (3).  PLANCK RADIATION FUNCTION CONSTANT, C2 = 1.4380
C          (4).  PLANCK RADIATION FUNCTION CONSTANT, C6 = 1.1909E-12
C          (5).  DESCALING (DIGITIZING) MULTIPLIER.
      DIMENSION XNU(710),TEMP(710),XIT(710),BTI(710),APRIME(710),
     1BPRIME(710),IT(710),BTT(710),BNU(710),XINTEN(3425)
    1 CONTINUE
      READ INPUT TAPE 2,2,SW1,SW2,SW3,NUMIN,NUTOP,JTOP,DNU,F,TI
    2 FORMAT(3F2.0,3I4,F3.1,F4.1,F3.0)
    3 CONTINUE
      CALL READ2( XINTEN(3425))
      IF(SW2) 7,7,4
    4 CALL DESCAL(XINTEN(1))
      WRITE OUTPUT TAPE 3,5
    5 FORMAT(1H1,13HDESCALED I(J)//)
      WRITE OUTPUT TAPE 3,6,(XINTEN(J),J = 1,JTOP)
    6 FORMAT(1X,10E13.5)
      GO TO 10
    7 CONTINUE
      WRITE OUTPUT TAPE 3,8
    8 FORMAT(1H1,4HI(J)//)
      WRITE OUTPUT TAPE3,9,(XINTEN(J),J = 1,JTOP)
    9 FORMAT(1X,10E13.5)
   10 CONTINUE
      WRITE OUTPUT TAPE 3,11
   11 FORMAT(1H1,11X,3HSW1,4X,3HSW2,4X,3HSW3,4X,5HNUMIN,4X,5HNUTOP,4X,
     14HJTOP,4X,3HDNU,4X,1HF,4X,2HTI//)
      WRITE OUTPUT TAPE 3,12,SW1,SW2,SW3,NUMIN,NUTOP,JTOP,DNU,F,TI
   12 FORMAT(F15.0,2F7.0,I8,I10,I8,F7.1,F6.1,F6.0//)
C     BEGIN FOURIER
      XNUMIN = NUMIN
      XNUTOP = NUTOP
      PMIN = XNUMIN / DNU
      XITOP = ((XNUTOP - XNUMIN) / F) + 1.0
      ITOP = XITOP
      XJTOP = JTOP
      PI = 3.14159265
      ARG1 = 2.0 * PI * PMIN / XJTOP
      ARG2 = 2.0 * PI * F / (DNU * XJTOP)
      C = COSF(ARG1)
      S = SINF(ARG1)
      C1 = COSF(ARG2)
      S1 = SINF(ARG2)
      C3 = 2.0 / (DNU * XJTOP)
      DO 14 I = 1,ITOP
      U2 =0.0
      U1 =0.0
```

6.2.2 ANALYSIS PROGRAM LISTING

```
      INTERFEROGRAM ANALYSIS

          J =JTOP
          DO 13 K = 1,JTOP
          UZERO = XINTEN(J) + 2.0 * U1 * C - U2
          J = J - 1
          U2 = U1
          U1 = UZERO
       13 CONTINUE
          ZEROIN = 0.0
          APRIME(I) = C3 * (ZEROIN + U1 * C - U2)
          BPRIME(I) = C3 * U1 * S
          Q = C1 * C - S1 * S
          S = C1 * S + S1 * C
          C = Q
       14 CONTINUE
          DO 15 I = 1,ITOP
          BNU(I) = APRIME(I)**2.0 + BPRIME(I)**2.0
          BNU(I) = SQRTF(BNU(I))
       15 CONTINUE
          IT(1) = 0
          DO 16 I = 2,ITOP
          IT(I) = I - 1
       16 CONTINUE
          DO 17 I = 1,ITOP
          XIT(I) = IT(I)
          XNU(I) = XNUMIN + (F * XIT(I))
       17 CONTINUE
          IF(SW3) 24,24,18
       18 CONTINUE
C         BEGIN PLANCK
          C6 = 1.1909E-12
          C2 = 1.4380
          DO 20 I = 1,ITOP
          E = C2 * XNU(I) / TI
          E = EXPF(E) - 1.0
          BTI(I) = C6 * (XNU(I)**3.0) / E
          IF(APRIME(I)) 19,20,20
       19 BNU(I) = -BNU(I)
       20 BTT(I) = BTI(I) - BNU(I)
C         END PLANCK, BEGIN INVERSE PLANCK
          DO 21 I = 1,ITOP
          TEMP(I) = C6 * XNU(I)**3.0 / BTT(I) + 1.0
          TEMP(I) = LOGF(TEMP(I))
          TEMP(I) = C2 * XNU(I) / TEMP(I)
       21 CONTINUE
          WRITE OUTPUT TAPE 3,22
       22 FORMAT(6X,1HI,9X,5HNU(I),10X,6HBNU(I),7X,9HBPRIME(I),9X,
         19HAPRIME(I),9X,6HBTT(I),9X,7HTEMP(I))
          WRITE OUTPUT TAPE 3,23,(IT(I),XNU(I),BNU(I),BPRIME(I),APRIME(I),
         1BTT(I),TEMP(I),I = 1,ITOP)
       23 FORMAT(1X,I6,F14.1,E18.5,E15.5,E18.5,E16.5,F13.1)
C         END OF INVERSE PLANCK
          CALL WRITE7(TEMP(710))
          CALL WRITE7(XNU(710))
       24 CONTINUE
          WRITE OUTPUT TAPE 3,25
       25 FORMAT(6X,1HI,9X,5HNU(I),10X,6HBNU(I),7X,9HBPRIME(I),9X,
```

→ go to 27

```
      INTERFEROGRAM ANALYSIS

     19HAPRIME(I))
      WRITE OUTPUT TAPE3,26,(IT(I),XNU(I),BNU(I),BPRIME(I),APRIME(I),
     1I = 1,ITOP)
   26 FORMAT(1X,I6,F14.1,E18.5,E15.5,E18.5)
   27 IF(SW1) 28,28,1
   28 PAUSE 7
      CALL EXIT
      END(1,1,0,0,0,0,1,1,0,1,0,0,0,0,0)
```

```
*       AFS....WRITE A7
*       FAP

                    00C00           ENTRY   WRITE7
00000   0500 00 4   00001   WRITE7  CLA     1,4
00001   0621 00 0   00014           STA     CMD
00002   0766 00 0   01227           WTBA    7
00003   0540 00 0   00014           RCHA    CMD
00004   0060 00 0   00004           TCOA    *
00005   0022 00 0   00007           TRCA    *+2
00006   0020 00 0   00012           TRA     CLAM
00007   0764 00 0   01207           BSRA    7
00010   0060 00 0   00010           TCOA    *
00011   0020 00 0   00000           TRA     WRITE7
00012   0761 00 0   00000   CLAM    NOP
00013   0020 00 4   00002           TRA     2,4
00014   3 01306 0   00000   CMD     IORT    **,,710
                            END
```

```
*       SIMMONS READ TAPE..
*       FAP

                    00000           ENTRY   READ2
00000   0500 00 4   00001   READ2   CLA     1,4
00001   0621 00 0   00021           STA     CMD
00002   0762 00 0   01230           RTBA    8
00003   0540 00 0   00021           RCHA    CMD
00004   0060 00 0   00004           TCOA    *
00005   0022 00 0   00007           TRCA    *+2
00006   0020 00 0   00012           TRA     *+4
00007   0764 00 0   01210           BSRA    8
00010   0060 00 0   00010           TCOA    *
00011   0020 00 0   00002           TRA     READ2+2
00012   0762 00 0   01230           RTBA    8
00013   0540 00 0   00017           RCHA    CMD2
00014   0060 00 0   00014           TCOA    *
00015   0022 00 0   00016           TRCA    *+1
00016   0020 00 4   00002           TRA     2,4
00017   3 06541 2   00020   CMD2    IORTN   A,,3425
00020                       A       BSS     1
00021   3 06541 0   00CC0   CMD     IORT    **,,3425
                            END
```

```
•       SIMMONS  DESCAL...
•       FAP

                        00000           ENTRY    DESCAL
00000   0774 00 2 00000 DESCAL AXT      0,2
00001   0500 00 4 00001         CLA      1,4
00002   0621 00 0 00036         STA      CAT
00003   0500 60 0 00036 TERN    CLA*     CAT
00004  -0320 00 0 00037         ANA      =0000400000000
00005   0100 00 0 00026         TZE      NOSCAL
00006  -0500 60 0 00036 GO      CAL*     CAT
00007  -0320 00 0 00043         ANA      =0400377000000
00010   0602 00 0 00034         SLW      TEMP
00011   0500 00 0 00034         CLA      TEMP
00012   0771 00 0 00022         ARS      18
00013  -0501 00 0 00042         ORA      =0233000000000
00014   0300 00 0 00042         FAD      =0233000000000
00015   0131 00 0 00000         XCA
00016   0260 00 0 00040         FMP      =.56858268E-05
00017   0601 60 0 00036         STO*     CAT
00020   0520 00 0 00035         ZET      SWIT
00021   0020 00 0 00030         TRA      TRAP            NON ZERO  NO SCALE
00022   0560 60 0 00036         LDQ*     CAT
00023   0260 00 0 00041         FMP      =10.0
00024   0601 60 0 00036         STO*     CAT
00025   0020 00 0 00030         TRA      TRAP
00026  -0625 00 0 00035 NOSCAL  STL      SWIT
00027   0020 00 0 00006         TRA      GO
00030   0600 00 0 00035 TRAP    STZ      SWIT
00031   1 00001 2 00032         TXI      *+1,2,1
00032  -3 06541 2 00003         TXL      TERN,2,3425
00033   0020 00 4 00002         TRA      2,4
00034                   TEMP    BSS      1
00035                   SWIT    BSS      1
00036   0 00000 2 00000 CAT     PZE      0,2
                                END
```